AD NUMBER

AD241240

NEW LIMITATION CHANGE

TO

Approved for public release, distribution unlimited

FROM

Distribution authorized to U.S. Gov't. agencies and their contractors; Specific Authority; 27 May 1960. Other requests shall be referred to Naval Radiological Defense Lab, San Francisco CA.

AUTHORITY

USNRDL ltr 19 Apr 1967

NOTICE: When government or other drawings, specifications or other data are used for any purpose other than in connection with a definitely related government procurement operation, the U. S. Government thereby incurs no responsibility, nor any obligation whatsoever; and the fact that the Government may have formulated, furnished, or in any way supplied the said drawings, specifications, or other data is not to be regarded by implication or otherwise as in any manner licensing the holder or any other person or corporation, or conveying any rights or permission to manufacture, use or sell any patented invention that may in any way be related thereto.

Copy No. 90

A THEORY OF FORMATION OF FALLOUT FROM LAND-SURFACE NUCLEAR DETONATIONS AND DECAY OF THE FISSION PRODUCTS

Research and Development Technical Report USNRDL-TR-425

27 May 1960

by

C. F. Miller

U.S. NAVAL RADIOLOGICAL DEFENSE LABORATORY

SAN FRANCISCO 24 · CALIFORNIA

A THEORY OF FORMATION OF FALLOUT FROM LAND-SURFACE NUCLEAR DETONATIONS AND DECAY OF THE FISSION PRODUCTS

Research and Development Technical Report USNRDL-TR-425
S-FO11 05 11
OCDM

27 May 1960

by

C.F. Miller

Chemical Technology Division
C.F. Miller, Head

Scientific Director
P.C. Tompkins

Commanding Officer and Director
Captain J.H. McQuilkin, USN

U.S. NAVAL RADIOLOGICAL DEFENSE LABORATORY
San Francisco 24, California

ABSTRACT

The current concepts of the formation of fallout from land surface nuclear detonations have been reviewed. Thermodynamic equations have been developed for a part of the overall condensation process to account for fractionation of the radioactive species. Empirical functions for some of the fireball parameters have been developed from available data and assumptions about the utilization of the energy released in a nuclear explosion. These functions and available data on the vapor pressure of fission product elements and compounds (mainly oxides) and on the fission yields from fission of U^{235}, U^{238}, and Pu^{239} were utilized to compute decay curves for the unfractionated mixtures and for an idealized fallout condition from a surface nuclear detonation.

SUMMARY

The Problem

The radiological hazard from nuclear detonations arises from the fact that radioactive materials produced in the explosion become associated with rather large particles of environmental materials that fall back to earth shortly afterward. The accumulation of these particles on the earth's surface creates a gamma radiation hazard because of radioactive content of the particles.

The nature, degree, and type of hazard over a prolonged time period depends upon the radioactive composition of the particles. It is known that the decay rates of the fission products produced in weapons tests differs from one shot to another and also differs from one location to another for a given shot. It is also known that, in a nuclear war for which countermeasures are to be developed and planned, the materials at likely targets are different from those at weapons test sites. Therefore to explain the causes of the different observed radiation decay of fallout and better define the radiological hazards and countermeasure requirements, a better understanding of the mechanism(s) of fallout formation is required.

Findings

In this report an attempt is made to describe mathematically some of the processes of fallout formation. A general process of fallout formation is outlined based on the observed structures and types of fallout particles produced by nuclear explosions. Thermodynamic equations are developed to describe some of the possible types of condensation that could occur. The conditions of temperature, pressure, volume, time, and energy utilization for establishing the boundary conditions of the condensation processes are obtained from some of the data in The Effects of Nuclear Weapons[14] together with numerous assumptions in order to make estimates for land surface detonations. The boundary conditions and thermal data are used to estimate the amount of melted soil present in the fireball when the temperature has decreased to the soil melting point.

Data on the vapor pressures of the fission product elements and compounds (mainly oxides) is summarized. The fission yields for slow and fast fission of U^{235}, U^{238}, and Pu^{239} are discussed and summarized.

For some of the fission processes, estimates of the fission yield were made to complete the yield curve for use in computations.

Using an ideal non-reactive soil with a defined melting point of 1400°C and which formed ideal dilute solutions with the fission product (usually as the oxide) elements, computations are made for a surface land detonation with an estimated yield of 2.3 MT and in which the temperature of 1400°C occurs at 60 sec after detonation. For this case, it is estimated that 6.3 % of the total energy was contained in the liquid particles just prior to their solidification at the melting point.

Calculations are made of the disintegration rates, photon emission rates, photon-energy emission rates, and air-ionization rates from the unfractionated or normal mixture of fission products from the slow- and fast-neutron fission of U^{235}, U^{238}, and Pu^{239}. The six ionization rate decay curves gave ratios of the r/hr at 1 hr (at 3 ft above an infinite smooth plane) to KT equivalents per sq mi that range from 3400 to 3950.

For the idealized detonation conditions in which the computations assume only one particle size (i.e., that none fall out of the fireball up to 60 sec, and then all the particles leave in solid form), computations of the disintegration rates and air-ionization rates for thermal and fission-neutron fission of U^{235}, 8 Mev-neutron (broad band) fission of U^{238}, and fission-neutron fission of Pu^{239}. In these cases, the ratios of the r/hr at 1 hr (at 3 ft above an infinite smooth plane) to KT equivalents per sq mi are found to range from 1480 to 1560. If induced activities, instrument response, and terrain roughness factors are considered, this ratio could be as low as 1000. However, for a fractionated mixture, the ratio has no real meaning. In addition, the ratio is not constant, except for a single computation; in a real fallout area it will change with particle size and distance from shot point. The report gives some suggestions for further improvements in the theory and suggests possible methods for making more realistic and comprehensive computations.

ADMINISTRATIVE INFORMATION

This work is based on and formulated for studies made under the sponsorship of Office of Civil and Defense Mobilization. The studies are part of Problem 3, Program B-1, and Problem 3, Program B-3, described in this laboratory's USNRDL Technical Program For Fiscal Years 1960 and 1961, Revision #1, 1 July 1959. Progress in These Problems is reported most recently in Quarterly Progress Report, 1 January Through 31 March 1960, USNRDL-P-22, April 1960.

ACKNOWLEDGEMENTS

The author wishes to thank Mr. P.D. LaRiviere for establishing the procedure and preparing the data for the computation of the decay curves and for his many technical contributions to the material presented in this report. The author also wishes to thank Mr. C.E. Adams for many helpful comments and suggestions.

CONTENTS

FIGURES

TABLES

SECTION 1

INTRODUCTION

1.1 OBJECTIVES

The major objectives of this report are to formalize some of the current concepts of formation of fallout from land-surface detonations and to develop approximating formulae, by use of thermodynamics logic and empirical functions, for the purpose of computing - or estimating - the radioactive decay of such fallout. Test detonations from which this type of information could be obtained have not yet been conducted. Another objective was to develop a procedure for computing decay curves and to demonstrate its use by making sample calculations.

1.2 SCOPE

The report is divided into seven sections. In this section (INTRODUCTION), the general background material is summarized. Inferences are made from analyses of fallout particles with regard to how they must have been formed, and some definitions of fractionation are given.

In Section 2, the condensation process in the formation of fallout is described and equations are derived for several alternate processes.

In Section 3, data on the vapor pressures of the fission product oxides, elements, and some compounds together with the oxides of a few other elements are summarized. Some equations are given to illustrate the use of the data in the computations.

In Section 4, some empirical functions are derived for estimating the amount of energy from a land surface nuclear explosion that is available for vaporizing and/or melting soil particles. In the development of the material for this section, correlation of the information given in The Effects of Nuclear Weapons,[14] which is the only unclassified source available, led to the finding of a number of inconsistencies in data and data treatment in that document. However, it is emphasized that the scope of this report does not include criticizing that document but rather utilizing its contents to establish the approximating formulae necessary for this study.

In Section 5, available data on the fission yields for several fissile materials are summarized. Correlation techniques were used to estimate the yields of mass chains for which data were not available.

In Sections 6 and 7, the computational methods and sample calculations of the decay curves are described for both unfractionated and fractionated fission products. The calculations are made for different fissile materials. The comparisons given for the fractionated mixture are based on calculations for a non-reactive soil that formed an ideal solution with all fission product oxides in the liquid state. Further study and experimental results will be required before the calculations can be made for a process that more closely corresponds to the real one.

1.3 LIMITATIONS

The many items considered in the general treatment all have a common limitation: the lack of sufficient available unclassified data for testing the validity of individual formula or the completed computation.

In the text itself, the assumptions and postulates are stated usually only once in order to minimize undue interruption of the main line of the argument and development of the material. Conclusions and comparisons are often stated without definite repeated reference to the original assumptions. This limitation is given here as a caution to the reader in the use of the computational results given in this report.

The computational results were made for illustrative use only since an idealized chemical system was used. A great deal of additional work can be done to improve the quantitative aspects of the theory. This report may be most helpful in identifying the type of information needed for improving both the conceptual basis for deriving the mathematics and the quantitative use of the theory.

1.4 BACKGROUND

In a nuclear detonation employing fissionable materials about 90 fission-product mass chains (40 elements) are produced. The high temperatures immediately following the detonation virtually assure that all of these elements are immediately vaporized so that the fallout formation process is one in which these elements condense from a vapor phase during the cooling of the fireball. Among the 90-odd mass-chains produced, with specific fission yields depending on the fissile material and the neutron energy, there are many atomic species and compounds whose volatilities at high temperatures are very different. Hence, at a given temperature, the range of values of the equilibrium partial vapor pressure of the various species and compounds will be large. A condensation process that occurs in a system of a rapidly decreasing high temperature can be expected therefore to result in the preferential condensation of the less volatile elements. This should, in turn, result in an alteration of the relative abundance of the fission product mass chains or radionuclides as found in fallout compared to the amounts initially produced. Any such alteration, when observed, is usually called fractionation.

A general description of some of the fallout particles found in local fallout from surface and tower shots and of how they could have originated has been given by Adams and coworkers.[1,2,3,4,5,6,7] The essential details of this work that have been used in this report are: (1) condensation of the fission product elements can begin at the highest temperature at which a macroscopic liquid phase can exist in the fireball and this liquid phase will essentially consist of substances such as iron oxide (tower shots) or aluminum and silicon oxides (surface ground shot), and (2) the fission products that co-condense with or into liquid particles are dissolved into the melts and remain there as compounds or in solid solution when the particles solidify.

In low tower shots, it appears that the very small drops of vapor-condensed iron oxide are later dissolved by melted soil particles to form a glassy iron oxide-silicon oxide solution. Data on the solubility of fission product elements into dilute acids and complexing agents, obtained by Fuller[8] from the larger particles from a low tower shot that fell close to ground zero, show that only a very small fraction of the fission products are soluble. However, data on the solubility, obtained by Larson[9] from smaller particles collected at greater distances from shot point, give larger fractions of soluble fission products; his data show also that radioelements other than just the daughter products of rare gas nuclides are among the soluble group of elements.

The essential facts from these data are that some of each of the fission products condenses into liquid particles and that some of each condensed onto the surfaces of solidified particles. Also, the particles that fall in the local areas downwind from shot point (and where the amount that falls out is large enough to produce a significant radiation hazard) are too large to have been produced by a vapor condensation process. These particles therefore are formed either from the break-up of a bulk liquid melt or from the melting of single grains of soil that enter the fireball after it has cooled to some given temperature.

The general condensation process can therefore be divided into two time periods. The first period of the process is characterized by the presence of gas and liquid phases and the second period by the existence of gas and solid phases. The first period of condensation ends when the bulk carrier or substrate material of the particles solidifies. The degree to which the change of phase of the carrier affects the continuity of the process and the distribution of each fission product element in or on a particle will depend on the thermo-chemical properties of the interacting materials. Some fission product elements may condense by sublimation on the surface of the particle and be readily available for solution upon contact with water. Others may react with the substrate material and/or diffuse through the surface of the particle.

One particular aspect of first period of condensation is important. This is that the fission product vapors condense into the liquid phase of the carrier material to form a very dilute solution.

The fraction of each fission product element that condenses into the liquid carrier particles depends on the melting point of the carrier and the time after fission at which that temperature occurs. If the melting point of the carrier is high, the fractions condensed will be low. If the melting point of the carrier is low, the fractions condensed will be high. The fraction which had not condensed into the liquid phase of the carrier can condense on or react with the surface of the solid particles. These could consist of the smaller of the melted particles or of unmelted particles that enter the gas volume at later times.

1.5 FACTORS CONTROLLING FRACTIONATION IN FALLOUT

In an overall sense, the amount of each fission product found in fallout relative to some standard of comparison depends on five

main factors: (1) the original fission yields or relative abundance of the fission products, (2) neutron capture by the fission products themselves, (3) the degree to which each fission product condenses into or onto the carrier particles, (4) neutron emissions in the decay chain, and (5) the radiochemical standards used to measure the fractionation.

The relative abundance of each fission product element originally produced depends on the fissile material used -- i.e. whether the material is U^{235}, U^{238}, Pu^{239}, or some other element. The fission chain yields also depend on the energy spectrum of the incident neutrons. In comparison with the fission yields from thermal neutrons on U^{235}, usually taken as the reference standard, the yields of the elements in the lighter-mass peak for other types of fission in general, shift more than do those in the heavier mass peak. With the heavier fissile elements, the center of the lighter-mass group moves toward the higher mass numbers. As the incident neutron energy increases, the yields of the valley elements and those of highest and lowest mass numbers rise and the neutron yield per fission increases. The increase in neutron yield per fission tends to spread the two peaks farther apart and, again, the lighter-mass group is shifted more than the heavy group.

Neutron capture by the fission product elements would result in a general shift of the whole yield curve to higher mass numbers. The result would be a decrease in the yields of the elements with the smaller mass numbers (left side of the peaks) of both groups, and an increase in the yields of the elements with the larger mass numbers of both groups. Relatively little change would result in the yields of elements in the peaks excepting for those that may have extremely high capture cross-sections. The subject is not discussed further in this report because of insufficient data.

Section 2 of this report discusses the role of the condensation process in fallout formation and in fractionation. This process is often assumed (and erroneously) to be the only cause of observed fractionation in fallout.

Neutron emission during the decay process results in a product nuclide with a mass number one unit less than the parent. This chain "shift" can be accounted for if the decay scheme is known. However for many of the short-lived radionuclides there is insufficient data for its further consideration in this report.

The experimental measure of fractionation is most often given as an "R" factor or value relative to thermal fission of U^{235} and a selected radionuclide. The most commonly selected radionuclide

for comparison is Mo^{99}. Thus, relative to these standards, a radiochemical assay of a fallout sample that gives an "R" value different from one does not necessarily mean that the nuclide in question has, in fact, been fractionated. Knowledge of the true initial fission yields are required to correct the observed assay data to determine whether fractionation has, in fact, occurred.

SECTION 2

THE CONDENSATION PROCESS

2.1 THE FIRST PERIOD OF CONDENSATION

2.1.1 Description of the Formation Process

As is implied by the general description of the formation process given in Section 1, no single well-defined condensation time for the fission product mixture can exist. Rather, it is a continuing process that can be separated into the two more or less well-defined time periods described above. In the first time period (during the cooling of the fireball), the major feature of the condensation process is the existence of vapor-liquid phase equilibria. This period of condensation ends when the carrier material solidifies, with the fission products being either fixed in a solid solution matrix or compounded with the carrier material.

The major feature of the second period of condensation is the existence of vapor-solid phase equilibria in which the remaining fission product elements condense at lower temperatures on the surface of solid particles. The second period of condensation never ceases in an absolute sense, except for those particles which fall out or otherwise leave the space containing the residual gases. Actually, the process can reverse for a fission product element that later decays to a more volatile element; for example, elements like iodine and the rare gases could sublime as fast as they form from non-volatile precursors (i.e., at ordinary temperatures) condensed on the surface of fallout particles. This process is unlikely when the fission products are trapped within a glassy matrix, since the vapor pressures due to the low concentration of dissolved fission products (ca. 10^{-10} moles/mole) would be extremely low, and diffusion through the glass solid would be very slow.

The essential problem in the theory for the process during the first period of condensation is to establish the vapor-liquid phase equilibria of each fission product element at the time that the carrier material solidifies; that is, to determine the fraction of each element present, condensed, inside the carrier melt when it solidifies.

When one of two phases in contact is a gas, simple kinetic theory can be used to show that condensation-vaporization equilibrium can be established within a small fraction of a second at temperatures above 1000°K. Thus those gaseous species of each fission product element that do not react with the liquid carrier but dissolve into it should obey Henry's law of dilute solutions. In fact, the solutions should be sufficiently dilute as to result in no change in the free energy of the liquid carrier so that the free energy of each element in the solution should be independent of any other. Therefore, it is possible to consider the solubility of each element as making a two-component system with the carrier. Moreover, there should be no appreciable surface loading (large excess surface concentrations) during the condensation process if the temperature range over which the liquid carrier exists exceeds 200 or 300°C. A concentration gradient in a particle, however should exist especially for the larger particles of which some may not be melted in the center when the air or gas temperature about the particle falls below the melting point of the bulk carrier.

2.1.2 Condensation Thermodynamics

For the condensation of dn_j moles of element j from a gaseous mixture to a liquid solution, the change in the partial molar free energy, $\bar{F}_j^\circ$, of the element in the gas is given by

$$d\bar{F}_j^\circ = RT\left(\frac{\delta \ell n f_j^\circ}{\delta P}\right)_{T,N_j^\circ}^{dP} + RT\left(\frac{\delta \ell n f_j^\circ}{\delta T}\right)_{P,N_j^\circ}^{dT} + RT\left(\frac{\delta \ell n f_j^\circ}{\delta N_j^\circ}\right)_{P,T}^{dN_j^\circ} \qquad (1)$$

and the corresponding change in its partial molar free energy, $\bar{F}_j$, in the solution is

$$d\bar{F}_j = RT\left(\frac{\delta \ell n f_j}{\delta P}\right)_{T,N_j}^{dP} + RT\left(\frac{\delta \ell n f_j}{\delta T}\right)_{P,N_j}^{dT} + RT\left(\frac{\delta \ell n f_j}{\delta N_j}\right)_{P,T}^{dN_j} \qquad (2)$$

where P is the total pressure, T is the temperature, N_j^o is the mole fraction of element j in the gas mixture, N_j is its mole fraction in the liquid, f_j^o is its fugacity (idealized pressure) in the gas phase and f_j is its fugacity in the liquid phase. At moderate and low total pressures, the fugacity of the element in the gas phase is given by

$$f_j^o = N_j^o f_j^* \tag{3}$$

in which f_j^* is the fugacity of the gas at the total pressure of the mixture and therefore

$$\left(\frac{\delta \ell n f_j^o}{\delta N_j^o}\right)_{P,T} = \frac{1}{N_j^o} \tag{4}$$

The fugacity of the element in the liquid phase, according to Henry's law is given by

$$f_j = N_j k_j \tag{5}$$

in which k_j is the Henry's law constant at a given temperature and total pressure; hence

$$\left(\frac{\delta \ell n f_j}{\delta N_j}\right)_{P,T} = \frac{1}{N_j} \tag{6}$$

In an equilibrium process, the two changes in the partial molar free energies for the transfer of dn_j moles from the gas mixture to the liquid solution are equal. Equating Eqs. 1 and 2 and substituting the appropriate thermodynamic equivalents for the indicated partial differentials gives

$$\frac{\bar{V}_j^o}{RT}\,dP - \frac{\bar{L}_j^o}{RT^2}\,dT + d\ell n N_j^o = \frac{\bar{V}_j}{RT}\,dP - \frac{\bar{L}_j}{RT^2}\,dT + d\ell n N_j \tag{7}$$

in which $\bar{V}_j^o$ is the partial molar volume of element j in the gas mixture, $\bar{L}_j^o$ is its relative partial molar heat content in the gas mixture, $\bar{V}_j$ is its partial molar volume in the liquid solution, $\bar{L}_j$ is its relative partial molar heat content in the liquid solution, R is the molar gas constant, P is total pressure, and T is the temperature in ^oK. For dilute solutions,

$$\bar{L}_j^o - \bar{L}_j = \Delta H_v \tag{8}$$

where ΔH_v is the heat of vaporization of the condensing specie of element j. Actually, ΔH_v is the heat of the reaction for the vaporization of the gas from its form in solution. If it exists as a different compound in solution, the heat of formation of this compound is included in the value of ΔH_v. For an ideal solution, or one in which there is no heat of dilution or compound formation, ΔH_v is the actual heat of vaporization. Since $\bar{V}_j^o >> \bar{V}_j$, $(\bar{V}_j/RT)dP$ (or, $\delta \ell n f_j/\delta P$) can be neglected. For an ideal gas, f_j^o can be replaced by $N_j^o P$. Then

$$\left(\frac{\delta \ell n f_j^o}{\delta P}\right)_{T,N_j^o} = \frac{\bar{V}^o}{RT} = \frac{1}{P} \tag{9}$$

Substituting Eqs. 8 and 9 into Eq. 7 and integrating gives

$$N_j^o/N_j = \frac{k_j^1}{P} e^{-\Delta H_v/RT} \tag{10}$$

in which k_j^1 is an integration constant and where the term $k_j^1 e^{-\Delta H_v/RT}$ is identifiable via Eqs. 3 and 5 ($f_j^o = f_j = p_j$, the partial pressure of element j; and $f_j^* = P$) as the Henry's law constant. It may be noted from Eq. 10 that an increase in P results in a decrease in the ratio N_j^o/N_j or an increase in the mole fraction of the minor constituent j, in the liquid phase relative to its mole fraction in the gas phase. For early time condensations (high M.P. of carrier), when the temperature is high and the gas volume not fully expanded, the total pressure should be high; thus the effect of the pressure alone would tend to produce a more complete condensation at shorter times after detonation. However, the Henry's law constant also is larger at higher temperatures so that the two terms in Eq. 10 would decrease (or increase) simultaneously and the change in the ratio of the two mole fractions with time (or temperature) in the expanding gas volume will be less than for just the decrease in temperature.

2.1.3 Effect of Carrier Particle Size on Mole Fraction Ratio

A dependence of the ratio of the mole fractions on the size of the liquid drop, itself may exist because the dependence of the total pressure about each drop on drop-size.

This dependence is given by

$$RT\ell np/p_o = 4\gamma M/\rho d \qquad (11)$$

in which p_o is the vapor pressure of the carrier material over the liquid with a flat surface, p is the pressure over the drop of diameter, d, γ is the surface tension of the drop (assumed independent of T), M is the molecular weight of the carrier, and ρ is the density of the liquid. For Al_2O_3 at 2050°C and SiO_2 at 1800°C, the value of γ is 690 dynes/cm and 307 dynes/cm, respectively.[10] The value of the ratio, p/p_o, for these values of γ is not very different from unity for diameters larger than a few tenths of a micron. Hence, unless the carrier material has a surface tension larger than do these two oxides by more than two orders of magnitude, the increased vapor pressure of the carrier material over the larger drops should not be enough to result in larger values of N_j. If the surface tension were extremely large, the fission product elements most likely to be preferentially condensed on the smaller particles are those whose volatilities are the same or lower than that of the carrier itself. These would co-condense with the volatilized carrier molecules as soon as the temperature dropped to the carrier boiling point, since at this time the vapor pressure of the carrier material would be a large fraction of the total pressure. At the melting point of the carrier, its own vapor pressure would be so small a fraction of the total pressure that it could not influence the mole fraction ratio even if the surface tension were extremely large.

For particles with a fairly large range in sizes, the mole fraction, N_j, needs to be precisely defined. Carrier materials such as silicate soils containing metal oxides are refractory materials with low heat conductance. As mentioned above, a particle need not be completely melted throughout its volume in order to condense gaseous molecules. Only a liquid layer of film on its exterior is required for the process. Also, since the time spent in the liquid state is short, the condensates may not diffuse more than a short distance from the surface of the particle before it solidifies. Thus for particles of a given temperature history, a maximum size particle should exist that is completely melted before it resolidifies. Elements or nuclides that condense first (less volatile than the carrier) should penetrate somewhat farther into the completely melted particles than those that are more volatile and condense more rapidly just before the particle solidifies if the penetration depended only on diffusion.

The penetration of the condensates into the liquid drop and its rate of distribution throughout the volume would be more rapid if caused by turbulence and convection - especially in the peripheral regions of the liquid particles. The general uniformity of the

radioactive concentration in the silicate fallout particles indicate a process of distribution other than by diffusion. The resultant process appears to be one in which the condensates are deposited to a given depth from the surface of the very largest particles and in a more or less uniform concentration throughout the medium-size and smaller particles. The more volatile elements may form solutions with the larger surface concentration excesses if they are condensing in large amounts just as the particles are solidifying.

If the average depth of the surface layer is designated as h and is assumed to be the same for all particles, then the number of moles of carrier per particle (spherical) that was involved in forming the dilute solution (i.e. was melted during the formation process) is given by

$$n(\ell,p) = \frac{\pi \rho_h}{M}\left[d(d-2h) + (4/3)h^2\right], \quad d>2h \tag{12}$$

in which $n(\ell,p)$ is the number of moles of the carrier (that was melted) in the surface layer of the particle.

For dilute solutions, the mole fraction is

$$N_j = n_j(p)/n(\ell,p) \tag{13}$$

in which $n_j(p)$ is the number of moles of element j in the particle; the latter is then given by

$$n_j(p) = N_j \frac{\pi \rho h}{M}\left[d(d-2h) + (4/3)h^2\right], \quad d>2h \tag{14}$$

If $n_o(p)$ is taken as the total number of moles of the carrier in the particle, then

$$n_j(p)/n_o(p) = 6.00\, N_j h \frac{\left[d(d-2h) + (4/3)h^2\right]}{d^3}, \quad d>2h \tag{15}$$

$$n_j(p)/n_o(p) = N_j, \quad d\leq 2h \tag{16}$$

The mole fraction in Eq. 16 is for the particles that were completely melted. The ratio, $n_j(p)/n_o(p)N_j$, for Eqs. 15 and 16 is shown in Fig. 1 for several values of h. If the value of N_j for each fission product is the same for all sizes via Eq. 10 and discussion of Eq. 11,

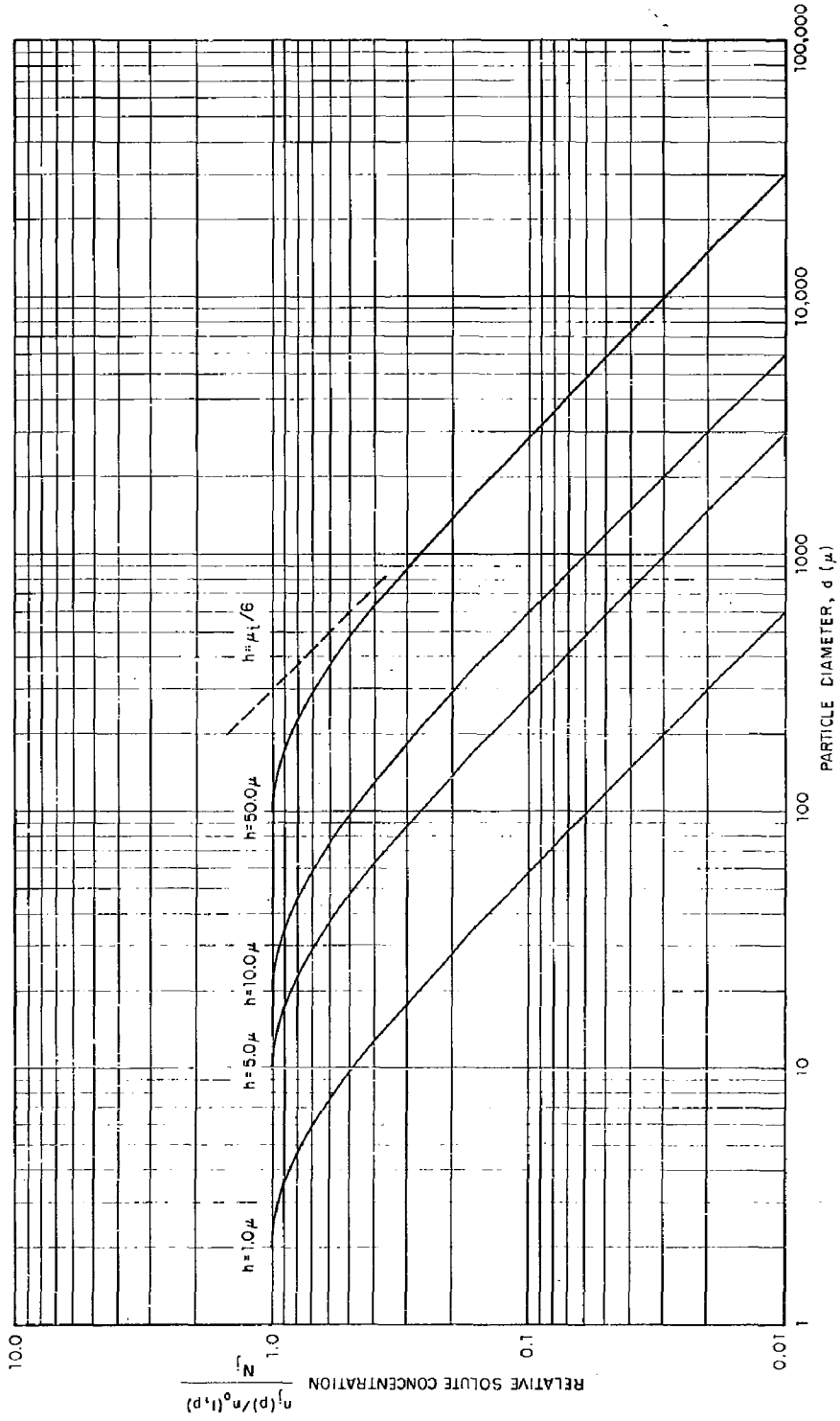

Fig. 1 Variation of $[n_j(p)/n_o(\ell,p)]/n_j$ With Particle Size for Several Values of the Surface Layer Thickness

then the gross average concentration of fission products per unit mass of particles should be a multiple of a curve similar to those in Fig. 1 for some value of h. The value of h could be determined from an experimentally determined curve by extending the straight line portions of the curve with logarithmic slopes of 0 and -1 to their intercept at a size, μ_i, which is 6 times the value of h.

The case for a non-uniform concentration in the surface layer or throughout the particle was not treated for presentation in this report. Its consideration requires estimates of the gaseous diffusion rates for condensation at the particle surface as well as estimates of subsequent mixing rates of the condensates in the liquid layer of the particle. Such estimates may be required for a more complete treatment of the condensation process.

There are two additional factors that could have some bearing on the relative amount of an element condensing into the liquid particles. The larger particles may either fall out of the gaseous volume before they solidify or may be melted only on one side (not sufficiently melted to form a spherical particle). Both of these two groups of particles would condense smaller amounts of all elements per particle than would be estimated from Eq. 15 and also would be most deficient in the more volatile elements.

The origins of the melted particles in the fireball may be several in number. The small vapor-condensed particles originating from vaporized soil have been mentioned. Some of the fallout particles are particles that were originally lying on the ground out to some distance from shot point. Some of these probably are melted by the heat absorbed from the radiant energy emitted at detonation. These particles are then drawn into the fireball as it rises. This mechanism probably is the dominant one for low air bursts where a small crater is formed. In this case the size distribution of the fallout particles that are produced should be the same as the original size distribution of the surface soil. In the detonation, the blast wave would powder the soil to some depth and the resulting dust particles, like the surface-melted particles, would retain their sizes in the formation process. However, these particles would not be melted until after they enter the fireball.

For surface detonations, a layer of soil may be melted in the process of crater formation. It would seem reasonable that a liquid layer of soil would intervene between the vapor in the fireball and a layer of shock-powdered earth as long as the fireball remained in contact with the earth's surface. If enough "fluxing" material such as the carbonates are present, a rather large amount of fluid material could be formed. As the fireball lifts, the liquid would break up

into drops and enter the fireball, followed by the powdered soil. The mechanical break-up of the fluid mass should produce about the same size distribution of particles from liquids that have about the same surface tension. If most of the fallout particles originate from the bulk liquid layer, then the particle size distributions in the fireball from detonations on different soils would be more nearly alike than if most of them originate from the surface soils and the shock-powdered dust from the crater.

There is no unique method, then, of selecting a size distribution for the liquid particles present in the fireball up to the time they solidify. But since Eqs. 12 through 16 will not lead to a variation in the relative amount condensed in the particles for different elements because of size, it is convenient to consider all the melted particles as one bulk liquid phase in a volume of space and designate the distribution in general terms only as

$$n(\ell) = \sum_{i=1}^{i=m} J_i n_i(\ell, p) \tag{17}$$

where $n(\ell)$ is the total moles of liquid carrier in the volume V at any time, J_i is the number of particles of size i, and $n_i(\ell,p)$ is the same as $n(\ell,p)$ for the size i. With Eq. 17, the mole fraction of element j in the liquid phase is

$$N_j = n_j/n(\ell) \tag{18}$$

where n_j is the number of moles of element j dissolved in the $n(\ell)$ moles of liquid carrier. The mole fraction of element j in the vapor phase is given by

$$N_j^o = n_j^o/n \tag{19}$$

where n_j^o is the number of moles of element j mixed with n moles of vapor. If the perfect gas law is used for n, Eq. 19 becomes

$$N_j^o = \frac{n_j^o RT}{PV} \tag{20}$$

Substitution of Eqs. 18 and 20 into Eq. 10 gives

$$N_j^o = \frac{n_j k_j}{(n(\ell)/V)RT} \tag{21}$$

where k_j is the Henry's law constant. It may be noted that the ratio, n_j^o/n_j, depends on k_j, T, and the number of moles of liquid carrier per unit volume in the fireball. Since the mole fractions are small, the n_j^o/n_j ratio is independent of the total amount of the element present. Thus the same fraction of the element is condensed for a 100 % fission weapon as for a "clean" thermonuclear weapon of the same total yield. The value of $n(\ell)/V$ depends only on the total yield (see Section 4).

2.1.4 The Material Balance and "R" Factor Equations

Since the elements considered are radioactive, the number of moles of each is constantly changing; therefore the material balance of a given element also changes with time. On the other hand, the fission yield of a given mass chain (except for neutron emitters) is constant. If the amount of a radionuclide of element j and mass number A present at the time, t, after fission is given by $y_{jA}(t)$, then the total amount of element j present at time t is

$$Y_j(t) = \sum_A y_{jA}(t) \text{ atoms or moles} \tag{22}$$

The corresponding sum for the chain yield of mass number A is

$$Y_A = \sum_j y_{jA}(t) \text{ atoms or moles} \tag{23}$$

in which Y_A is constant except for the mass chains containing neutron emitters. The material balance for element j between gas and liquid phases is

$$Y_j(t) = n_j^o(t) + n_j(t) \tag{24}$$

where the time dependence of n_j^o and n_j of Eq. 21 is indicated. If n_{jA}^o and n_{jA} are taken for the amounts of each nuclide in the gas and liquid phases, respectively, the material balance for each element is

$$\sum_A y_{jA}(t) = \sum_A n_{jA}^o(t) + \sum_A n_{jA}(t) \tag{25}$$

If k_j^o is used for $k_j/[(n(\ell)/V)RT]$, substitution of Eq. 21 in Eq. 25 (Eq. 21 holds for all nuclides of element j) gives

$$\sum_A y_{jA}(t) = (1+k_j^o) \sum_A n_{jA}(t) \tag{26}$$

and since $(1+k_j^o)$ is the multiplier for each of the $n_{jA}(t)$ terms, the terms for each nuclide can be separated out. The separated terms give the amount of each nuclide condensed, which is

$$n_{jA}(t) = \frac{y_{jA}(t)}{1+k_j^o} \tag{27}$$

The fraction of the mass chain condensed, $r_o(A,t)$, is defined by

$$r_o(A,t) = \frac{1}{Y_A} \sum_j n_{jA}(t) \tag{28}$$

Substitution of Eq. 27 and replacing the $y_{jA}(t)/Y_A$ ratios by $y_j(A,t)$ in Eq. 28 gives

$$r_o(A,t) = \sum_j \frac{y_j(A,t)}{1+k_j^o} \tag{29}$$

in which $y_j(A,t)$ is the fraction of the chain yield of element j with mass number A. According to Eq. 29, the fraction of the chain condensed in the liquid phase depends only on k_j^o and the fractions of the chain yield of the elements present. The use of Eq. 29 therefore requires values of the independent yields of each member element of the chain at times from a few seconds after fission, or, at least for the time of the end of the first period of condensation.

The experimental radiochemical "R" factor for a given sample or quantity of mixed fission products is usually defined as the ratio of the number of atoms of a given mass present to the number of atoms of mass number 99 present, divided by the expected value of their ratio for thermal neutron fission of U^{235}. In mathematical notation, this is

$$R^{99}(A) = \frac{n(A)}{K_o(A)\, n(99)} \tag{30}$$

Ordinarily, count-rate ratios are used along with the appropriate decay corrections from the time of analysis to zero time with a corresponding value of $K_o(A)$ that has been previously determined from an analysis of a sample of U^{235} bombarded with thermal neutrons. For analyses made more than several days after fission, only the last or last two members of a decay chain of most mass numbers will be present in appreciable amount. Since, as mentioned in the introduction, the observed "R" factors give an overall measure of variation from U^{235} thermal fission, another factor is needed to account only for that part due to the first period of the condensation process. For this, let

$$r(A) = \frac{n(A)}{K(A)\ n(99)} \tag{31}$$

in which K(A) is the true yield ratio, Y_A/Y_{99}, of mass number A to 99, which varies with the kind of fissioning nuclide and incident neutron spectrum (the same definition holds if some mass number other than 99 is selected as the reference nuclide). The value of the ratio, n(A)/n(99), should be the same as the ratio of the sum over j of the respective $n_{jA}(t)$ terms. Making the substitution in Eq. 31 gives

$$r(A) = \frac{\sum_j n_{jA}(t)}{K(A)\sum_j n_{j99}(t)} \tag{32}$$

or, with Eq. 27,

$$r(A) = \frac{1}{K(A)} \frac{\sum_j y_{jA}(t)/(1+k_j^o)}{\sum_j y_{j99}(t)/(1+k_j^o)} \tag{33}$$

and finally, replacing K(A) with Y_A/Y_{99}, gives

$$r(A) = \frac{\sum_j y_j(A,t)/(1+k_j^o)}{\sum_j y_j(99,t)/(1+k_j^o)} \tag{34}$$

Thus r(A) is equal to $r_o(A,t)/r_o(99,t)$ of the theory and equal to $K_o(A)R^{99}(A)/K(A)$ for experimentally determined "R" factors.

2.1.5 Condensation by Compound Formation With Carrier Material

Compound formation of an element with the carrier in the gas phase, followed by condensation of the heavier gas molecule into a liquid solution with the melted carrier material, would be described by use of Henry's law for the dilute solution. However when the compound is formed with the (bulk) liquid carrier, then the free energy of formation of the compound and its vaporization and that of the carrier is involved. The overall reaction for a direct combination of fission product element A with carrier material B to form the compound AB may be written as follows:

$$A(g) + B(\ell) \rightarrow AB(\ell), \text{ dilute solution in } B(\ell) \qquad (35)$$

This reaction may be written as a sum of three or four separate reactions depending on whether the combination of A and B occurs as A condenses or with B in the vapor phase prior to condensation. There should be no difference in the two processes with regard to the total change in free energy between the same initial and final states. The difference, if any, would be in the kinetics of the process. In the first process, the separate reactions and the standard free energy changes are:

1. $$A(g) \rightarrow A(\ell) \qquad (36a)$$

$$\Delta F_1^o = RT\, \ell n\, p_A \qquad (36b)$$

2. $$A(\ell) + B(\ell) \rightarrow AB(\ell) \qquad (37a)$$

$$\Delta F_2^o = -RT\, \ell n\, K_{AB} \qquad (37b)$$

where K_{AB} is the equilibrium constant for the formation of $AB(\ell)$ from $A(\ell)$ and $B(\ell)$ at the temperature, T.

3. $$AB(\ell) \rightarrow AB(\ell), \text{ dilute solution in } B(\ell) \qquad (38a)$$

$$\Delta F_3^o = -RT\, \ell n\, a_{AB} \qquad (38b)$$

where a_{AB} is the thermodynamic activity of AB(ℓ) in B(ℓ) and is equal to $N_{AB}\ k_{AB}$ if N_{AB} is the mole fraction and k_{AB} is the Henry's law constant. The sum of the standard free energy changes for the three reactions, or, the free energy of the reaction given by Eq. 35, is

$$\Delta F^{o} = RT \ell n \frac{p_A}{N_{AB}\ k_{AB}\ K_{AB}} \tag{39}$$

In the second process, the separate reactions and the standard free energy changes are:

1. $A(g) + B(g) = AB(g)$ (40a)

$$\Delta F_1^{o} = -RT \ell n \frac{p_{AB}}{p_A p_B} \tag{40b}$$

2. $B(\ell) \longrightarrow B(g)$ (41a)

$$\Delta F^{o} = -RT \ell n\ p_B \tag{41b}$$

3. $AB(g) \longrightarrow AB(\ell)$ (42a)

$$\Delta F^{o} = RT \ell n\ p_{AB} \tag{42b}$$

4. $AB(\ell) \longrightarrow AB(\ell)$, dilute solution in $B(\ell)$ (43a)

$$\Delta F^{o} = -RT \ell n\ N_{AB}\ k_{AB} \tag{43b}$$

The sum of the standard free energy changes for these reactions is

$$\Delta F^{o} = RT \ell n \frac{p_A}{N_{AB}\ k_{AB}} \tag{44}$$

The free energy changes given by Eqs. 39 and 44 would be equal if $p_A/N_{AB}\ K_{AB}$ of Eq. 39 is equal to p_A/N_{AB} of Eq. 44, or if K_{AB} is unity. If the perfect gas law is used to estimate the number of moles of A, n_A, in the gas volume from p_A in Eqs. 39 or 44 and replacing N_{AB} by $n_{AB}/n(\ell)$, the two equations become

$$n_A = \frac{n_A\, k_{AB}\, K_{AB}\, e^{\Delta F^\circ/RT}}{(n(\ell)/V)\, RT} \qquad (45)$$

and

$$n_A = \frac{n_A\, k_{AB}\, e^{\Delta F^\circ/RT}}{(n(\ell)/V)\, RT} \qquad (46)$$

respectively. Replacing either $k_{AB}\, K_{AB}\, e^{\Delta F^\circ/RT}$ (Eq. 45) or $k_{AB}\, e^{\Delta F^\circ/RT}$ (Eq. 46) by k'_{AB} reduces the two equations to the same form as Eq. 21. The same summation formulae following Eq. 21 for the material balances would therefore apply except that the standard free energy functions, if available, could be used to calculate the free energy change for the reaction given by Eq. 35 or for those of the various separate reactions.

The reaction described by Eq. 35 did not include any reaction between the atmospheric oxygen and the element A in the condensation process. Of course, even in the presence of oxygen many of the fission product oxides are partially or completely dissociated in the vapor phase. For those that are completely dissociated at the temperatures where the carrier material exists as a liquid, the reaction described by Eq. 35 is applicable. Also, if the oxides are completely associated, A(g) may be taken to represent the oxide molecule, and the reaction of Eq. 35 can be applied. However, for the elements in which the oxide molecule is partially dissociated in the vapor state and associates further with oxygen in the condensed state, the oxygen partial pressure will influence the relative amounts of the element in each state.

The overall reaction for this condensation process is

$$A(g) + xO_2(g) + B(\ell) \longrightarrow AO_{2x}\, B(\ell), \text{ dilute solution in } B(\ell) \qquad (47)$$

in which x is the number of oxygen molecules that combine with each atom of element A. Separate reactions for this overall reaction can be set up in the same way as for Eq. 35. For the reaction of Eq. 47 to be different from Eq. 35 (or competing with it), the gas atoms of A and O_2 must be in equilibrium with the oxide of element A in the vapor state. The oxide molecules then either react with $B(\ell)$ as they condense or react with B(g) in the vapor and then the larger

molecules condense to form the dilute solution. In the first process, the separate reactions and the standard free energy changes are:

$$1.\quad A(g) + xO_2(g) \longrightarrow AO_{2x}(g) \tag{48a}$$

$$\Delta F^\circ = RT\,\ell n\, p_{AO}/p_A p_O^x \tag{48b}$$

$$2.\quad AO_{2x}(g) \longrightarrow AO_{2x}(\ell) \tag{49a}$$

$$\Delta F^\circ = RT\,\ell n\, p_{AO} \tag{49b}$$

$$3.\quad AO_{2x}(\ell) + B(\ell) \longrightarrow AO_{2x}\,B(\ell) \tag{50a}$$

$$\Delta F^\circ = -RT\,\ell n\, K_{AOB} \tag{50b}$$

where K_{AOB} is the equilibrium constant for the formation of $AO_{2x}\,B(\ell)$ from the two liquid compounds at the temperature, T.

$$4.\quad AO_{2x}\,B(\ell) \longrightarrow AO_{2x}\,B(\ell),\ \text{dilute solution in } B(\ell) \tag{51a}$$

$$\Delta F^\circ = RT\,\ell n\, N_{AOB}\, k_{AOB} \tag{51b}$$

The sum of these reactions and standard free energy changes give, for Eq. 47,

$$\Delta F^\circ = RT\,\ell n\, \frac{p_A p_O^x}{N_{AOB}\, k_{AOB}\, K_{AOB}} \tag{52}$$

In the second process, the separate reactions and standard free energy changes are:

$$1.\quad A(g) + xO_2(g) \longrightarrow AO_{2x}(g) \tag{53a}$$

$$\Delta F^\circ = -RT\,\ell n\, p_{AO}/p_A p_O^x \tag{53b}$$

2. $AO_{2x}(g) + B(g) \longrightarrow AO_{2x}\ B(g)$ (54a)

$$\Delta F^{\circ} = -RT\,\ell n\ p_{AOB}/p_{AO}p_{B} \quad (54b)$$

3. $B(\ell) \longrightarrow B(g)$ (55a)

$$\Delta F^{\circ} = -RT\,\ell n\ p_{B} \quad (55b)$$

4. $AO_{2x}\ B(g) \longrightarrow AO_{2x}\ B(\ell)$ (56a)

$$\Delta F^{\circ} = RT\,\ell n\ p_{AOB} \quad (56b)$$

5. $AO_{2x}\ B(\ell) \longrightarrow AO_{2x}\ B(\ell)$, dilute solution in $B(\ell)$ (57a)

$$\Delta F^{\circ} = -RT\,\ell n\ N_{AOB}\ k_{AOB} \quad (57b)$$

The sum of the five standard free energy changes for Eq. 47 is

$$\Delta F^{\circ} = RT\,\ell n\ \frac{p_A p_O^x}{N_{AOB}\ k_{AOB}} \quad (58)$$

Equations 52 and 58, when solved for n_A by use of the perfect gas law give

$$n_A = \frac{n_{AOB}\ k_{AOB}\ K_{AOB}\ e^{\Delta F^{\circ}/RT}}{(n(\ell)/V)\ RT\ p_O^x} \quad (59)$$

and

$$n_A = \frac{n_{AOB}\ k_{AOB}\ e^{\Delta F^{\circ}/RT}}{(n(\ell)/V)\ RT\ p_O^x} \quad (60)$$

respectively. The values of n_A in Eqs. 59 and 60 are sensitive to the oxygen partial pressure. If p_O is greater than 1 atmosphere, the value of n_A will be decreased (most with largest x value) and the amount of element A condensed is increased. If p_O is less than 1 atmosphere, the value of n_A will be increased (most with largest x value) and the amount of element A condensed is decreased. If

p_0^x is incorporated into the k^o_{AOB} in the same way as was done for the factors of Eqs. 45 and 46, then Eqs. 59 and 60 can also be reduced to the same form as Eq. 21 for material balance and other general summation formulae.

Equations 35 to 60 are perhaps more rigorous in the definition of the condensation process than those of Sections 2.2 and 2.3 that describe the process only in terms of Henry's law. In a real case, the carrier material is not an inert substance but capable of forming compounds with many of the fission product elements. Also, the above equations will be applicable for elements that react with the carrier in the solid state (see Section 2.6); for these, the notations only need be changed from (ℓ) to (s) to refer to the solid rather than the liquid state.

2.2 THE SECOND PERIOD OF CONDENSATION

2.2.1 Description of the Formation Process

In the second period of condensation, the carrier material is in the solid state and the condensation of the remaining radioelements can only occur on the surface of the carrier particles. The latter can consist of unmelted particles and the smaller particles that had been melted but have not fallen out of the cooling fireball. Although this period of condensation may continue indefinitely with the exchange of rare gas elements that are formed by decay or that decay into alkali metal daughter elements, it should be essentially complete with respect to most of the radioactive elements between 5 and 7 minutes after detonation. For a given group of particles, it should be complete when they fall away from the volume containing the radioactive gases.

Of the elements that condense, or adsorb, on the surface of the larger particles, some consist of decay products of the more volatile elements (present at the end of the first period of condensation) and would tend to be soluble in rain water and salt solutions. Others, consisting of the more reactive elements, may form compounds with the solid carrier and even diffuse into the interior of the particles. In either case, the elements condensing during this period would be more available for solution than those condensed into the liquid phase.

Since a surface condensation is indicated for this process, the effective specific activity (i.e. activity/gram) carried by various particle sizes should be inversely proportional to the

particle "diameter". In a sample of fallout containing particles from both types of condensates, the measured specific activity would not correspond to any of the curves of Fig. 1; the flat portion of the curve(s) indicated for the smaller particles would instead show an increase in the value of $n_j(p)/N_j n_o(\ell,p)$ as the particle diameter decreased.

2.2.2 Condensation Mathematics

The mathematical equations for describing the processes that can occur in this period of condensation have not been fully developed. Completion of the current work by C.E. Adams[11] should aid the treatment. However, tentative treatment of two rather simplified types of interactions allow approximate formulae to be given. For the less volatile elements and a large amount of available surface, the simplified form of Langmuir's adsorption isotherm (low partial pressures) is given, in the terms used previously, by

$$n_j' = a_j(s) n_j^o \tag{61}$$

in which n_j' is the amount of element adsorbed, $a_j(s)$ is a constant including the surface area, and n_j^o is proportional to the partial pressure of the element j. The value of the constant, $a_j(s)$, would presumably depend on the kind of gas molecule that is adsorbed. If n_j^o is to be the same as that given by Eq. 21 for the amount of element j remaining at the end of the first period of condensation, then the adsorption reaction described by Eq. 61 must occur within a very short time. Otherwise its value must be adjusted to account for decay. This adjustment would not be required if all the elements in the chain are adsorbed and remain so. For a short-time condensation, n_j^o may be replaced by $k_j^o n_j$ and the "R" factor for this condensation process can be written as

$$r'(A) = \frac{\sum_j a_j(s)\, k_j^o\, y_j(A,t)/(1+k_j^o)}{\sum_j a_j(s)\, k_j^o\, y_j(99,t)/(1+k_j^o)} \tag{62}$$

If $a_j(s)$ is the same for all elements, Eq. 62 reduces to

$$r'(A) = \frac{\sum_j k_j^o\, y_j(A,t)/(1+k_j^o)}{\sum_j k_j^o\, y_j(99,t)/(1+k_j^o)} \tag{63}$$

Although the sum of the numerators and denominators in Eqs. 34 and 63 will both be equal to 1, the sum of r(A) and r'(A) will not equal 1 (unless one is zero).

Another, and probably more realistic, process is to consider the adsorption condensation as one in which the relative amount of each element condensed is related to its sublimation pressure (as if the solid carrier would act as pure compound of each of the condensing species). The computational values from such a process will reflect the relative volatility of constituent molecules at all temperatures at which this kind of condensation can occur. If an excess of solid surface area is present, the amount condensed by the process (assuming it to be reversible) at any time after solidification of the carrier is given by

$$n'_j = n^o_j - n^{oo}_j \tag{64}$$

in which n'_j is the amount of element j condensed on the surface of the solid particles, n^o_j is the amount of the element that had not condensed in the liquid carrier, and n^{oo}_j is the amount in the vapor phase. All three quantities depend on the time after solidification because of decay. For a perfect gas

$$n^{oo}_j = \frac{p^s_j V}{RT} \tag{65}$$

in which V is the volume containing the n^{oo}_j moles of the gaseous species and p^s_j is the sublimation pressure and is given by

$$p^s_j = e^{\Delta S_s/R}\ e^{-\Delta H_s/RT} \tag{66}$$

in which ΔS_s is the entropy of sublimation and ΔH_s is the heat of sublimation at the temperature, T. If uniform mixing in the fireball volume is assumed for the particles and gaseous species, then V is the fireball volume. The material balance for element j (all time-dependent) is

$$Y_j = n_j + n'_j + n^{oo}_j \tag{67}$$

so that, Eq. 64, with Eqs. 21, 65, and 67, becomes

$$n'_j = \frac{k_j^o y_j}{1 + k_j^o} - \frac{V p_j^s}{RT} \tag{68}$$

or

$$\sum_A n'_{jA} = \frac{k_j^o}{1 + k_j^o} \sum_A y_{jA} - \frac{V}{RT} \sum_A p_{jA}^s \tag{69}$$

Separating out the equal terms for each nuclide gives

$$n'_{jA} = \frac{k_j^o y_{jA}}{1 + k_j^o} - \frac{V p_{jA}^s}{RT} \tag{70}$$

The "R" factor for this process is now

$$r'(A) = \frac{\sum_j y_j(A,A) k_j^o/(1+k_j^o) - (V/RT)\sum_j p_j^s(A,t)}{\sum_j y_j(99,t) k_j^o/(1+k_j^o) - (V/RT)\sum_j p_j^s(99,t)} \tag{71}$$

in which $p_j^s(A,t)$ is equal to p_{jA}^s/Y_A and Y_A is the total chain yield. For elements with very low sublimation pressures, Eq. 71 reduces to Eq. 63. For chains with very volatile elements, r'(A) could approach zero.

2.3 SUMMARY OF FALLOUT PARTICLE FORMATION PROCESS

A general description of the over-all fallout particle formation process, from the foregoing treatment, is as follows. The larger particles that fall out of the fireball earliest and land near ground zero should contain radioelements that were condensed during the liquid phase and very little, if any, radioelements that were condensed during the second period of condensation. The smaller particles that enter late and stay in the rising fireball and cloud for longer times should carry radioelements that were condensed on their surfaces. The smallest of these particles would make up the world-wide fallout

and the others are deposited at large distances from ground zero.* The intermediate size particles that deposit at intermediate distances from ground zero should contain radioelements that were condensed during both periods of condensation. It is reasonable to assume that individual particles at these locations could contain condensates from either or both types of condensation. In a radiochemical determination of an "R" factor for a given mass chain from a gross sample of the fallout in which a given fraction of a mass chain had condensed during the first period of condensation and the remainder during the second period, the expected "R" factor would be given by

$$R(A) = \frac{1}{K(A)} \frac{\left[(1-x)\sum_j n_{jA} + x\sum_j n'_{jA}\right]}{\left[(1-x)\sum_j n_{j99} + x\sum_j n_{jA}\right]} \tag{72}$$

in which x is the fraction of element j condensed during the second period of condensation. Substitution of the appropriate equalities in Eq. 72 gives

$$R(A) = \frac{\sum_j y_j(A,t)/(1+k_j^o) - x\left[\sum_j y_j(A,t)(1-k_j^o)/(1+k_j^o) + (V/RT)\sum_j p_j^s(A,t)\right]}{\sum_j y_j(99,t)/(1+k_j^o) - x\left[\sum_j y_j(99,t)(1-k_j^o)/(1+k_j^o) + (V/RT)\sum_j p_j^s(99,t)\right]} \tag{73}$$

The variation of x from 0 to 1 corresponds respectively to the close-in and world-wide (or far distant) fallout compositions discussed above.

In all the condensation processes, no variation of fractionation with particle size (for sizes larger than a few tenths of a micron) was indicated. Any variation in the amounts condensed to give a variation in fractionation with particle size would be caused by a combination of time of particle fall from the gas volume and the value of x. It is possible that some amount of the larger particles would fall out of the gas volume or move through it like projectiles at

*The present world-wide fallout from air, seawater, tower, and surface bursts also contains a large fraction of vapor-condensed particles with the activity more or less uniformly distributed through their volumes.

temperatures (and times) between the boiling and melting point of the carrier. The description of this computationally as a continuous process via Eq. 73, for example, would be to initiate the calculations for the phase of condensation at the boiling point of the carrier (with $\dot{x} = 0$ until the melting point is reached) and continue the process up to the time of 6 or 7 minutes after detonation. Such a process should give, in relative terms, the overall variation of fractionation with size and downwind distance from ground zero.

SECTION 3

THE VAPOR PRESSURE OF SOME OXIDES, COMPOUNDS, AND ELEMENTS OF FISSION PRODUCTS AND OTHER SUBSTANCES

If the Henry's law constants for all the radionuclides and a silicate soil material (as the carrier) were known, the condensation and/or fractionation "R" factors of Section 2 could be calculated, also provided some estimate of the term $(n(\ell)/V)RT$ could be made. The necessary data has not yet been measured. Estimates of the Henry's law constants can be made, however, if appropriate properties are assumed for the carrier material and the gaseous fission products. For such calculations, presented in Sections 4 and 7, the following properties were stipulated: (1) the gaseous species of each fission product element (with a few exceptions) was the same as that in equilibrium with its own liquid (or solid) oxide in the presence of oxygen; (2) the liquid mixture formed a perfect (ideal) solution; (3) the carrier material was non-reactive so that no compound formation was involved (alternately, if a compound was formed its vapor pressure was the same as the oxide); and (4) the melting point of the carrier was taken to be 1400°C.

For the formation of one mole of gas from either the liquid (vaporization) or solid (sublimation), the standard free energy is given by

$$\Delta F^\circ = \Delta H^\circ - T\Delta S^\circ \qquad (74)$$

in which ΔH° is the difference in heat content of the gas and the liquid or solid, and ΔS° is the change in entropy. Also,

$$\Delta F^\circ = -RT\ell nK = -RT\ell np \qquad (75)$$

in which p is the vapor pressure of the gas in contact with the liquid or solid and K is the equilibrium constant for the vaporization or sublimation process. Combining Eqs. 57 and 58 gives

$$\log p = -\frac{A}{T} + B \tag{76}$$

in which

$$A = \frac{\Delta H^\circ}{4.576} \tag{77}$$

and

$$B = \frac{\Delta S^\circ}{4.576} \tag{78}$$

The notation A_v, B_v will be used for vaporization and A_s, B_s for sublimation. In general, both ΔH° and ΔS° vary with temperature so that A and B are not actually constants. They were considered constant here however and evaluated from the data at the boiling point (p = 1 atmos) and the temperature at which the total vapor pressure is 10^{-3} atmos. For the oxides that decompose on vaporization or sublimation, the constants were then adjusted to a constant oxygen pressure of 1 atmos. For example, sodium oxide decomposes to Na(g) and O_2(g) as follows:

$$2\ Na_2O \rightleftharpoons 4Na(g) + O_2(g) \tag{79}$$

For this reaction,

$$p = p(Na) + p(O_2) \tag{80}$$

and

$$p(Na) = 4p(O_2) \tag{81}$$

so that

$$p = 5p(O_2) \tag{82}$$

Also,

$$K = p^4(Na)\ p(O_2) = p_1^4(1) \tag{83}$$

where p_1 is the sodium vapor pressure when the oxygen pressure is 1 atmosphere. Combining the above equations gives

$$\log p_1 = \log 4 - (5/4) \log 5 + (5/4) \log p \tag{84}$$

or,

$$\log p_1 = - 0.272 - 1.25A'/T + 1.25B' \tag{85}$$

For oxygen pressures other than 1 atmos., p(Na) can be determined from the ratio $p_1/p^{1/4}(O_2)$. The constants for Eqs. 76, via equations similar to Eq. 85, and the various vaporization and sublimation reactions and melting points for the oxides or other assumed gaseous species are summarized in Table 1. Some values of the entropies of vaporization and sublimation and even of the melting points and boiling points were obtained from correlations or were otherwise estimated. Most of the data, however, should give values fairly close to the true pressures between 10^{-3} and 1 atmos., as well as for pressure of several atmospheres for temperatures higher than the boiling points. For most mass chains in the condensation process, this range of vapor pressure is the most critical one if the melting point of the carrier material falls within the corresponding temperature range. If the vapor pressure of the element or its oxide is either very low or very high at the carrier melting point temperature, the fraction condensed will be essentially one or zero, respectively; the exact value of the pressure is then not required.

For a perfect solution, the relation between the vapor pressure of the solute and its mole fraction is given by Raoult's law which, in terms of the notation given here, is

$$p_j = N_j p_o \tag{86}$$

where p_o is the vapor pressure of the pure compound and, for a perfect solution, is the same as k_j for Henry's law. No estimate can be given for the magnitude of the deviations that might be expected from perfect solution behavior in the dilute solutions at high temperatures in the silicate systems of all of the fission product

TABLE 1

Vapor Pressure Data for the Oxides of Fission Products and Other Elements
Constants for $\log p_1 = (A/T) + B$

Oxide	Reaction	M.P. (°K)	A_v	B_v	A_s	B_s	p_j
Na_2O	$2M_2O \rightarrow 4M(g) + O_2(g)$	1193	14,320	6.75	16,060	8.21	$p_1/p^{1/4}(O_2)$
K_2O		(975)[a]	12,600	6.93	14,000	8.38	
Rb_2O		(855)	13,190	7.97	14,440	9.42	
Ca_2O		763	11,250	7.23	12,360	8.68	
MgO	$MO \rightarrow MO(g)$	3075	21,830	6.51	29,090	8.87	p_1
CaO		2860	24,750	6.51	31,520	8.87	
SrO		2730	20,450	5.84	26,890	8.20	
BaO		2196	20,980	6.99	26,180	9.35	
CdO	$2MO \rightarrow 2M(g) + O_2(g)$	d1750[b]	16,460	8.98	19,110	10.50	$p_1/p^{1/2}(O_2)$
FeO		1644	31,980	8.98	24,500	10.50	
Fe_3O_4	$M_3O_4 \rightarrow 3M(g) + 2O_2$	1870	84,350	40.44	96,350	46.85	$p_1/p^{2/3}(O_2)$
Y_2O_3	$2MO_3 \rightarrow 4MO(g) + O_2(g)$	2690	40,500	8.61	56,600	15.33	$p_1/p^{1/4}(O_2)$
La_2O_3		2590	39,700	(8.61)	50,400	(15.33)	
Pr_2O_3		(2420)	38,900	(8.61)	48,800	(15.33)	
Nd_2O_3		(2380)	38,500	(8.61)	48,300	(15.33)	
Pm_2O_3		(2300)	37,500	(8.61)	47,000	(15.33)	
Al_2O_3	$M_2O_3 \rightarrow M_2O(g) + O_2(g)$	2300	58,800	14.868	73,900	21.25	$p_1/p(O_2)$
Ga_2O_3		1998	44,300	(14.87)	57,400	(21.25)	
In_2O_3		1560	31,600	(14.87)	41,800	(21.25)	
As_2O_3	$2M_2O_3 \rightarrow 4MO(g) + O_2(g)$, $T > 1400°K$	588	8,700	8.61	-	-	
As_2O_3	$2M_2O_3 \rightarrow M_4O_6(g)$	588	3,670	5.01	5,400	7.96	p_1
Sb_2O_3	$2M_2O_3 \rightarrow 4MO(g) + O_2(g)$, $T > 2000°K$	928	16,400	8.61	-	-	
Sb_2O_3	$2M_2O_3 \rightarrow M_4O_6(g)$	928	9,170	5.01	11,900	7.96	
Cu	$M \rightarrow M(g)$	1356	24,400	9.45	-	-	p_1
Pd		1823	19,600	5.70	20,670	6.29	
Ag		1234	13,340	5.44	-	-	
ZrO_2	$MO_2 \rightarrow MO_2(g)$	2960	32,360	6.73	36,950	8.28	
CeO_2		(3000)	29,500	(6.77)	34,200	(8.33)	
UO_2		2680	26,500	(6.77)	30,700	(8.33)	
U_3O_8	$2M_3O_8 + O_2(g) \rightarrow 6MO_3(g)$	(2450)	11,030	3.55	19,600	7.05	$p_1 p^{1/6}(O_2)$
SiO_2	$2MO_2 \rightarrow 2MO(g) + O_2(g)$	(2040)	39,250	12.55	39,700	12.79	$p/p^{1/2}(O_2)$
GeO_2		1389	20,900	11.85	22,730	13.15	
SnO_2		1898	26,750	11.91	29,230	13.22	
RuO_2	$M + O_2(g) \rightarrow MO_2(g)$	2700	5,330	0.52	6,670	1.02	$p_1 p(O_2)$
RhO_2		2240	10,300	0.84	11,670	0.95	
Ru	$M \rightarrow M(g)$	2700	32,500	7.22	33,700	7.67	p_1
Rh		2240	27,300	6.58	28,400	7.00	
SeO_2	$2MO_2 \rightarrow 2MO(g) + O_2(g)$, $T > 1500°K$	613	13,060	12.74	14,030	14.29	$p/p^{1/2}(O_2)$
SeO_2	$MO_2 \rightarrow MO_2(g)$	613	3,970	6.78	4,920	8.33	p_1
TeO_2	$2MO_2 \rightarrow 2MO(g) + O_2(g)$, $T > 1800°K$	1006	18,500	11.35	19,850	12.68	$p/p^{1/2}(O_2)$
TeO_2	$MO_2 \rightarrow MO_2(g)$	1006	11,300	7.37	12,000	8.07	p_1
Nb_2O_5	$M_2O_5 \rightarrow M_2O_5(g)$	1785	22,300	6.75	27,700	9.77	
MoO_3	$3MO_3 \rightarrow M_3O_9(g)$; $T < 1575$	1068	7,620	5.64	17,430	14.82	
MoO_3	$MO_3 \rightarrow MO_3(g)$	1068	10,200	6.66	13,590	9.73	
Tc_2O_7	$M_2O_7 \rightarrow M_2O_7(g)$	392	3,570	6.12	7,205	15.40	
NaBr	$MX \rightarrow MX(g)$	1028	8,830	5.30	-	-	
NaI		924	8,800	5.58	-	-	
Kr	$X \rightarrow X(g)$		485	4.04			
Xe			524	4.00	-	-	

a. Values in parentheses are estimated values.
b. d for decomposition point.

Bibliography for Table 1:

Leo Brewer, The Thermodynamic Properties of the Oxides and Their Vaporization Processes, Chem. Revs. 52, p. 1, 1953.

James P. Coughlin, Contributions to the Data on Theoretical Metallurgy, XII. Heats and Free Energies of Formation of Inorganic Oxides, Bulletin 542, Bureau of Mines, 1954.

P.E. Blackburn, et al. J. Phys. Chem. 62, No. 7, 769, 1958.

J. Berkowitz, et al., J. Chem. Phys. 26, No. 4, 842, 1957.

W.A. Chupka and J. Berkowitz, J. Chem. Physics 26, No. 5, 1207 (1957).

K.K. Kelley, Contributions to the Data on Theoretical Metallurgy, X. High-Temperature Heat-Content, Heat Capacity, and Entropy Data for Inorganic Compounds, Bulletin 476, Bureau of Mines, 1949.

elements. For many of them, the deviations should certainly be large. In assuming a liquid silicate as the condensing surface, then those elements whose ionic character differs most from Si^{+4} will probably deviate most from ideal behavior. The elements that would be expected to deviate most would therefore be those of the alkali metals. However, similar oxides should give similar deviations so that the relative values of p_j for similar oxides should be in the same numerical order as the k_j values. The fact that the solutions are dilute does not necessarily indicate that the solution is perfect or make p_j a good estimate of k_j.

The melting point selected is approximately that of a silicate soil containing fairly large amounts of Al_2O_3 and K_2O or Na_2O along with SiO_2. For a surface detonation, large amounts of this material would be vaporized. The Al_2O_3, with a boiling point of 3950°K (1 atmos O_2), could start vapor-condensing at some temperature less than this (depending on the partial pressure) into liquid drops and co-condense some of the less volatile radioelements. The latter cannot vapor-condense by themselves because their actual vapor pressures are lower than those which would be calculated from the data in Table 1. These small vapor-condensed particles of Al_2O_3 will solidify when they cool to 2300°K and/or combine with SiO_2 as alumino-silicate liquid particles that can be formed between about 3100°K and 2040°K. The influx of larger liquid particles at these and lower temperatures can dissolve the very small vapor-condensed particles upon collision as well as condense more of other elements still in the gaseous state. The establishment of equilibrium vapor pressures for elements that decay from a non-volatile to a volatile element in the liquid state may be slower than for the gas-to-liquid equilibrium since diffusion through the liquid to the surface is slower than diffusion through the gas to the liquid surface.

A carrier material such as a silicate soil contains elements and compounds that could form other compounds with the fission product elements whose vapor pressures and solubilities in the liquid state could be different from that calculated for the oxide (aside from use of Raoult's law). For example, Na and K form compounds with all reactive non-metals and most metallic elements form silicate compounds. However, many also form silicate glasses as solutions and for these the assumed process applies. The vapor pressure data for the possible gaseous species of the fission-product elements over silicate solutions have not been measured. The exact gaseous species need not be known if the Henry's law constants for the liquid solutions are known as a function of temperature.

SECTION 4

EVALUATION OF THE $n(\ell)/V$ RATIO

4.1 CALCULATION OF THE RATIO $n(\ell)/V$ FROM RADIOCHEMICAL DATA

Radiochemical data from samples of fallout that give the content of one or more radionuclides per gram of fallout (preferably consisting of the larger fused particles) can be used to make estimates of the concentration of the carrier material in the fireball during the first period of condensation. In order to do this, however, the assumption of uniform mixing in the fireball must be made, the volume of the fireball at the time when the particles solidified must be known, and the total yield of the radionuclide(s) (i.e. total chain yield) is required. Also, the molecular weight of the carrier material must be known. The mole fraction, N_j, can then be calculated in terms of the ratio of the number of moles of the mass number, A, to the number of moles of the carrier. With this information, the ratio, $n(\ell)/V$, can be estimated from

$$n(\ell) = \frac{Y_A}{N_j} \sum_j \frac{y_j(A,t)}{\left(1 + \frac{k_j}{(n(\ell)/VRT}\right)} \qquad (87)$$

in which Y_A is the total weapon yield of the mass number A and V is the volume of the fireball at the time the carrier melting point occurs. The best estimates of $n(\ell)/V$ will result from analyses for mass chains that are neither condensed in large amount nor missing from the sample in large amount. Equation 87 can be solved by successive approximations and, if data for several mass numbers are available, the final value of the ratio should be selected from those in which the summed term has values between 0.2 and 0.8.

No complete set of unclassified data have been reported for use of Eq. 87. However, Kimura[12] gives values of the specific activity of the fallout from the 1 March 1954 detonation at the Eniwetok Proving Grounds. His values are 0.37 mc/gm of fallout on 23 April (D+53) and 8×10^{-8} gm fission products/gm of fallout. In terms of unfractionated fission products where the activity at 53 days is 3.7×10^{-8} d/s/fission,[13] the first value can be converted to 7×10^{14} fission product atoms per gram of fallout. The second value converts to 4×10^{14} fission product atoms per gram of fallout. The report also gives data on the relative yields of some of the individual radionuclides present. However, the carrier material, CaO, has a much higher melting point than siliceous soil minerals and the end of the firstperiod of condensation would occur much earlier for the CaO carrier, for the yield of that device. The gross fission product concentrations given above indicate at least the order of magnitude of the specific activity of fallout from large yield weapons. The information in the remainder of this Section will show that large variations in the specific activity in the fallout from weapons of different yield is not expected (i.e. for surface detonations) if the fraction of fission yield is held constant. It should, however, vary directly with the fraction of fission yield. For example, if the 1 March 1954 detonation were 50 percent fission, then a fission weapon might be expected to produce fallout with specific activities between 8×10^{14} and 14×10^{14} fission product atoms per gram of fallout.

According to data from The Effects of Nuclear Weapons (ENW),[14] the crater radius for a surface detonation is $62W^{1/3}$ feet (W in KT) and its depth is $25W^{1/4}$ ft. For a cone-shaped crater, which is more representative of the crater shape for a large yield detonation than is an ellipsoid of revolution (as given in ENW[14]), and a soil density of 110 lb/cu ft, the mass of material thrown out of the crater is given by

$$M = 5.03 \times 10^{9} W^{0.92} \text{ gm} \qquad (88)$$

If all the activity produced in a 20-KT fission weapon were mixed uniformly with the ejected mass, the fission-product concentration would be about 7.3×10^{13} atoms/gm; for a 1-MT fission weapon, it would be about 1.0×10^{14} atoms/gm; and for a 15-MT fission weapon, it would be about 1.2×10^{14}. With the assumption of uniform mixing of the fission products with all the crater material, the concentration changes rather slowly with yield (i.e., only as $W^{0.08}$). However, even for the 15-MT yield, the "uniform mixing" concentrations are lower by a factor of 7 to 12, assuming 50 % fission for

the 1 March 1954 detonation, or 3 to 6, assuming 100 % fission, than those found by Kimura. Thus these percentages indicate that only the order of 5 to 10 percent of the crater material must come in contact with the radioactive material and is involved in the formation of radioactive fallout particles.

4.2 CALCULATION OF THE RATIO $n(\ell)/V$ FROM THERMAL DATA AND EMPIRICAL SCALING EQUATIONS

4.2.1 Description of Calculation

The scaling equations and other data for an air burst given in ENW will be used along with modifications and idealized scaling assumptions for a description of the fireball volume and temperature, with time, for a surface detonation. The air burst model assumes detonation at sea level without an air-soil interface. For the surface detonation, the air-soil interface will be added. The reference time of the second maximum in the observed temperature used in ENW will be retained as a reference point in time.

In the two model detonations, a certain fraction of the total energy released will be estimated as still being in the fireball at the second maximum in the form of gaseous atoms of high internal energy. Some of the energy is still in the blast wave (or transferred to substances outside the fireball volume by the blast wave). Another portion of the energy has been radiated from the fireball (ENW calls this portion the "thermal energy"). Some of the energy has been used in expansion of the hot gases against the atmosphere. At times after the second maximum, the gases in the fireball release their internal energy and cool by heating inflowing air and/or soil material, expanding further against the atmosphere, and radiating energy out into the atmosphere. The thermal balances for these processes will be estimated in order to compute the amount of soil that can be heated and melted when the fireball has cooled to 1400°C. In addition, the energy balances will be computed as a function of yield so that the total amount of the major constituents contained in the volume of the fireball can be estimated.

In the calculations, the energy used to heat the surrounding air and/or soil is that required to dissociate these substances, originally in their normal thermodynamic state at 298°K and 1 atmos, to atomic gases and then heat the latter (as ideal gases) to the temperature of the second maximum. For cooling to 1400°C, the energy released comes from the change in kinetic energy of the gases and from the association of the gas atoms to gas molecules

or to liquid molecules at 1400°C. Except for consideration of the heat lost by radiation, ionization energies will not be taken into account.

4.2.2 Partition of Energy at Second Maximum

In ENW (p. 6), the distribution of energy for the air burst is 15 percent for nuclear radiation, 35 percent for thermal radiation (i.e. radiant energy), and 50 percent for blast and shock. The time or time period of the detonation at which these values apply is not given, nor is energy allotted for the processes given in 4.2.1. Of the energy distribution values given in ENW, the 15 percent for nuclear radiation will be assumed to be unavailable or lost from the fireball with respect to the processes discussed above for both the air burst and surface burst. The remaining 85 percent is, then, to be distributed among (1) the energy in the fireball at the second maximum, (2) the energy lost by radiance, and (3) the energy carried beyond the fireball perimeter by the blast wave.

The energy content of the fireball at the second maximum will be taken to include the dissociation energy for air ($0.8N_2 + 0.2O_2$), the change in internal energy for a temperature rise of 8000°K, and the work for expanding the gases to the fireball volume at the second maximum against a 1.0 atmosphere external pressure. The energy contained in the fireball for this process is

$$Q_1 = 2n_1(3 \times 8000 + 79{,}200) + P_oV_2 - n_1RT_o \quad (89)$$

in which n_1 is the number of moles of undissociated air, the value 3 is used for heat capacity (C_v) in cals/mile of an ideal gas, the value 79,200 cal/mole is the dissociation energy (ΔE) for one mole of dissociated gas atoms at 298°K, V_2 is the fireball volume at the second maximum, n_1RT_o is equal to P_oV_o where V_o is the original volume of the heated air molecules, and T_o is taken as 298°K (standard conditions at sea level). For a 20-KT yield air burst the value of V_2 as calculated from ENW for a spherical fireball is 2.5×10^{13} cm^3 so that P_oV_2 is 2.5×10^{13} cm^3-atmos or 6.1×10^{11} cals (1 cal = 41.29 cm^3-atmos). With these values, Eq. 89 reduces to

$$Q_1 = 2.06 \times 10^5 n_1 + 6.1 \times 10^{11} \quad (90)$$

The energy lost from the fireball by radiance, from ENW, p. 333, up to the second maximum is 0.2 X W/3, or 6.7 %. Using the conversion of 1.11×10^{12} cals/KT, the radiant energy lost for a 20-KT air burst is 1.5×10^{12} cals.

The energy content of the blast wave as it separates from the fireball should consist of the internal energy content of the air molecules expressed as a temperature rise, the compression energy (i.e., the dynamic pressure of the pulse), and a potential energy or work term expressed in terms of outward velocity of the wave. The measured fireball temperature decrease prior to the second maximum (see ENW, p. 69) will be taken as the decrease of the air temperature within the blast wave itself. The temperature curve in this period of time, expressed as an increase in the air temperature from ambient can be represented by

$$\Delta T = 304 t^{-0.423} \tag{91}$$

for t in seconds and T in ^{o}K. For a breakaway time (i.e. the time the blast wave leaves the fireball) of 0.015 secs, ΔT is 1800^{o}. For this temperature rise, ΔE for air is 10,860 cals/mole.[15] The peak overpressures from ENW, p. 109, can be represented, in part, for a 20 KT air burst by

$$p = 1.20 \times 10^{12} r^{-2.31}, \quad r = 2.4 \times 10^{4} \text{ to } 5.0 \times 10^{4} \tag{92}$$

for r in cm and p in psi overpressure. The variation of the fireball radius with time up to the breakaway from ENW, p. 65, can be represented by

$$r_{20} = 4.98 \times 10^{4} t^{0.372}, \quad t = 10^{-4} \text{ to } 0.015 \text{ secs} \tag{93}$$

for r in cm and t in secs. At 0.015 sec, r is 1.04×10^{4} cm, and, extrapolating Eq. 92 to 1.04×10^{4} cm, p is 620 psi (42 atmos). The corresponding value of the peak dynamic pressures is 1330 psi which is equal to 2.19 cal/cm3 (1 psi = 1.65×10^{-3} cal/cm3). For a temperature of $2100^{o}K$ (1800 + 300), the number of moles of gas atoms per cm3 at a pressure of 43 atmospheres, using the perfect gas law, is 2.4×10^{-4}. The energy absorbed by the gas due to the compression is then 9.1×10^{3} cals/mole. The outward velocity of the blast wave is obtained by differentiating Eq. 93 to give

$$v_r = 1.85 \times 10^4 t^{-0.628} \tag{94}$$

Using the gross kinetic energy, $1/2\ mv_r^2$, as measure of the potential work of the wave in moving the air molecules outward and converting to number of moles of air and to caloric units, the energy content at 0.015 secs is

$$Q_r = 2.28 \times 10^4 n_2 \tag{95}$$

where n_2 is number of moles of air in the blast wave at the breakaway. The total energy in the blast wave is

$$\begin{aligned} Q_2 &= 1.09 \times 10^4 n_2 + 0.91 \times 10^4 n_2 + 2.28 \times 10^4 n_2 \\ &= 4.28 \times 10^4 n_2 \end{aligned} \tag{96}$$

The sum of Q_1 and Q_2 should be equal to $0.78 \times 2.22 \times 10^{13}$, or 1.73×10^{13}, cals for the 20 KT air burst. Thus,

$$1.73 \times 10^{13} = 2.06 \times 10^5 n_1 + 6.1 \times 10^{11} + 4.28 \times 10^4 n_2 \tag{97}$$

In order to solve Eq. 97 for n_1 and n_2, a relation between n_1 and n_2 was required. Since none was directly available, it was assumed that all the gas molecules in the fireball at the second maximum and in the blast wave at breakaway originally occupied the volume enveloped by the fireball at the breakaway. That is to say, the air molecules outside the blast wave do not absorb any of the Q_1 or Q_2 energies until the blast wave hits them. With this assumption, the perfect gas law estimate is that the volume originally contained 1.94×10^8 moles air and

$$n_1 + n_2 = 1.94 \times 10^8 \tag{98}$$

With Eq. 98, the value of n_1 is 5.15×10^7 moles and n_2 is 1.42×10^8 moles. The corresponding value of Q_1 is 1.12×10^{13} cals or 0.51 of the total energy; the value of Q_2 is 6.08×10^{12} cals which is 0.27 of the total energy. The latter value for the fraction of the energy carried by the blast (and shock) wave is about half of that given in **ENW**.

For a surface detonation, about the same energy partition should occur except that the fraction of the energy lost from the fireball up to the second temperature maximum by radiation should be less. If, for a given yield, the variation of the temperature and fireball radius with time before the second maximum for the surface burst is similar to that for the air burst, then the ratio of radiant energy lost for the two types of bursts should be equal to the ratio of the products of the fourth power of the temperature(s) at the second maximum and the surface area of the fireball at that time. Taking a spherical fireball for the air burst and a hemispherical shape for the surface burst, the ratio of the two energies radiated into the air space around the two is

$$q(s)/q(a) = \frac{T_2^4(s)\, R_2^2(s)}{2T_2^4(a)\, R_2^2(a)} \tag{99}$$

where T_2 and R_2 are the temperature and fireball radius at the second maximum, respectively, and (s) and (a) refer respectively to the surface or air burst. If it is further assumed that the volume of the fireball at the second maximum is the same for both types of detonations (i.e. and contains approximately the same fraction of the total energy), then

$$R_2(s)/R_2(a) = 2^{1/3} \tag{100}$$

For this ratio of radii, Eq. 99 is

$$q(s)/q(a) = 0.79 \left[T_2(s)/T_2(a)\right]^4 \tag{101}$$

The probable maximum value of $T_2(s)/T_2(a)$ is one; then for a q(a) value of 0.067W, q(s) is 0.053W. A probable minimum value of $T_2(s)/T_2(a)$ might be 0.5; the corresponding value of q(s) is 0.0033W. The fraction of the total energy in the fireball at the second maximum for the surface burst should therefore be between 0.53W and 0.58W. These calculations assume that the radiant energy that strikes the ground surface has been utilized to vaporize soil whose vapors are contained in the fireball volume. Some of this energy might be lost in heating soil that may enter at later times. But on the other hand, the shock wave would contribute some energy in heating soil materials whose gaseous (or liquid) products cannot

escape the fireball volume by outward movement as in the air burst. A mean value, 0.55W, was therefore selected as the estimate of energy contained in the surface burst fireball at the second temperature maximum. In the calculations to follow, these energy partitions were assumed to be invariant with yield; this assumption, as is shown in the following paragraphs, leads to a particular set of solutions to the derived scaling equations for the fireball temperature and vapor concentration.

4.2.3 Fireball Temperature, Volume, and Energy Content Scaling Functions for Model Air Burst

The scaling equations for the air burst are presented here as a basis for deriving comparable functions for the surface burst in the following subsection. Geometry, energy content, and assumptions about the differences and/or similarities in the two types of bursts have been used to alter or retain the necessary scaling functions. Also, some of the scaling functions in the ENW have been altered to obtain consistent sets of functions for the model bursts.

The variation of the fireball radius after the second temperature maximum was derived from Fig. 2.85, p. 65 of ENW; for a 20-KT yield, the values of 620 ft at 0.15 sec (t_2, time of the second maximum) and 760 ft at 0.75 sec (t_m, time of maximum expansion of fireball) were used. These values give the variation of the 20 KT yield fireball radius with time as

$$R(20\ KT) = 1.89 \times 10^4 (t/t_2)^{0.128} \qquad (102)$$

for R in cm and t in secs. For the yield scaling of the radius, the geometrical scaling function, $W^{1/3}$, was used instead of $W^{2/5}$ as given in ENW. The higher power of W given in ENW may have been used to account for the decrease in external air pressure for the required air burst height. For the model air burst, however, the external pressure is assumed to be constant at 1 atmosphere. Using the 20-KT fireball radius at the second maximum to solve for the coefficient of $W^{1/3}$ (i.e., as being representative of the model burst conditions), Eq. 102 becomes

$$R = 6.96 \times 10^3 W^{0.333} (t/t_2)^{0.128},\ t_2 \leq t \leq t_m \qquad (103)$$

for W in KT. If the time for full wxpansion of the fireball is also taken to scale according to $W^{1/3}$, then (from $t_m = 0.75$ sec and W = 20 KT),

$$t_m = 0.276W^{0.333} \tag{104}$$

From ENW, p. 331, the scaling for t_2 (note change of notation from ENW), adjusted to give 0.15 sec for 20 KT, is

$$t_2 = 0.0336W^{0.500} \tag{105}$$

The ratio t_m/t_2 is

$$t_m/t_2 = 8.21W^{-0.167} \tag{106}$$

By eq. 106, t_2 and t_m approach each other with increasing yield and, if the relation held for all yields, the time of maximum expansion and of second temperature maximum would coincide for a yield of about 3×10^5 KT (300 MT). Substitution of Eq. 106 in Eq. 103 gives, for the fireball radius at maximum expansion,

$$R_m = 0.12 \times 10^3 W^{0.312} \tag{107}$$

for R_m in cm.

Scaling relationships for the fireball temperature can be derived from the information given by ENW, pp. 300-333. The thermal power, P, is given by

$$P = 1.73 \times 10^{-11} T^4 R^2 \text{ cals/sec} \tag{108}$$

for T in $^\circ$K and R in cm. The radiant energy lost up to t_2 is given by

$$q_1(a) = \int_o^{t_2} P \, dt \tag{109}$$

To evaluate Eq. 109 from the curve in ENW, p. 333, let

$$Z = P/P_2 \tag{110}$$

where P_2 is the thermal power at the second maximum, and

$$y = t/t_2 \tag{111}$$

With these variables, Eq. 109 becomes

$$q_1(a) = P_2 t_2 \int_0^{t_2} Z \, dy \tag{112}$$

The graphical integration is tabulated in Table 2; the value of the integration for Eq. 112 is 0.569. Substituting Eqs. 103, 104, and 108 into Eq. 112 gives

$$q_1(a) = 1.61 \times 10^{-5} T_2^4 \, W^{1.167} \text{ cals} \tag{113}$$

A logarithmic plot of the curve in ENW, p. 333, for t/t_2 greater than one can be represented quite accurately by the equation

$$Z = 1.28 y^{-1.590}, \quad 1.4 \leq y \leq 10 \tag{114}$$

The radiant energy lost at times greater than t_2 is given by

$$q_2(a) = \int_{t_2}^{t} P \, dt \tag{115}$$

so that

$$q_2(a) = P_2 t_2 \int_{1.0}^{1.4} Z \, dy + P_2 t_2 \, 1.28 \int_{1.4}^{y} y^{-1.590} \, dy \tag{116}$$

TABLE 2

Summary of Graphical Integration of Scaled Thermal Power Function up to the Time of the Second Maximum

y	Z	$0.1\Delta Z$	$\int_0^y Z\,dy$
0.1	0.05	0.0022	0.002
0.2	0.12	0.0085	0.011
0.3	0.24	0.0180	0.029
0.4	0.43	0.0322	0.061
0.5	0.67	0.0555	0.116
0.6	0.82	0.0755	0.192
0.7	0.91	0.0866	0.278
0.8	0.96	0.0935	0.372
0.9	0.99	0.0974	0.469
1.0	1.00	0.0995	0.569

Graphical integration of the first term of Eq. 116 gives 0.356; the complete integral up to y values larger than 1.4 is then given by

$$q_2(a) = P_2 t_2 \left\{0.356 + 2.17\left[(1.4)^{-0.59} - y^{-0.59}\right]\right\} \qquad (117a)$$

$$= P_2 t_2 \left(2.135 - 2.17 y^{-0.59}\right)$$

According to Eq. 108, the thermal power at the second maximum is

$$P_2 = 1.73 \times 10^{-11} T_2^4 R_2^4 \qquad (118)$$

Substitution of Eqs. 103, 105, and 118 into Eq. 117 gives

$$q_2(a) = 2.82 \times 10^{-5} T_2^4 W^{1.167} (2.135 - 2.17 y^{-0.59}) \qquad (119)$$

At temperatures below about 1000°K, the energy loss by radiation should drop very rapidly and be negligible for T/T_2 less than 0.1 In order to estimate a value of y for which T/T_2 is 0.1, Eqs. 103, 107, 108, 110 and 114 can be combined to give

$$T^4R_m^2 = T_2^4R_2^2 \times 1.28(t/t_2)^{-1.590},\ t \geq t_m \qquad (120)$$

It may be noted here that, for the 20 KT yield, R_m occurs at t/t_2 equal to 5.0 whereas the right hand side of Eq. 120 applies for t/t_2 values as low as 1.4 which would imply that, for the curve given, R_m occurred at a t_m/t_2 value of 1.4 independent of yield rather than at the value given by Eq. 106 for 20 KT. It is likely that the P/P_2 curve, at least up to t_m/t_2, is yield-sensitive and that the curve in ENW, if an observed curve, is for a yield much greater than 20 KT. At any rate, for times near t_m and longer, the curve indicates T is proportional to $(t/t_2)^{-0.398}$. Complete substitution of the indicated equations into Eq. 120 and solving for T gives

$$T = 0.929W^{0.0108}\ T_2\ (t/t_2)^{-0.398},\ t \geq t_m \qquad (121)$$

For a large range of yields the value of $0.929W^{0.0105}$ is near one; hence the value of t/t_2 or y for T/T_2 equal to 0.1 is about $325(2.17y^{-0.59} = 0.072)$. Using this value in Eq. 119 gives

$$q_2(a) = 5.82 \times 10^{-5}T_2^4\ W^{1.167} \qquad (122)$$

The total radiant energy is then

$$q_T(a) = 7.43 \times 10^{-5}T_2^4\ W^{1.167} \qquad (123)$$

The fraction of this amount up to t_2 is 0.22. Now, if $q_T(a)$ is taken as 1/3 W in KT (or 3.70×10^{11} W in Cals), then

$$T_2 = 8{,}390W^{-0.042} \qquad (124)$$

Equation 124 shows that when the energy partition is postulated to be independent of yield, the temperature at the second maximum decreases with yield.

For a yield of 20 KT, Eq. 124 gives 7400°K as the value for T_2; this value is almost 1000°K lower than shown in ENW, p. 68 and 69. A lower temperature results even when the fireball radius equations, p. 66, are used for R in Eq. 120. If $q_T(a)$ is taken as 0.58

W(KT), as has been found in the previous section, then Eq. 123 would give a second maximum temperature of

$$T_2 = 9{,}640W^{-0.042} \tag{125}$$

For a yield of 20 KT, Eq. 125 gives 8500°K as the value for T_2 which is in better agreement with the values given in ENW, p. 68 and 69. To obtain the temperature given by Eq. 125, all of the energy in the fireball is used as radiant energy; none of the energy has been allocated to further expansion of the fireball and atomic cloud or for the work against gravity in raising the gas and particle mass to high altitudes. However, there are two additional sources of energy that have not been mentioned that could easily provide this "extra" energy; these are: (1) the buoyant force of the atmosphere to lift the warm gas mass, and (2) the kinetic energy and the energy of cooling and expansion of the air, originally at 1 atmos and 298°K, to a lower final pressure and temperature at higher altitudes; this is a net gain from the air molecules, themselves, that were enveloped in the fireball. Also, some of the blast energy will be reclaimed as preheated air in the rising cloud. Thus, Eq. 125 may well not be the maximum value for T_2 with respect to the fraction of the total bomb energy lost by radiation.

If $q_T(a)$ is taken as equal to $1.11 \times 10^{12}\alpha$ W calories (α being the fraction of the total energy released which is lost by radiance), then T_2 from Eq. 112 is

$$T_2 = 1.10 \times 10^4 \alpha^{1/4} W^{-0.042} \tag{126}$$

Substitution of Eq. 126 into Eq. 121 gives

$$T = 1.02 \times 10^4 \alpha^{1/4} W^{-0.031} (t/t_2)^{-0.398}, \quad t \geq t_m \tag{127}$$

And further substitution of Eq. 105 for t_2 gives

$$T = 2660\alpha^{1/4} W^{0.168} t^{-0.398}, \quad t \geq t_m \tag{128}$$

In view of the possibility of variations in the scaled power curve of ENW due to yield, it may be assumed that the lower time limit

for application of Eqs. 127 and 128 is t_2 rather than t_m. With this assumption, the substitution of Eqs. 103 (or 107) and 127 in Eq. 108 gives

$$P = 9.16 \times 10^{12} \alpha W^{0.543} (t/t_2)^{-1.334}, \quad t_2 \leq t \leq t_m \tag{129}$$

and

$$P = 1.57 \times 10^{13} \alpha W^{0.500} (t/t_2)^{-1.590}, \quad t \geq t_m \tag{130}$$

For these approximations of the thermal power, the energy lost by radiance after t_2 is

$$q_2(a) = 9.16 \times 10^{12} \alpha W^{0.543} t_2^{1.334} \int_{t_2}^{t_m} t^{-1.334}\, dt + 1.57 \times 10^{13} \alpha W^{0.500} t_2^{1.590} \int_{t_m}^{t_f} t^{-1.490}\, dt \tag{131}$$

If the final limit of integration, t_f, is again defined as the time when T/T_2 is 0.1, then by use of Eq. 126 and Eq. 127 or 128, t_f is given by

$$t_f = 9.09 W^{0.527} \tag{132}$$

Integration of Eq. 131 up to this limit yields

$$q_2(a) = 9.22 \times 10^{11} \alpha W^{1.043} (1 - 0.235 W^{0.056} - 0.0357 W^{-0.059}) \tag{133}$$

Thus, even though the scaling equations were derived on the basis of $q_2(a)$ being proportional to W, the combination of the T and R functions from EMW (with some alterations for R) gives $q_2(a)$ as not being directly proportional to W. However, the power of W is not far from one so that $q_2(a)$ from Eq. 133 conforms approximately to the original postulation. The main difference is that most of the yield dependence in P/P_2 occurs in the period from t_2 to t_m when the fireball is still

expanding; the extrapolation of the variation of T with t/t_2 back to this time period may also account for some of the difference in the yield dependence.

4.2.4 Estimate of Difference in Fireball Temperature at Second Maximum Between Model Air and Surface Bursts

The main assumptions that were made to obtain an estimate of the difference in the fireball temperature at the second maximum between the model air and surface bursts are: (1) in the surface burst, 1/2 of the energy in the fireball is utilized to heat, dissociate, and expand air molecules and 1/2 of the energy to vaporize, heat, dissociate, and expand molecules of soil; (2) the air and surface bursts are equally efficient in the heating process with respect to the number of gas atoms heated to the temperature of the second maximum per unit of yield, and (3) the fraction of the total yield utilized at the second temperature maximum is 0.51 for the air burst and 0.55 for the surface burst.

The first law of thermodynamics for the utilization of 0.51 of the total energy at the second maximum for the model air burst is

$$Q_1 = n_2 \left[C_v(T_2 - T_o) + \Delta E_a^o \right] + P_o(V_2 - V_o) \qquad (134)$$

in which n_2 is the number of air atoms (N and O atoms), C_v is the heat capacity of (an ideal) monatomic gas (3 cal/mole-deg), T_2 is the temperature at the second maximum, T_o is the original temperature of the gas atoms (298°K), ΔE_a^o is the heat of dissociation of air molecules at 298°K (79,200 cal/mole of gas atoms), P_o is the external pressure (1 atmosphere), V_2 is the volume of the fireball at the second maximum, V_o is the original volume of the air molecules at P_o, V_o, and T_o, and Q_1 is 0.51W in KT or 5.66×10^{11}W in cal. For a spherical fireball, the volume from Eq. 103 is

$$V = 1.41 \times 10^{12} W \, (t/t_2)^{0.385} \text{ cm}^3 \qquad (135)$$

so that

$$V_2 = 1.41 \times 10^{12} W \qquad (136)$$

Using the perfect gas law, the value, of $P_o V_o$ for the original air molecules is

$$P_o V_o = (n_2/2)RT_o \qquad (137)$$

Substitution of the appropriate terms in Eq. 134 (1 cal = 41.29 cm^3 atoms) gives

$$5.66 \times 10^{11} W = n_2 3(T_2-298) + 79{,}200 + 3.42 \times 10^{10} W - 300 n_2 \qquad (138)$$

so that

$$n_2/W = \frac{5.32 \times 10^{11}}{(3\ T_2 + 78{,}000)} \qquad (139)$$

In order to make a similar computation for the model surface burst, the thermal properties of the "ideal" soil must be specified. The nonreactive "ideal" soil will be assigned the thermal properties of anorthoclase ($Na_2O \cdot Al_2O_3 \cdot 6SiO_2$) to be consistent with the selected melting point (1400°C). One mole of the soil upon complete dissociation gives 26 moles of gas atoms; the molecular weight is 524. In estimating the energy computations, the bonding energy between the three oxides was assumed to be small compared to the oxygen bonding to the metal atoms. The changes in energy for any process involving the whole molecule therefore may be equated to the sum of the energy changes for the individual oxide molecules indicated in the formula. The entropy of fusion was taken to be 29 cal/mole/deg; the heat of fusion is then 48,000 cal/mole.

The change in internal energy of the atoms and molecules was estimated from

$$\Delta E = \Delta H - \Delta(PV) \qquad (140)$$

and when gas atoms are involved, the perfect gas law was used and the quantity ΔnRT substituted for $\Delta(PV)$ for a constant temperature process. The dissociation energy of the soil at 298°K was calculated as follows from the data of Shell and Sinke[15] (s = solid; g = gas; ΔH and ΔE values in cal for indicated reaction in number of moles):

(1) $2\ Na(s) + 1/2\ O_2(g) \longrightarrow Na_2O(s)$, $\quad \Delta H^\circ = -61{,}100$

(2) $2\ Na(s) \longrightarrow 2Na(g)$, $\quad \Delta H^\circ = 24{,}500$

(3) $1/2\ O_2(g) \longrightarrow O(g)$, $\Delta H^\circ = 59,100$

Sum: (3)+(2)-(1) $Na_2O(s) \longrightarrow 2Na(g) + O(g)$, $\Delta H^\circ = 144,700$

$$\Delta E^\circ = 144,700 - 3 \times 2 \times 298 = 142,900$$

(1) $2\ Al(s) + 3/2\ O_2(g) \longrightarrow Al_2O_3(s)$, $\Delta H^\circ = -400,200$

(2) $2\ Al(s) \longrightarrow 2Al(g)$, $\Delta H^\circ = 154,300$

(3) $3/2\ O_2(g) \longrightarrow 3O\ (g)$, $\Delta H^\circ = 177,300$

Sum: (3)+(2)-(1) $Al_2O_3(s) \longrightarrow 2Al(g) + 3O(g)$, $\Delta H = 731,800$

$$\Delta E^\circ = 731,800 - 5 \times 2 \times 298 = 728,800$$

(1) $Si(s) + O_2(g) \longrightarrow SiO_2(s)$, $\Delta H^\circ = -210,200$

(2) $Si(s) \longrightarrow Si(g)$, $\Delta H^\circ = 90,000$

(3) $O_2(g) \longrightarrow 2O\ (g)$, $\Delta H^\circ = 118,200$

Sum: (3)+(2)-(1) $SiO_2(s) \longrightarrow Si(g) + 2O(g)$, $\Delta H^\circ = 418,400$

$$\Delta E^\circ = 731,800 - 3 \times 2 \times 298 = 416,600$$

For the process,

$$Na_2O \cdot Al_2O_3 \cdot 6SiO_2(s) \longrightarrow 2Na(g) + 2\ Al(g) + 6Si(g) + 16\ O(g) \quad (141a)$$

$$\Delta E^\circ = 142,900 + 731,800 + (6 \times 418,400)$$

$$= 3,370,000 \text{ cal/mole of soil} \quad (141b)$$

or,

$$\Delta E^\circ = 129,600 \text{ cal/mole of gas atoms formed} \quad (141c)$$

The first law of thermodynamics for the utilization of 0.55 of the total energy at the second maximum for the model surface burst is

$$Q_1' = n_2' \left[C_v(T_2'-T_o) + 72,200\right] - (n_2'/2)RT_o + n_2'' \left[C_v(T_2'-T_o) + 129,600\right] + 3.42 \times 10^{10} W \qquad (142)$$

in which n_2' is the number of moles of air atoms in the fireball, n_2'' is the number of soil atoms in the fireball, T_2' is the temperature of the gas mixture at the second maximum, and Q_1' is 0.55W in KT or 6.10×10^{11}W in cals. Making the substitutions indicated and letting the sum of n_2' plus n_2'' be represented by n gives, for Eq. 142,

$$5.76 \times 10^{11} W = n(3\ T_2' + 78,000) + 51,600 n_2'' \qquad (143)$$

The model surface burst was defined as one in which half the energy in the fireball at the second maximum was utilized in dissociating and heating air molecules and half for the soil molecules. If each of the two component gases are expanded from their original volumes to V_2 (same as for the air burst), then

$$n_2' \left[C_v(T_2'-T_o) + 79,200\right] + \left[P_o V_2 - (n_2'/2)RT_o\right] = n_2'' \left[C_v(T_2'-T_o) + 129,600\right] + P_o V_2 \qquad (144)$$

Substitution of $(n - n_2'')$ for n_2' and solving for n_2'' gives

$$n_2'' = n \frac{(3T_2' + 78,000)}{(6T_2' + 207,600)} \qquad (145)$$

With Eq. 145, Eq. 143 becomes

$$5.76 \times 10^{11} W = n\ (3T_2' + 78,000) \left[1 + \frac{51,600}{6T_2' + 207,600)}\right] \qquad (146)$$

The values of n_2/W for Eq. 139 and n/W for Eq. 146 are summarized in Table 3 and the values of n/W is plotted as a function of T_2 in Fig. 2. The values of T_2 and T_2' for equal values of n_2/W and n/W are given in Table 4. The assumption of equal values of the "vaporization efficiency" (n/W) for the two types of burst gives, approximately, a constant difference in the temperatures at the second maximum of about 3800°K.

TABLE 3

Values of n_2/W and n/W for Several Values of T_2 and T_2', Respectively

T_2 or T_2' (^oK)	n_2/W (10^6 moles/KT)	n/W (10^6 moles/KT
4,000	5.91	5.24
5,000	5.72	5.09
6,000	5.54	4.95
7,000	5.37	4.82
8,000	5.21	4.70
9,000	5.06	4.58
10,000	4.93	4.47
11,000	4.79	-
12,000	4.67	-

TABLE 4

Values of T_2 and T_2' for Equal Values of n_2/W and n/W

n/W or n_2/W (moles/KT)	T_2 (^oK)	T_2' (^oK)	T_2-T_2' (^oK)	T_2'/T_2
4.7	11,750	8,000	3,750	0.681
4.8	10,910	7,150	3,760	0.658
4.9	10,150	6,370	3,780	0.628
5.0	9,420	5,640	3,780	0.599
5.1	8,730	4,930	3,800	0.565
5.2	8,050	4,250	3,800	0.528
			Av.: 3,780	

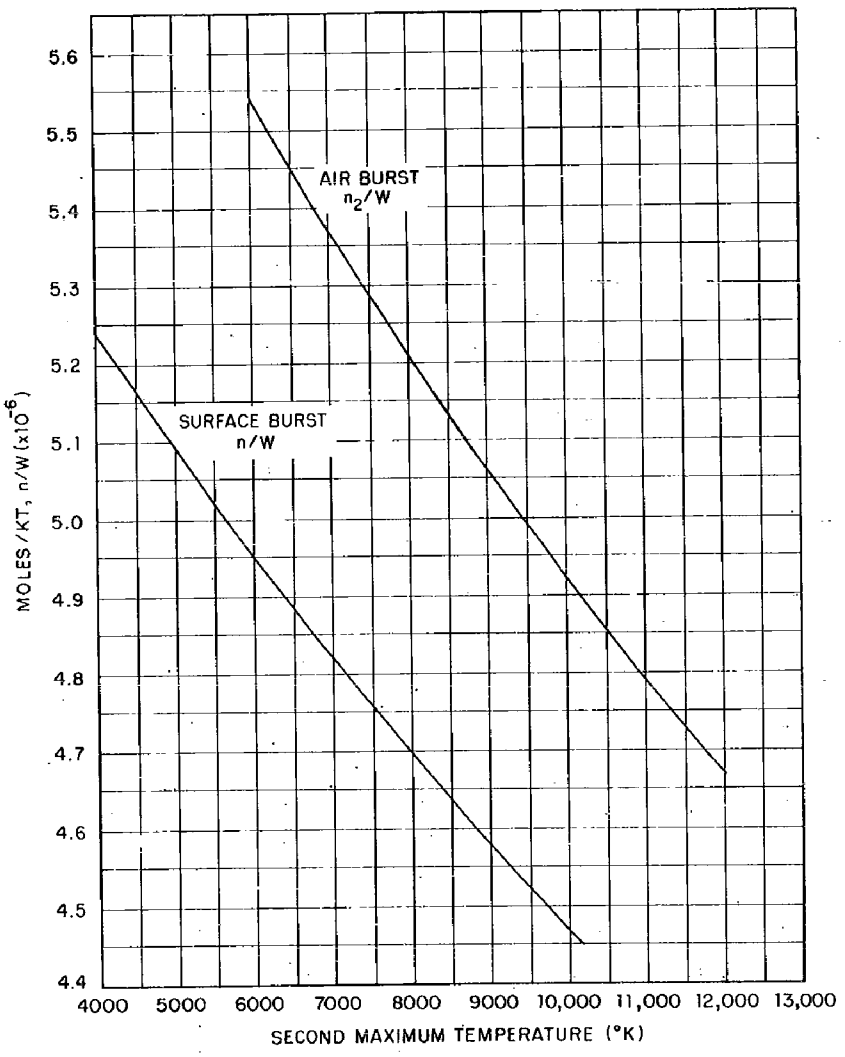

Fig. 2 Variation of the Moles Gas per KT in the Fireball With the Second Maximum Temperature

If the value of T_2 for the model air burst for a yield of 20 KT is 8300°K as given in ENW, p. 68 and 69, then T_2' is 4500°K. This value of T_2' seems to be too low to be consistent with the energy utilization and energy partition. The temperature of 4500°K is not high enough to completely dissociate all the air molecules and many of the more stable oxide molecules. If the dissociation energies in Eq. 142 were reduced, a larger value of n/W at a given value of T_2' would result. This, in turn, would give a smaller difference between T_2 and T_2'; and, if the original value of T_2 is retained a higher value of T_2' would be indicated. A higher value of T_2' would require use of the dissociation energies (i.e. Eq. 142) and a return to the above temperature values. This inconsistency can be removed if T_2 is increased.

The data from ENW used in the previous sections to obtain the various scaling functions was associated with the model air burst. However, as was noted, ENW does not state the type of burst; except for the blast curves, p. 109, no mention of the burst type is given. Many of the inconsistencies found in the ENW information with respect to the fireball temperature, energy partition, and thermal power would be resolved if it were assumed that the data actually applied to a tower-mounted explosion. If this assumption is applied and if it is also assumed that the temperature at the second maximum for a tower shot is midway between that for a surface burst and an air burst, then the latter two temperatures can be estimated from

$$T_2 + T_2' = 16,600 \tag{147}$$

and

$$T_2 - T_2' = 3,800 \tag{148}$$

The resulting values of T_2 and T_2' are 10,200 °K and 6400 °K, respectively.

The assumed scaling equations for R and t_2 and the assumption that the radiant energy was proportional to the yield led to the result that T_2 was proportional to $W^{-0.042}$ since $q_T(a)$ was proportional to $T_2^4 W^{1.167}$ when the yield dependence of the term $R^2 t_2$ were substituted. If, however, instead of assigning the excess over 1.000 in the exponent of W to T_2 alone, the excess, 0.167, is divided equally and assigned to the scale functions for T_2^4 and t_2, and, if $q_2(a)$ is adjusted to 0.51W (in KT) for the 20 KT yield model air burst, the following scaling functions result:

$$R = 5.74 \times 10^{3} W^{0.333} (t/t_2)^{0.128} \text{ cm}, \quad t_2 \leq t \leq t_m \tag{149a}$$

$$R = 8.58 \times 10^{3} W^{0.280} t^{0.128} \text{ cm}, \quad t_2 \leq t \leq t_m \tag{149b}$$

$$t_2 = 0.0431^{*} W^{0.416} \text{ sec} \tag{150}$$

$$t_m = 0.286^{***} W^{0.321^{**}} \text{ sec} \tag{151}$$

$$R_m = 7.32 \times 10^{3} W^{0.321^{**}} \text{ cm} \tag{152}$$

$$T = 1.02 \times 10^{4} W^{-0.021} (t/t_2)^{-0.400} {}^{o}K, \quad t \geq t_2 \tag{153a}$$

$$T = 2.90 \times 10^{3} W^{0.145} t^{-0.400} {}^{o}K, \quad t \geq t_2 \tag{153b}$$

$$T_2 = 1.02 \times 10^{4} W^{-0.021} {}^{o}K \tag{154}$$

$$t_f = 13.63 W^{0.416} \text{ sec, for } T = 0.1\, T_2 \tag{155}$$

$$P = 9.06 \times 10^{10} W^{1.143} t^{-1.344} \text{ cals/sec}, \quad t_2 \leq t \leq t_m \tag{156}$$

$$P = 6.59 \times 10^{10} W^{1.225} t^{-1.600} \text{ cals/sec}, \quad t_m \leq t \leq t_f \tag{157}$$

$$q_1(a) = 7.77 \times 10^{10} W \text{ cals (7 \% of total)} \tag{158}$$

$$q_2(a) = 7.76 \times 10^{11} W(1 - 0.222 W^{0.031} - 0.0295 W^{-0.025}) \tag{159}$$

For Eq. 159, $q_2(a)/W$ (both in same units) is 0.52 for 1 KT, 0.50 for 100 KT, 0.49 for 1 MT, and 0.48 for 10 MT. This relative decrease with yield in the loss of fireball energy by radiance, due to the second term in the parenthesis of Eq. 159, is a result of the scaling function for t_m. If the t_m scaling function exponent on W were the same as that for t_2, this term in Eq. 159 would not be yield-dependent. The indicated drift of t_m towards t_2 with increasing yield also results in a decrease in the difference between R_2 and R_m with yield and hence less relative increase in the surface area of the fireball from which the energy is radiated.

Besides the difference in temperature at the second maximum, the main difference in the above scaling functions from those given in the preceeding paragraph is that due to the 18 % decrease in the fireball radius. This decrease resulted from the adjustment of $q_2(a)$ to 0.51W (in KT) at 20 KT. This "used up" all the energy so that the

*Adjusted to 0.15 secs for 20 KT.
**Taken to be equal; determined from Eq. 121b.
***Adjusted to 0.75 secs for 20 KT.

fireball radius thus determined is a maximum value. Lapple[16] indicates that the fireball radius may actually be only about 0.5 of the values given by EMW. The decrease in the radius does not result in a significant change in difference in temperature at the second maximum between the model air burst and model surface burst; the difference is decreased by only about 100°K. The reestimate of T_2' is therefore 6500°K.

4.2.5 Scaling Functions for Temperature, Fireball Radius, and Utilization of Fireball Energy for Model Surface Burst

The scaling functions for the model surface burst were based on those for the model air burst given in the previous subsection and altered to account for assumed differences between the two types of bursts.

Assuming equal fireball volumes for the two and a hemispherical shape for the surface burst fireball up to maximum expansion results in a radius for the latter that is $2^{1/3}$ times that for the air burst, or

$$R = 7.23 \times 10^{3} W^{0.333} (t/t_2)^{0.128} \text{ cm}, \quad t_2 \leq t \leq t_m \qquad (160)$$

The dependence of the time of the second maximum on yield for the model surface burst will be assumed to be intermediate between that given by EMW and that given by Eq. 150 for the model air burst; at 1 KT the times at which the second maximum occur will be taken to be equal for the two types of burst. In other words, the change(s) in temperature with time for the surface burst is assumed to be just a little slower for the surface burst than for the air burst. The value of t_2, according to the above assumptions, is then

$$t_2 = 0.0431 W^{0.460} \text{ secs} \qquad (161)$$

Substitution of Eq. 161 into Eq. 160 gives

$$R = 1.08 \times 10^{4} W^{0.274} t^{0.128} \text{ cm}, \quad t_2 \leq t \leq t_m \qquad (162)$$

By again letting the t_m and R_m dependence yield have the same exponent on W and, if the value of t_m for 1 KT is taken to be the same

as for the model air burst (Eq. 151), the time at which maximum expansion of the fireball occurs is given by

$$t_m = 0.286W^{0.314} \text{ sec} \tag{163}$$

Substitution of Eq. 163 in Eq. 162 gives

$$R_m = 9.22 \times 10^3 W^{0.314} \text{ cm} \tag{164}$$

The temperature at the second maximum for the surface burst will be assumed to be independent of yield so that, from the previous subsection

$$T_2 = 6,500 \ ^oK \tag{165}$$

For times just beyond t_2, the decrease in temperature will be assumed to be proportional to $(t/t_2)^{-1/3}$ rather than $(t/t_2)^{-0.400}$. This initial slower cooling was taken because of thermal reflection and possible entry of preheated materials from the earth's surface into the fireball after t_2. The slower cooling curve was assumed to apply until the fireball cooled to 2500 ^oK at which temperature the cooling rate is increased by use of Newton's law of cooling to approximate the shape of the fireball cooling curve at later times. The fireball temperature is then

$$T = 6,500(t/t_2)^{-1/3} \ ^oK, \ t_2 \leq t \leq t_x \tag{166}$$

or, with Eq. 161

$$T = 2,230W^{0.153} t^{-1/3} \ ^oK, \ t_2 \leq t \leq t_x \tag{167}$$

where t_x is the time at which T is 2500 ^oK. Substitution of 2500 for T in Eq. 167 gives

$$t_x = 0.759W^{0.460} \text{ sec} \tag{168}$$

For times longer than t_x, where Newton's law of cooling is used,

$$T = T_o + (2500-T_o)e^{-K(t-t_x)} \qquad (169)$$

in which T_o is the external temperature and K is the cooling constant. The value of T_o will be taken to be 273 ^oK (0^oC) and the value of K can be determined from the differential of Eq. 167 evaluated at t_x and 2500 ^oK so that Eqs. 167 and 169 join smoothly at that temperature. Namely

$$K = \frac{(dT/dt)}{2,227} \text{ sec}^{-1} \text{ at } t = t_x \qquad (170)$$

When the appropriate substitutions from Eqs. 167 and 168 are made in Eq. 169, Eq. 170 is

$$K = 0.508W^{-0.460} \text{ sec}^{-1} \qquad (171)$$

Use of Eqs. 168, 169, and 171 to determine the time at which the fireball temperature is 1400^oC (1673 ^oK) gives

$$t\ (1400^oC) = 1.69W^{0.460} \text{ sec} \qquad (172)$$

For t (1400^oC) equal to 60 sec, W is 2.3 MT. If Eq. 167 were assumed to apply up to 60 secs, the yield would be about 1.0 MT. Of the two yields, the larger value associated with the more rapid decrease in temperature below 2500 ^oK is probably the better of the two estimates.

The thermal power and energy lost from the fireball for the model surface burst, for times after the second thermal maximum, is calculated for energy transmission from a hemispherical fireball up to the time of maximum expansion. At about this time or very shortly thereafter, the fireball should be breaking clear of the ground surface in its upward rise (see EMW, p. 23, where for 1 MT the top of the cloud is at 10,000 ft in about 16.5 sec, at 20,000 ft in 40 sec, and at 25,000 ft in 60 sec, etc.). For calculating the distribution of the thermal energy during the fireball rise (until it cools to 1400^oC), it is more convenient to "remove" the ground surface and allow the fireball to remain at constant volume with a constant external pressure. In this procedure, the shape of the fireball

changes from hemispherical to spherical with a decrease in radius. The fireball volume, however, is assumed to remain constant until the temperature falls below 500 ^{o}K or at least until the fireball separates from the surface. The spherical fireball radius at separation time, t_s, with the constant volume assumption, is

$$R_s = 7.32 \times 10^3 W^{0.314} \text{ cm}, \quad t \geq t_s \tag{173}$$

The height of the top of the fireball at this time would then be $14.64 \times 10^3 W^{0.314}$ cm and since it was $9.22 \times 10^3 W^{0.314}$ cm at t_m, its height is increased by $5.42 \times 10^3 W^{0.314}$ cm between t_m and t_s.

Using the value of R_m as the height of the cloud at t_m and the data of ENW, Fig. 2.12, for the 1-MT burst, the height of the cloud top can be represented, with a fair degree of precision, by

$$h_t = 4.24 \times 10^4 t^{0.704} \text{ cm}, \quad t_m \leq t \leq 60 \text{ sec} \tag{174a}$$

and

$$h_t = 6.46 \times 10^4 t^{0.600} \text{ cm}, \quad 60 \text{ sec} \leq t \leq 390 \text{ sec} \tag{174b}$$

Since h_t is equal to $2R_s$ at t_s, the use of Eq. 173 can be made to find t_s for the 1-MT yield. It is 4.82 sec. Assuming the equation form at^n for the dependence of R on t between t_m and t_s and solving by use of Eqs. 164 and 173 for a 1-MT yield, gives a value of n of -0.354. Use of the general equations for t_m and R_m with this power of t gives, for the fireball radius,

$$R = 5.92 \times 10^3 W^{0.425} t^{-0.354} \text{ cm}, \quad t_m \leq t \leq t_s \tag{175}$$

The time that the fireball separates from ground surface is then

$$t_s = 0.550 W^{0.314} \text{ sec} \tag{176}$$

The thermal power equations for the time limitations on the temperature and radius functions are four in number. For the hemispherical shape, the energy radiated between t_2 and t_m from the portion of the fireball in contact with the ground is lost from the fireball. The four functions are given by

$$P = 4.11 \times 10^{10} W^{1.161} t^{-1.077} \text{ cals/sec}, \quad t_2 \leq t \leq t_m \tag{177a}$$

$$P = 2.18 \times 10^{10} W^{1.320} t^{-1.585} \text{ cals/sec}, \quad t_m \leq t \leq t_s \tag{177b}$$

$$P = 2.51 \times 10^{10} W^{1.241} t^{-1.333} \text{ cals/sec}, \quad t_s \leq t \leq t_x \tag{177c}$$

and

$$P = 5.16 \times 10^{6} W^{0.628} \left[1 + 32.6e^{-K(t-t_x)} + 399e^{-2K(t-t_x)} + 2170e^{-3K(t-t_x)} + 4430e^{-4K(t-t_x)}\right] \text{ cals/sec}, \quad t \geq t_x \tag{177d}$$

Eq. 177b was determined, by joining Eq. 177a at t_m to Eq. 177c at t_s with a straight line in a logarithmic coordinate system, as an approximation of the change in radiant energy emission occurring with the change both in temperature and surface area while the shape of the fireball changes from hemispherical to spherical without change in total volume as it rises from the ground.

The radiant energy lost from the fireball, from integration of Pdt for Eq. 176, is

$$q_2(a) = 6.81 \times 10^{11} W^{1.126}(1 - 0.693W^{0.010} - 0.121W^{-0.038}) + 5.16 \times 10^{6} W^{0.628} \left[t + W^{0.460}(4060 - 64.2e^{-K(t-t_x)} - 393e^{-2K(t-t_x)} - 1420e^{-3K(t-t_x)} - 2180e^{-4K(t-t_x)}\right] \text{ cals} \tag{178}$$

For T equal to 1673 ^{o}K (1400^{o}C), substitution of the values for K and $(t-t_x)$ into Eq. 178 gives

$$q_2(a) = 6.81 \times 10^{11} W^{1.126}(1 - 0.693W^{0.010} - 0.0971W^{-0.038}) \tag{179}$$

For a yield of 2.3 MT, Eq. 179 gives a value of $q_2(a)$ that is 0.29 of the total weapon yield. It may be noted that Eqs. 177 through 179 do not support the postulate that requires $q_2(a)$ to be directly proportional to W. Since generalized yield limits were used to solve for $q_2(a)$, Eq. 179 is valid for a range of yields for the radiant energy lost between t_2 and the time at which the fireball temperature is 1400^{o}C.

4.2.6 Estimation of $n(\ell)/V$ for Model Surface Burst

The estimate of $n(\ell)/V$ for the model surface burst was made for the soil melting point of 1400°C. The time after detonation of 60 sec was used to minimize, to a degree, errors in the relative abundance of the short-lived fission product nuclide composition (many of the half-lives are estimated) and so that computations would apply to a surface detonation in the megaton yield range.

The discussion in the previous subsections was concerned with establishing the energy content and gas composition in the fireball at the time of the second temperature maximum. In order to estimate the molar concentration of the soil in the fireball at the time and temperature stated above, estimates of the energy utilization between the time of the second maximum and 60 secs are required. In this period, the following processes were considered: (1) cooling of the gases from T_2' to 1400°C and liquifaction of the vaporized soil with a resultant release of energy, (2) association of the gas atoms with a resultant release of energy, (3) loss of energy due to radiation from the fireball, (4) loss of energy due to expansion of the fireball gases against the atmosphere, (5) loss of energy due to heating and expansion of additional air, and (6) loss of energy due to heating and melting of a given amount of additional soil. These losses and gains in the energy among the fireball constituents and external substances have to be estimated and balanced in order to estimate the amount of soil present in the fireball that can be melted at 1400°C in process (6).

For a temperature of 6500 °K at the second maximum, Fig. 2 gives, for the surface burst

$$n = 4.88 \times 10^6 W \text{ moles of gas atoms} \qquad (180)$$

The value of the ratio of n_2''(gas atoms from the soil) to n(total gas atoms) from Eq. 145 is 0.395 so that

$$n_2' = 2.95 \times 10^6 W \text{ moles of air gas atoms} \qquad (181)$$

and

$$n_2'' = 1.93 \times 10^6 W \text{ moles of soil gas atoms} \qquad (182)$$

Upon complete condensation of the soil vaporized at t_2, the number of moles of soil formed would be 26 atoms per molecule

$$n''(\ell) = 7.42 \times 10^{4} W \text{ moles soil} \qquad (183)$$

The computational procedure for estimating the energy releases and losses for the first four processes is given by the following steps: (1) cool the gases from 6500 °K to 1673 °K at constant volume, (2) recombine the air gas atoms to gas molecules and the soil gas atoms to liquid soil, (3) subtract the radiant energy emitted, and (4) expand the gas volume from V_2 to V_m against the external pressure of 1 atm. The gases will be assumed to behave like an ideal monatomic gas so that the energy released in cooling to 1673° is, using 3 cal $mole^{-1}$ deg^{-1} for the heat capacity,

$$-Q_1^1 = 7.07 \times 10^{10} W \text{ cals} \qquad (184)$$

For the soil composition of $Na_2O \cdot Al_2O_3 \cdot 6SiO_2$ (as given previously), the single oxide energies were calculated from Reference 15 data as follows:

(1) $Na_2O(s)$, 298°K $\rightarrow$ 2Na(g), 298°K + O(g), 298°K, ΔH = 144,700 cal/mole

(2) $Na_2O(s)$, 298°K $\rightarrow$ $Na_2O(s)$, 1673°K, ΔH = 24,750 cal/mole

(3) O(g), 298°K $\rightarrow$ O(g), 1673°K ΔH = 6,880 cal/mole

(4) 2Na(g), 298°K $\rightarrow$ 2Na(g), 1673°K, ΔH = 13,750 cal/2 moles

(5) $Na_2O(s)$, 1673 $\rightarrow$ $Na_2O(\ell)$, 1673°K, ΔH = 7,200 cal/mole

Sum: (1)-(2)+(3)+(4)-(5): $Na_2O(\ell)$, 1673°K $\rightarrow$ 2Na(g), 1673°K + O(g), 1673°K, ΔH = 133,380 cal/mole

$$\Delta E = 133,380 - 3 \times 2 \times 1673 = 123,300 \text{ cal/mole}$$

Similar computations for Al_2O_3 and SiO_2 give, for

$Al_2O_3(\ell)$, 1673°K $\rightarrow$ 2Al(g), 1673°K + 3O(g), 1673°K, ΔH = 696,700 cal/mole

ΔE = 680,000 cal/mole

and, for

$$SiO_2(\ell),\ 1673^\circ K \rightarrow Si(g),\ 1673^\circ K + 2O(g),\ 1673^\circ K,\ \Delta H = 412{,}200 \text{ cal/mole}$$

$$\Delta E = 402{,}200 \text{ cal/mole}$$

For the dissociation of the molecule, $Na_2O \cdot Al_2O_3 \cdot 6SiO_2(\ell)$ as pure single component oxides to gas atoms at $1673^\circ K$, $\Delta E = 123{,}700$ cal per mole of gas atoms formed. The energy of dissociation of the air molecules $0.8\ N_2(g)$ and $0.2\ O_2(g)$ at $1673^\circ K$ is 79,400 cal/mole. Thus, for the second process,

$$-Q_2' = 2.95 \times 10^6 W \times 7.94 \times 10^4 + 1.93 \times 10^6 W \times 1.24 \times 10^5$$

$$= 4.73 \times 10^{11} W \text{ cals} \qquad (185)$$

The radiant energy lost for the 2.3 MT yield surface burst is

$$Q_3' = 0.290 \times 1.11 \times 10^{12} W \qquad (186)$$

$$= 3.22 \times 10^{11} W \text{ cals}$$

Eq. 186 applies only for W equal to 2.3 MT; for other yields Eq. 178 (divided by $1.11 \times 10^{12} W$) can be used to estimate Q_3'.

The fireball volume at the second maximum, from Eq. 160, is

$$V_2 = 7.92 \times 10^{11} W \text{ cm}^3 \qquad (187)$$

and the volume at maximum expansion, from Eq. 164, is

$$V_m = 1.64 \times 10^{12} W^{0.942} \text{ cm}^3 \qquad (188)$$

The change in volume is

$$\Delta V = 1.64 \times 10^{12} W \left[W^{-0.058} - 0.482\right] \qquad (189)$$

or, for the 2.3 MT yield ($W^{-0.058} = 0.638$),

$$V_m = 1.05 \times 10^{12} W \text{ cm}^3 \tag{190}$$

and

$$\Delta V = 2.56 \times 10^{11} W \text{ cm}^3 \tag{191}$$

The work associated with the expansion of the original fireball gases against 1 atmosphere is (1 cal = 41.29 cm^3-atmospheres)

$$Q_4' = P_o \Delta V = 0.062 \times 10^{11} W \text{ cals} \tag{192}$$

When the fireball reaches its maximum volume in expanding against the atmosphere, the total internal pressure in the fireball should be very close to the external pressure, which, for the model surface burst, has been taken to be 1 atmosphere. The total number of air molecules (plus a small amount of gaseous detonation products) in the fireball at 1400°C, by use of the perfect gas law, is then

$$n_T = 1.20 \times 10^7 W^{0.942} \text{ moles} \tag{193}$$

or, for 2.3 MT ($W^{-0.058} = 0.638$),

$$n_T = 7.66 \times 10^6 W \text{ moles} \tag{194}$$

With the exception of the Na_2O component, the partial pressure of the "soil" at its melting point should be negligible in comparison to a total pressure of 1 atmos.

The number of air molecules that have entered the fireball up to this time, neglecting the Na_2O soil component, is

$$n_3 = n_T - n_2'/2 \tag{195a}$$

$$= 1.20 \times 10^7 W \left[W^{-0.058} - 0.123 \right] \text{ moles} \tag{195b}$$

or, for 2.3 MT ($W^{-0.058} = 0.638$)

$$n_3 = 6.18 \times 10^6 W \text{ moles} \tag{196}$$

This number of moles of air is about 81 % of the gas molecules present in the fireball.

The change in internal energy of the air molecules in being heated from 298 °K to 1673 °K is 10,800 cals/mole. The total change in internal energy for this is

$$\Delta E_5 = 1.30 \times 10^{11} W \left[W^{-0.058} - 0.123 \right] \text{ cals} \tag{197}$$

For the n_3 moles of air initially at 298 °K and 1 atmos, the energy, or work, required for their expansion to V_m (against 1 atmos) is

$$q_5 = 3.27 \times 10^{10} W \left[W^{-0.058} + 0.027 \right] \text{ cals} \tag{198}$$

Some energy is also required for the mechanical mixing of the incoming gases with the gases already present in the fireball. The postulated assumption that the fireball volume remains constant after t_m until the gases are near ambient (i.e. 500 °K or lower) would require either that external gases enter before t_m or that the internal pressure be larger than 1 atmos. The yield-independent perfect gas law estimate of the pressure at t_2 is 3.3 atmos. If no additional gases enter before t_m, the pressure at t_m would be $0.84\ W^{0.106}$ atmos, or 1.9 atmos for the 2.3 MT yield. The temperature at this time is $3.46 \times 10^3\ W^{0.048}$ °K, or about 5000 °K for 2.3 MT so that recombination of the gas atoms would be occurring at this time. By the time the temperature decreased another 1000 °K, most of the O and N atoms would have recombined (note that the formation of nitrogen oxides has not been considered in this treatment) to form O_2 and N_2 atoms; also, many of the metallic atoms would have formed oxide molecules. The recombination should result in a drop in the pressure (between 4000 and 5000 °K) of about 30 % not considering the drop in temperature. At about 2500 °K, the soil constituents will start condensing into liquid droplets. This process should also tend to reduce the pressure further.

Assuming complete recombination when the fireball has cooled to 4000 °K, the number of gas molecules of the material originally

present at t_2 would be $3.41 \times 10^6 W$ moles so that the number of additional air molecules would be, from use of the perfect gas law,

$$n_3\ (4000^\circ K) = 5.00 \times 10^6 W\ (P W^{-0.058} - 0.682)\ \text{moles} \qquad (199)$$

where P is the total pressure of the gases in atmospheres. For n_3 equal to zero, the pressure would be about 1.1 atmos for the 2.3 MT yield. If the additional gas were as much as 25 % of the total present, the pressure would be about 1.4 atmos (2.3 MT).

For a reliable estimate of the mixing energy, the variation of the gas concentration of content in the fireball (e.g., the total pressure) with time is required. Since that cannot be deduced from the scaling equations, the end-point composition will be used to estimate the entropy and heat of mixing for a process in which the gases are at the same initial temperature and pressure when mixing occurs. For the computation, the mixing process will be assumed to occur at 3300 $^\circ$K (mid-temperature of 5000 $^\circ$K at t_m and 1673 $^\circ$K) the heat of mixing is then given by

$$q_5' = 3300\ n_T\ \Delta S_m \qquad (200)$$

where ΔS_m is the entropy of mixing at constant temperature and pressure. This computation can be interpreted either as a recognition that the gases are nonideal and some heat of mixing is involved, or, that the gases are nearly ideal and the entropy change due to mixing at the selected temperature is essentially a measure of the reversible work required to do the mixing. The overall value of ΔS_m (constant T and P) for the estimation is defined by

$$\Delta S_m = -R\ \left[(n_2'/n_T)\ell n(n_2'/n_T) + (n_3/n_T)\ell n(n_3/n_T)\right] \qquad (201)$$

For the final mixture, ΔS_m is 0.98 cals/mole and

$$q_5' = 3.88 \times 10^{10} W^{0.942}\ \text{cals} \qquad (202)$$

The total energy for the heating, expansion, and mixing of the air, is the sum of Eqs. 197, 198, and 202 and is given by

$$Q_5' = 2.02 \times 10^{11} W \left[W^{-0.058} - 0.075\right] \quad (203)$$

or, for 2.3 MT ($W^{-0.058} = 0.638$)

$$Q_5' = 1.14 \times 10^{11} W \quad (204)$$

The summation of Eqs. 184, 185, 186, 192 and 204 gives a residual of 1.02×10^{11} W cals for heating and melting soil. If the temperature were uniform throughout the fireball and if the soil particles melted instantaneously, only liquid soil would exist. This condition undoubtedly does not occur because of the low thermal conductivity of soils. Many of the particles that enter the fireball at the time the highest temperature for the existence of a liquid phase is reached (about 2500 °K) would be completely melted (it takes about 33 secs for the temperature to drop from 2500 °K to 1673 °K for the 2.3 MT yield) while those that were entering just as the melting temperature occurred would not be melted at all. The latter would, however, be heated to some degree and therefore would have absorbed some of the available energy -- as would the solid phase in the interior of other particles that entered at intermediate times and were partially melted. Considering that more soil would be vaporized between t_2 (1.5 sec) and the time at which the temperature has decreased to 2500 °K at t_x (27 secs) together with the melting of additional soil from 2500 °K to 1673 °K, the fraction of available energy for melting should lie between 0.25 and 0.75. Thus, the final proportionment of the energy, like others previously, is an assigned amount; the fraction, 0.5 of the residual energy, or 0.51×10^{11} W cals for the 2.3 MT yield, was taken to make the estimate of the number of moles of liquid soil present in the fireball at the selected soil melting point.

The change in heat content of soil minerals such as the ideal soil defined previously, for a rise in temperature from 298 °K to 1673 °K, would be about 200,000 cal/mole. The heat of fusion would be about 50,000 cal/mole. The number of moles of melted soil is then

$$n(\ell) = 2.04 \times 10^5 W + 0.74 \times 10^5 W \text{ moles} \quad (205a)$$

$$= 2.78 \times 10^5 W \text{ moles} \quad (205b)$$

And, for the 2.3 MT yield, the average concentration of the liquid phase in the fireball is

$$n(\ell)/V_m = 2.65 \times 10^{-7} \text{ moles/cm}^3 \qquad (206)$$

The value of $(n(\ell)/V)RT$ ($T = 1673^\circ K$) is then 3.64×10^{-2} atmospheres; it is used in Section 7 to compute the fraction of each fission product element that has condensed into the liquid phase of the idealized carrier material.

Not considering the amount of soil vaporized initially (up to t_2), which by Eq. 205 was about 0.27 of $n(\ell)$, only 4.6 % of the total energy was used to melt soil for the 2.3 MT yield surface burst. For a low yield tower shot, Adams[6] estimated that about 3 % of the total energy was used in heating soil and tower materials. The total energy content of the liquid soil at its melting point therefore represents about 6.3 % of the total. According to Eq. 205, the total mass of liquid soil is 3.4×10^{11} gm (about 380,000 tons); this mass, from Eq. 88 represents about 5.4 % of the mass thrown out of the crater by the 2.3 MT yield detonation.

No argument can be given regarding the accuracy of the fireball scaling functions and the thermal data used to arrive at the final value of $n(\ell)/V$. Certainly many improvements can be made with more detailed treatment of the many parameters when more of the needed data become unclassified. The treatment of the data in this section, although preliminary in scope, has identified some types of information and parameters required, and has attempted to place them in a conceptual framework with respect to their role in the fallout formation process.

SECTION 5

FISSION YIELDS FOR FISSION OF U^{235}, U^{238}, AND Pu^{239}

One major factor that determines the amount of a fission product that condenses during the first period of condensation is the amount of that element present in each of the mass chains when the carrier solidifies. According to the equations given in Section 2, the fractional chain yield of each element is required for estimating the "R" factor for the chain relative to the number of fissions, or to the yield of Mo^{99} or some other reference nuclide.

The independent yields of all the radionuclides have been calculated by Bolles and Ballou[13] for thermal neutron fission of U^{235} according to the theories of independent fission yields of Glendenin[17] and of Present.[18] The fractional chain yields from these calculations are given from 0 to 189 sec in Table 5 for mass 89 and in Table 6 for mass 140; each chain contains a rare gas (Kr and Xe) element. The two mass chains selected lie on the outer edge of the two yield peaks. In each case, the independent yield distribution according to the Glendenin theory is the broader, with the short-lived, lowest-Z elements more heavily weighted. This difference diminishes as the mass number approaches the value 118.

The fractional yields themselves indicate what might be expected as to the fractionation of the chain members during condensation. For example, if the rare gas member only is considered, the maximum loss (minimum amount condensed) should occur for mass 89 between 19 and 28 secs (Glendenin); and for mass 140, the fraction not condensed (for both theories of yield) should decrease as the time period of the condensation process increases.

Similar calculations have not been made for the independent yields, for fission of U^{235} and Pu^{239} with fission-spectrum neutrons nor for U^{238} fission with 8 Mev broad-band spectrum neutrons which would be more applicable to nuclear detonations. Moreover, the chain yields themselves for Pu^{239} and U^{238} fission are not very well known. Most

TABLE 5

Fractional Chain Yields for Mass 89 for U^{235} Fission

t (sec)	Present					Glendenin				
	Se	Br	Kr	Rb	Sr	Se	Br	Kr	Rb	Sr
0	0.05	0.372	0.528	0.100	0	0.170	0.420	0.343	0.067	0
1		0.325	0.571	0.104	0	0.121	0.410	0.399	0.070	0
2		0.280	0.612	0.108	0	0.087	0.390	0.452	0.071	0
3		0.245	0.644	0.111	0	0.062	0.362	0.502	0.074	0
4		0.212	0.673	0.115	0	0.044	0.332	0.547	0.077	0
6		0.159	0.720	0.121	0	0.022	0.266	0.629	0.083	0
9		0.102	0.764	0.133	0.0014	0.008	0.182	0.720	0.090	0
13		0.056	0.794	0.147	0.0021	0.002	0.106	0.786	0.105	0.0012
19		0.022	0.809	0.166	0.0030		0.044	0.830	0.124	0.0020
28		0.0054	0.798	0.195	0.0043		0.011	0.832	0.155	0.0032
41			0.764	0.232	0.0064		0.002	0.800	0.192	0.0050
60			0.707	0.283	0.0097			0.744	0.249	0.0076
88			0.638	0.347	0.015			0.670	0.318	0.012
129			0.564	0.436	0.025			0.559	0.419	0.022
189			0.433	0.520	0.047			0.456	0.500	0.044

TABLE 6

Fractional Chain Yields for Mass 140 for U^{235} Fission

t (sec)	Present					Glendenin				
	I	Xe	Cs	Ba	La	I	Xe	Cs	Ba	La
0	0.074	0.493	0.399	0.034	0	0.138	0.408	0.366	0.088	0
1	0.047	0.498	0.416	0.039	0	0.087	0.441	0.380	0.092	0
2	0.029	0.495	0.433	0.043	0	0.055	0.453	0.395	0.097	0
3	0.019	0.485	0.449	0.048	0	0.034	0.454	0.412	0.100	0
4	0.012	0.470	0.466	0.052	0	0.022	0.447	0.426	0.105	0
6	0.005	0.438	0.493	0.064	0	0.009	0.423	0.453	0.115	0
9	0.001	0.389	0.531	0.079	0	0.002	0.377	0.491	0.130	0
13		0.328	0.570	0.102	0		0.318	0.531	0.151	0
19		0.252	0.609	0.139	0		0.246	0.569	0.185	0
28		0.170	0.632	0.198	0		0.167	0.592	0.241	0
41		0.097	0.619	0.284	0		0.095	0.584	0.321	0
60		0.043	0.555	0.402	0		0.041	0.526	0.433	0
88		0.013	0.439	0.548	0		0.012	0.416	0.572	0
129		0.002	0.294	0.704	0		0.002	0.278	0.720	0
189		0.001	0.157	0.842	0			0.149	0.851	0

of the available data and estimates of unmeasured yields are summarized in Table 7 for the fission of U^{235}, U^{238}, and Pu^{239}. The bulk of the data were taken from the summary by Katcoff.[19] The yield curve for thermal neutron fission of U^{235} gives an average value of 2.5 neutrons per fission. For fission-spectrum neutron fission of U^{238}, an average value of 3.1 neutrons per fission is obtained. These values, together with the referenced data in Table 7, were used to obtain a set of stylized yield curves for fission-neutron fission of U^{235} and Pu^{239} and the 8 Mev-neutron fission of U^{238}. In each case, the fission by fission-neutrons was assumed to yield about 3 neutrons per fission and the 8 Mev-neutron fission to yield 4 neutrons per fission. For this change in neutron yield per fission with neutron energy, 14-Mev neutron fission would give about 4.5 neutrons/fission. The increase in the neutron energy from thermal to fission-spectrum energies shifted the right side of the heavy-element peak to heavier masses by about 1/4 mass unit (for the same yield). Where there was no data to indicate possible changes in the "fine" structure shape of the yield curve at the peak, the general shape of the thermal-neutron yield curves was retained but adjusted in height so that the peak sum was reasonably near 100.0. The large discrepancy in the rare earth yields for thermal neutron fission of Pu^{239}, between Katcoff's values and those given by Bunney,[20] may be due to persistent errors in the counter calibration. The yield values given by Bunney are lower by a factor of 1.5 at mass number 144 and approach Katcoff's values as the mass increases; at mass number 156, Bunney's value is only about 20 percent lower. The values given by Katcoff give a peak sum nearer 100 and were therefore used in Table 7.

Comparison of the cumulative chain yields at the two peaks (A = 90 to 100 and A = 131 to 144) for the various types of fission indicates that no very large differences in the decay rates should be expected. Of the three mentioned yield curves, the yields for fission-neutron fission of Pu^{239} appear to differ most from those of thermal neutron fission of U^{235}. For mass numbers such as 140 and 95 whose radioisotopes may contribute more than 80 percent of the total gamma radiation at specific times after fission, the largest percentage difference is 5.0/6.44, or 28 percent (lower) for mass number 140 and 5.6/6.27, or 11 percent (lower) for mass number 95. The yield of mass number 90, however, is significantly lower for U^{238} (8 Mev neutrons) and Pu^{239} (fission neutrons); the percentage differences are 36 percent (lower) and 48 percent (lower), respectively. The yields of mass number 137 are all more nearly alike. The largest differences, of course, occur for the mass numbers in the valley between the peaks and those at the highest and lowest mass numbers. But even for U^{238} fission (8 Mev neutrons), where the yields of the mass numbers near 118 are more than a factor of ten larger than for

U^{235} fission (thermal neutrons), the contribution of these elements will be a small fraction of the total activity.

The "R" factors due to the different yields will be more sensitive to small changes in abundances than the gross decay curve. Using the U^{235} fission with thermal neutrons as a standard, the yield "R" factors for mass 144, for example, are 0.89 (U^{235}, fission neutrons), 0.74 (U^{238}, 8 Mev neutrons), and 0.87 (Pu^{239}, fission neutrons); for mass number 115 the respective yield "R" factors are 1.6, 14, and 6.8.

For the computations presented in the next two sections, the independent yields as calculated by Bolles and Ballou[13] for thermal neutron fission of U^{235} were converted to fractional chain yields. The same fractional chain yields were then used for all fission yield curves.

Although it appears that Glendenin's symmetrical charge-distribution curve is generally applicable for all fissile nuclides in low-energy neutron fission, it has been shown that the most probable charge, Z_p, for a given mass split shifts toward stability with increasing neutron energy; i.e. the higher fractional yields would appear farther to the right (higher Z) in any decay chain.[21] Pappas[22] used a discontinuous function for Z_p and considered the primary fragments before neutron boil-off; Wahl[23] has shown empirically however that the Z_p function in thermal fission of U^{235} is continuous, as originally postulated by Glendenin et al.[24] Herrington[25] proposes two charge-distribution curves, one for even-neutron nuclides and another showing lower yield for odd-neutron nuclides.

It is clear that there is no unequivocal choice in methods for estimating the independent yields of the chain members, even for thermal neutron fission of U^{235}. For higher-energy fission the experimental data on independent yield are rarer yet. It was therefore assumed that the fractional independent yields calculated by Bolles and Ballou on Glendenin's postulate for thermal fission of U^{235} would not be too inappropriate for any kind of low-energy fission. When more data on the total chain yields and the independent yields are available for each fissile nuclide, the indicated corrections can be applied to the computations.

TABLE 7

Cumulative Mass-Chain Yields of Fission Products
(Values are in percent of fissions)

Mass Number	U^{235}		U^{238}		Pu^{239}	
	Thermal Neutrons*	Fission Neutrons	Fission Neutrons	8-Mev Neutrons	Thermal Neutrons	Fission Neutrons
72	1.6×10^{-5}	4.6×10^{-4}	5.0×10^{-6}	-	1.2×10^{-4}*	-
73	1.1×10^{-4}	0.0012	3.7×10^{-5}	-	2.2×10^{-4}	-
74	(3.2×10^{-4})[a]	0.0034	1.1×10^{-4}	0.001	4.1×10^{-4}	0.0011
75	(8.8×10^{-4})	0.0062	8.3×10^{-4}	0.0040	7.5×10^{-4}	0.0023
76	(0.0029)	0.012	0.0012	0.0078	0.0014	0.0051
77	0.0083	0.023	0.0038*	0.014	0.0026	0.011
78	0.021	0.048	0.0095	0.026	0.0049	0.025
79	(0.041)	0.096	0.019	0.053	0.0090	0.043
80	(0.077)	0.19	0.045	0.096	0.016	0.075
81	0.14	0.21	0.088	0.18	0.030	0.14
82	(0.29)	0.50	0.20	0.35	0.056	0.23
83	0.544	0.80	0.40*	0.66	0.10	0.37
84	1.00	1.3	0.85*	1.02	0.17	0.60
85	1.30	1.85	0.80	1.45	0.28	0.92
86	2.02	2.5	1.38*	1.9	0.45	1.15
87	(2.94)	3.3	1.90	2.25	0.73	1.5
88	(3.92)	4.2	2.45	2.7	1.2	1.9
89	4.79	5.1	2.9*	3.17	1.9*	2.4

Continued

*Seymour Katcoff, Fission-Product Yields From U, Th and Pu, Nucleonics, Vol. 16, No. 4, p. 78-85 (1958).

**L.R. Bunney, E.M. Scadden, J.O. Abriam and N.E. Ballou, Radiochemical Studies of the Fast Neutron Fission of U^{235} and U^{238}, Second UN International Conference on the Peaceful Uses of Atomic Energy, A/Conf. 15/P/643, USA, June 1958.

***G.P. Ford, J.S. Gilmore, et al, Fission Yields, LADC-3083.

****L.R. Bunney, E.M. Scadden, J.O. Abriam, N.E. Ballou. Fission Yields in Neutron Fission of Pu^{239}, USNRDL-TR-268, 1958, Uncl.

a. Parentheses indicate estimated values or where Katcoff's value was altered in order to adjust the yields to a gross sum of 100 in each peak.

b. Line indicates division of two peaks that was used for individual peak sums.

TABLE 7 (Cont'd)

Cumulative Mass-Chain Yields of Fission Products
(Values are in percent of fissions)

Mass Number	U^{235}		U^{238}		Pu^{239}	
	Thermal Neutrons*	Fission Neutrons	Fission Neutrons	8-Mev Neutrons	Thermal Neutrons	Fission Neutrons
90	5.77	5.8	3.2*	3.7	2.4	3.0
91	5.84	5.85	3.6	4.3	3.0	3.7
92	6.03	6.0	4.1	4.8	3.7	4.4
93	6.45	6.4	4.85	5.2	4.6	5.0
94	6.40	6.4	5.3	5.45	5.5	5.4
95	6.27	6.3	5.7*	5.6	5.9*	5.6
96	6.33	6.3	5.8	5.7	5.7	5.3
97	6.09	6.1	5.7	5.64	5.6*	5.2*
98	5.78	5.8	5.7	5.6	5.4	5.4
99	6.06	6.1**	6.3*	6.2**	5.9*	5.9*
100	6.30	6.7	6.1	6.4	6.0	6.4
101	5.0	5.3	5.5	6.5	6.0	5.9
102	4.1	2.9	5.6	5.9	5.9	5.3
103	3.0	1.7	6.6	5.0	5.8*	4.6
104	1.8	0.95	5.4	3.2	5.0	3.5
105	0.90	0.54	3.9	2.2	3.9*	3.2
106	0.38	0.30	2.7*	1.5	5.0*	3.6
107	0.19	0.17	1.35	1.0	4.0	3.1
108	(0.085)	0.095	0.67	0.70	3.0	2.6
109	(0.039)	0.053***	0.32*	0.48	1.5*	1.9*
110	(0.020)	0.030	0.15	0.33	0.65	0.81
111	(0.015)	0.022***	0.073*	0.23***	0.27*	0.34
112	(0.013)	0.020***	0.046*	0.19	0.10*	0.14*
113	(0.012)	0.018	0.043	0.17	0.055	0.090
114	(0.011)	0.017	0.041	0.16	0.046	0.075
115	0.0104	0.017***	0.040*	0.15***	0.041*	0.069*
116	(0.010)[b]	0.017[b]	0.039	0.14	0.039	0.065
117	(0.010)	0.017	0.039	0.14[b]	0.038	0.064
118	(0.010)	0.017	0.040[b]	0.14	0.038[b]	0.064[b]
119	(0.011)	0.017	0.041	0.14	0.039	0.064

Continued

TABLE 7 (Cont'd)

Cumulative Mass-Chain Yields of Fission Products
(Values are in percent of fissions)

Mass Number	U^{235} Thermal Neutrons*	U^{235} Fission Neutrons	U^{238} Fission Neutrons	U^{238} 8 Mev Neutrons	Pu^{239} Thermal Neutrons	Pu^{239} Fission Neutrons
120	(0.011)	0.018	0.042	0.15	0.041	0.065
121	(0.012)	0.020	0.044	0.16	0.044*	0.066
122	(0.013)	0.022	0.046	0.17	0.047	0.069
123	(0.015)	0.030	0.050	0.19	0.052	0.076
124	(0.017)	0.053	0.055	0.23	0.058	0.082
125	0.021	0.095	0.072	0.33	0.072*	0.14
126	(0.058)	0.17	0.175	0.48	0.175	0.35
127	(0.145)	0.30	0.39	0.70	0.39*	0.80
128	0.37	0.54	0.77	1.0	0.77	1.9
129	0.90	0.95	1.45	1.5	1.45	2.5
130	2.0	1.7	2.5	2.2	2.5	3.2
131	(2.88)	2.9	3.2*	3.2	3.8*	3.8
132	(4.31)	4.3	4.7*	4.4	5.0	4.6
133	(6.48)	6.1	5.5*	5.4	5.27*	4.9
134	(7.80)	7.3	6.6*	6.5	5.69*	5.2
135	(6.40)	6.3	6.0*	5.9	5.53*	5.1
136	(6.36)	6.4	5.9*	5.8	5.06*	5.3
137	(6.05)	6.0	6.2	5.85	5.24*	6.4*
138	5.74	5.7	6.4	5.9	5.5	5.4
139	(6.34)	6.4	6.5	6.0	5.7*	5.2
140	6.44	6.4	5.7*	5.6	5.68*	5.0*
141	(6.30)	6.3	5.7	5.5	5.2*	4.7
142	(5.85)	5.9	5.7	5.4	6.69*	4.9
143	(5.87)	5.8	5.5	4.97	5.4*	5.0
144	5.67	5.1**	4.9*	4.3**	5.29*	4.8
145	3.95	4.2	3.7	3.7	4.24*	4.4
146	3.07	3.3	3.1	3.17	3.53*	3.7
147	2.38	2.5**	2.6**	2.7**	2.92*	3.0
148	1.70	1.85	2.0	2.27	2.28*	2.36
149	1.13	1.3**	1.45	1.9**	1.75	1.86

Continued

TABLE 7 (Cont'd)

Cumulative Mass-Chain Yields of Fission Products
(Values are in percent of fissions)

Mass Number	U^{235}		U^{238}		Pu^{239}	
	Thermal Neutrons*	Fission Neutrons	Fission Neutrons	8 Mev Neutrons	Thermal Neutrons	Fission Neutrons
150	0.67	0.80	1.05	1.45	1.38*	1.48
151	0.45	0.50	0.74	1.02	1.08	1.16
152	0.285	0.31	0.50	0.66	0.83*	0.92
153	0.15	0.19**	0.32	0.41**	0.52	0.60
154	0.077	0.096	0.19	0.25	0.32*	0.37
155	0.033	0.048	0.11	0.15	0.20	0.23
156	0.014	0.023**	0.066*	0.092**	0.12*	0.14
157	0.0078	0.012	0.034	0.057	0.064	0.075
158	0.002	0.0062	0.016	0.032	0.034	0.043
159	0.00107	0.0034**	0.0090**	0.017**	0.020****	0.025
160	3.5×10^{-4}	0.0012	0.0036	0.0085	0.0092	0.011
161	7.6×10^{-5}	4.6×10^{-4}**	9.4×10^{-4}	0.0044**	0.0038****	0.0051

*Seymour Katcoff, Fission-Product Yields From U, Th and Pu, Nucleonics, Vol. 16, No. 4, p. 78-85 (1958).

**L.R. Bunney, E.M Scadden, J.O. Abriam and N.E. Ballou, Radiochemical Studies of the Fast Neutron Fission of U^{235} and U^{238}, Second UN International Conference on the Peaceful Uses of Atomic Energy, A/Conf. 15/P/643, USA, June 1958.

***G.P. Ford, J.S. Gilmore, et al, Fission Yields, LADC-3083.

****L.R. Bunney, E.M. Scadden, J.O. Abriam, N.E. Ballou. Fission Yields in Neutron Fission of Pu^{239}, USNRDL-TR-268, 1958, Uncl.

a. Parentheses indicate estimated values or where Katcoff's value was altered in order to adjust the yields to a gross sum of 100 in each peak.

b. Line indicates division of two peaks that was used for individual peak sums.

SECTION 6

CALCULATION OF DISINTEGRATION RATES, PHOTON EMISSION RATES, PHOTON-ENERGY EMISSION RATES, AND AIR-IONIZATION RATES FROM NORMAL FISSION PRODUCTS OF U^{235}, U^{238}, AND Pu^{239}

6.1 DESCRIPTION OF COMPUTATIONS

In making the computations, the fractional chain yields were taken to be the same for all fissile nuclides as were discussed in Section 5. For this stipulation, the disintegration rate per fission of a given fission product nuclide from each fissile nuclide differs only by a constant. It was therefore convenient to use the disintegration rates calculated by Bolles and Ballou[13] for thermal fission of U^{235} and multiply them by the ratio of the yields from the fissile nuclide of interest to that from the thermal fission of U^{235}, in order to obtain the disintegration rates desired. These ratios are the same as the yield "R" values given in Section 3. The summation over all masses time-wise gives the total fission product disintegration rate.

Where decay schemes of individual fission products are known, gamma ray characteristics may also be computed. If the particular characteristics are evaluated per disintegration of each radionuclide, each disintegration rate value can be multiplied by the appropriate factor time-wise and the products for all nuclides summed to give the total characteristic of the mixture.

The disintegration rates, photon emission rates, photon energy emission rates, and air ionization rates were computed for times extending from 45.8 minutes to 25.7 years after fission for the 3 fissile nuclides. The first three rate curves were calculated for 10^4 fissions; the last was for the air ionization 3 ft above a smooth infinite plane uniformly contaminated with 10^4 fissions/sq ft. The required basic decay scheme information was taken from a previous report[26] and a current revision[27] including nuclear data through July 1959. Details of the method of calculation of the air ionization rates have been published.[28]

6.2 RESULTS OF COMPUTATIONS

The results of the computations are summarized in Table 8 as decay data for thermal-neutron fission of U^{235}, fission-neutron fission of U^{235}, 8 Mev-neutron fission of U^{238}, thermal-neutron fission of Pu^{239}, and fission-neutron fission of Pu^{239}. The use of Katcoff's yields[19] (adjusted) for thermal fission give disintegration rates that are almost identical with those of Bolles and Ballou. The air ionizations (U^{235}, thermal) are also very close to those of Reference 19; at 2.4 hr, they are about 8 % higher and at 2.6 y they are about 19 % lower (maximum fluctuation).

Dolan[29,30] has calculated the disintegration rates and photon emission rates for 14 Mev neutron fission of U^{238}; ratios of his values to those in Table 8 for the 8 Mev neutron fission of U^{238} are given in Fig. 3. It may be noted that the disintegration rates are within 5 % of each other from 1 to about 350 hours; the agreement in the photon emission rates is not quite as good, with Dolan's values being more than 10 % lower after 40 hrs. The maximum spread is +5 % (75 h) to -12 % (2500 h) for the d/s computations and +3 % (7.5 h) to -17 % (1200 h) for the photons/sec computations. A few more photons were counted in the method by which the data in Table 8 were obtained than by the method used by Dolan (chiefly in the energy range 0 to 20 Kev).

The air ionization-rate curves from each type of fission are of chief interest; these are compared in Figs. 4 and 5 in terms of an air ionization "R" factor. The factor, r_{fp}, is the ratio of the air ionization-rate from one type of fission to that from thermal neutron fission of U^{235}. The fluctuation in the curves of Figs. 4 and 5 reflect the relative prominence of the important gamma emitters in each mixture. The deviation in r_{fp} from the value 1 is a measure of the difference in the ionization rate from that of the U^{235} thermal fission reference curve. The order in the r_{fp} deviations, from least to most, is: (1) fission neutron fission of U^{235}, (2) 8 Mev neutron fission of U^{238}, (3) fission neutron fission of Pu^{239}, and (4) thermal neutron fission of Pu^{239}. The maximum relative deviation for the first three (combined) is from -16 % (2.5 h) to +5.5 % (110 h) between 1 and 7000 hours after fission. However, between 2 and 3 years after fission the U^{238} (8 Mev) r_{fp} value is almost 1.6 and the Pu^{239} (fission) r_{fp} value is almost 2.2, reflecting the higher yields for the rare earth elements (heavy mass peak).

The two main factors that determine the gross decay of the normal product mixtures (besides the half-lives and the individual

TABLE 8

Decay of Normal Fission Products From U^{235}, U^{238} and Pu^{239}
1. dis/sec for 10^4 fission (Glendenin)

Age			U^{235}		U^{238}	Pu^{239}	
Years	Days	Hours	Thermal	Fission	(8 Mev)	Thermal	Fission
		0.763	1.618	1.615	1.598	1.558	1.536
		1.12	1.072	1.076	1.043	1.008	1.001
		1.64	0.6860	0.6933	0.6578	0.6253	0.6269
		2.40	0.4361	0.4454	0.4152	0.3867	0.3936
		3.52	0.2818	0.2908	0.2691	0.2473	0.2568
		5.16	0.1847	0.1916	0.1780	0.1640	0.1734
		7.56	0.1228	0.1271	0.1195	0.1117	0.1186
		11.1	(1) 8171	(1) 8393	(1) 8000	(1) 7661	(1) 8036
		16.2	(1) 5280	(1) 5373	(1) 5201	(1) 5107	(1) 5245
		23.8	(1) 3311	(1) 3341	(1) 3291	(1) 3304	(1) 3318
	1.45	34.8	(1) 2037	(1) 2042	(1) 2049	(1) 2092	(1) 2062
	2.13	51.1	(1) 1223	(1) 1219	(1) 1250	(1) 1297	(1) 1260
	3.12	74.9	(2) 7417	(2) 7381	(2) 7698	(2) 8062	(2) 7751
	4.57		(2) 4787	(2) 4778	(2) 4978	(2) 5205	(2) 4982
	6.70		(2) 3239	(2) 3236	(2) 3323	(2) 3448	(2) 3290
	9.82		(2) 2227	(2) 2222	(2) 2247	(2) 2318	(2) 2198
	14.4		(2) 1523	(2) 1502	(2) 1501	(2) 1548	(2) 1453
	21.1		(2) 1025	(2) 1001	(2) 1002	(2) 1036	(3) 9635
	30.9		(2) 6823	(3) 6603	(3) 6662	(3) 6910	(3) 6385
	45.3		(3) 4456	(3) 4277	(3) 4365	(3) 4544	(3) 4191
	66.4		(3) 2872	(3) 2743	(3) 2814	(3) 2961	(3) 2733
	97.3		(3) 1838	(3) 1764	(3) 1790	(3) 1925	(3) 1780
	143		(3) 1117	(3) 1088	(3) 1082	(3) 1170	(3) 1080
	208		(4) 6162	(4) 6078	(4) 5938	(4) 7133	(4) 6507
	301		(4) 3192	(4) 3174	(4) 3140	(4) 4175	(4) 3722
1.2	438		(4) 1676	(4) 1666	(4) 1710	(4) 2506	(4) 2185
1.78	650		(5) 9854	(5) 9766	(4) 1025	(4) 1538	(4) 1341
2.60			(5) 6010	(5) 5978	(5) 6236	(5) 8855	(5) 7926
3.80			(5) 3715	(5) 3732	(5) 3740	(5) 4617	(5) 4406
5.58			(5) 2479	(5) 2536	(5) 2359	(5) 2332	(5) 2479
8.18			(5) 1915	(5) 1987	(5) 1731	(5) 1449	(5) 1683
12.0			(5) 1509	(5) 1589	(5) 1323	(5) 1036	(5) 1253
17.6			(5) 1189	(5) 1261	(5) 1027	(6) 7922	(6) 9719
25.7			(6) 9079	(6) 9624	(6) 7814	(6) 6061	(6) 7465

Continued

TABLE 8 (Cont'd)

Decay of Normal Fission Products From U^{235}, U^{238}, and Pu^{239}
2. betas/sec for 10^4 fissions (Glendenin)

Age			U^{235}		U^{238}	Pu^{239}	
Years	Days	Hours	Thermal	Fission	(8 Mev)	Thermal	Fission
		0.763	1.544	1.543	1.527	1.482	1.466
		1.12	1.009	1.015	0.9816	0.9432	0.9398
		1.64	0.6358	0.6444	0.6076	0.5724	0.5767
		2.40	0.3983	0.4081	0.3763	0.3457	0.3542
		3.52	0.2547	0.2637	0.2402	0.2170	0.2272
		5.16	0.1655	0.1722	0.1571	0.1420	0.1515
		7.56	0.1088	0.1130	0.1042	(1) 9556	0.1025
		11.1	(1) 7159	(1) 7377	(1) 6932	(1) 6518	(1) 6892
		16.2	(1) 4581	(1) 4680	(1) 4496	(1) 4346	(1) 4484
		23.8	(1) 2866	(1) 2905	(1) 2860	(1) 2840	(1) 2853
	1.45	34.8	(1) 1781	(1) 1697	(1) 1804	(1) 1831	(1) 1802
	2.13	51.1	(1) 1093	(1) 1095	(1) 1125	(1) 1165	(1) 1130
	3.12	74.9	(2) 6837	(2) 7117	(2) 6847	(2) 7450	(2) 7166
	4.57		(2) 4532	(2) 4558	(2) 4698	(2) 4911	(2) 4709
	6.70		(2) 3102	(2) 3130	(2) 3155	(2) 3268	(2) 3128
	9.82		(2) 2143	(2) 2158	(2) 2121	(2) 2180	(2) 2076
	14.4		(2) 1455	(2) 1460	(2) 1404	(2) 1440	(2) 1360
	21.1		(3) 9707	(3) 9701	(3) 9216	(3) 9454	(3) 9856
	30.9		(3) 6373	(3) 6350	(3) 5999	(3) 6158	(3) 5740
	45.3		(3) 4108	(3) 4083	(3) 3852	(3) 3963	(3) 3694
	66.4		(3) 2632	(3) 2608	(3) 2459	(3) 2559	(3) 2390
	97.3		(3) 1697	(3) 1684	(3) 1581	(3) 1690	(3) 1579
	143		(3) 1025	(3) 1025	(4) 9610	(3) 1075	(4) 9900
	208		(4) 5919	(4) 5920	(4) 5587	(4) 6756	(4) 6167
	301		(4) 3113	(4) 3110	(4) 3033	(4) 4070	(4) 3616
1.2	438		(4) 1639	(4) 1629	(4) 1666	(4) 2469	(4) 2140
1.78	650		(5) 9542	(5) 9455	(5) 9922	(4) 1511	(4) 1307
2.60			(5) 5708	(5) 5680	(5) 5921	(5) 8595	(5) 7605
3.80			(5) 3419	(5) 3442	(5) 3444	(5) 4364	(5) 7605
5.58			(5) 2194	(5) 2257	(5) 2080	(5) 2089	(5) 2181
8.18			(5) 1643	(5) 1723	(5) 1469	(5) 1218	(5) 1401
12.0			(5) 1255	(5) 1343	(5) 1082	(6) 8220	(6) 9919
17.6			(6) 9621	(5) 1041	(6) 8124	(6) 6002	(6) 7378
25.7			(6) 7129	(6) 7737	(6) 5974	(6) 4412	(6) 5456

Continued

TABLE 8 (Cont'd)

Decay of Normal Fission Products from U^{235}, U^{238}, and Pu^{239}
3. photons/sec for 10^4 fissions (Glendenin)

Age			U^{235}		U^{238}	Pu^{239}	
Years	Days	Hours	Thermal	Fission	(8 Mev)	Thermal	Fission
		0.763	1.937	1.934	1.928	1.965	1.921
		1.12	1.280	1.278	1.259	1.269	1.250
		1.64	0.8049	0.8068	0.7821	0.7688	0.7658
		2.40	0.4908	0.4977	0.4751	0.4495	0.4581
		3.52	0.2971	0.3060	0.2904	0.2654	0.2798
		5.16	0.1815	0.1893	0.1810	0.1628	0.1776
		7.56	0.1149	0.1204	0.1165	0.1052	0.1166
		11.1	(1) 7584	(1) 7901	(1) 7741	(1) 7156	(1) 7808
		16.2	(1) 4989	(1) 5146	(1) 5090	(1) 4866	(1) 5133
		23.8	(1) 3239	(1) 3310	(1) 3307	(1) 3268	(1) 3326
	1.45	34.8	(1) 2106	(1) 2140	(1) 2151	(1) 2180	(1) 2157
	2.13	51.1	(1) 1355	(1) 1372	(1) 1355	(1) 1444	(1) 1398
	3.12	74.9	(2) 8799	(2) 8907	(2) 9118	(2) 9597	(2) 9145
	4.57		(2) 5886	(2) 5968	(2) 6115	(2) 6461	(2) 6097
	6.70		(2) 3927	(2) 3974	(2) 4050	(2) 4267	(2) 3994
	9.82		(2) 2582	(2) 2590	(2) 2626	(2) 2753	(2) 2551
	14.4		(2) 1644	(2) 1629	(2) 1648	(2) 1720	(2) 1577
	21.1		(2) 1020	(3) 9949	(2) 1019	(2) 1064	(3) 9640
	30.9		(3) 6166	(3) 5895	(3) 6212	(3) 6526	(3) 5849
	45.3		(3) 3573	(3) 3334	(3) 3665	(3) 3895	(3) 3467
	66.4		(3) 2014	(3) 2100	(3) 1832	(3) 2268	(3) 2015
	97.3		(3) 1165	(3) 1053	(3) 1213	(3) 1330	(3) 1188
	143		(4) 6400	(4) 5830	(4) 6540	(4) 7310	(4) 6540
	208		(4) 3342	(4) 3179	(4) 3335	(4) 3810	(4) 3460
	301		(4) 1421	(4) 1393	(4) 1431	(4) 1728	(4) 1568
1.2	438		(5) 5158	(5) 5176	(5) 5631	(5) 7512	(5) 6714
1.78	650		(5) 2117	(5) 2158	(5) 2647	(5) 3752	(5) 3334
2.60			(5) 1109	(5) 1145	(5) 1534	(5) 2058	(5) 1884
3.80			(6) 6058	(6) 6348	(6) 9011	(5) 1040	(5) 1024
5.58			(6) 3762	(6) 3948	(6) 5505	(6) 5079	(6) 5644
8.18			(6) 3014	(6) 3080	(6) 3893	(6) 3199	(6) 3861
12.0			(6) 2709	(6) 2690	(6) 3088	(6) 2583	(6) 3153
17.6			(6) 2413	(6) 2357	(6) 2559	(6) 2238	(6) 2709
27.7			(6) 2074	(6) 2016	(6) 2141	(6) 1919	(6) 2310

Continued

TABLE 8 (Cont'd)

Decay of Normal Fission Products From U^{235}, U^{238}, and Pu^{239}
4. photon-Mev/sec for 10^4 fissions

Age			U^{235}		U^{238}	Pu^{239}	
Years	Days	Hours	Thermal	Fission	(8 Mev)	Thermal	Fission
		0.763	1.856	1.853	1.720	1.633	1.605
		1.12	1.243	1.240	1.147	1.084	1.065
		1.64	0.7757	0.7770	0.7127	0.6656	0.6550
		2.40	0.4550	0.4614	0.4170	0.3813	0.3795
		3.52	0.2584	0.2664	0.2379	0.2118	0.2170
		5.16	0.1463	0.1529	0.1368	0.1190	0.1271
		7.56	(1) 8549	(1) 8983	(1) 8172	(1) 7044	(1) 7786
		11.1	(1) 5212	(1) 5454	(1) 5096	(1) 4463	(1) 4940
		16.2	(1) 3121	(1) 3239	(1) 3113	(1) 2811	(1) 3053
		23.8	(1) 1817	(1) 1868	(1) 1844	(1) 1731	(1) 1826
	1.45	34.8	(1) 1068	(1) 1090	(1) 1093	(1) 1063	(1) 1086
	2.13	51.1	(2) 6328	(2) 6431	(2) 6521	(2) 6593	(2) 6495
	3.12	74.9	(2) 3897	(2) 3974	(2) 4064	(2) 4234	(2) 4044
	4.57		(2) 2570	(2) 2643	(2) 2695	(2) 2845	(2) 2669
	6.70		(2) 1751	(2) 1810	(2) 1817	(2) 1918	(2) 1778
	9.82		(2) 1199	(2) 1236	(2) 1216	(2) 1275	(2) 1170
	14.4		(3) 8006	(3) 8199	(3) 7926	(3) 8247	(3) 7484
	21.1		(3) 5202	(3) 5273	(3) 5068	(3) 5253	(3) 4726
	30.9		(3) 3226	(3) 3229	(3) 3125	(3) 3252	(3) 2911
	45.3		(3) 1862	(3) 1831	(3) 1809	(3) 1906	(3) 1706
	66.4		(3) 1038	(4) 9996	(3) 1011	(3) 1086	(4) 9784
	97.3		(4) 6179	(4) 5891	(4) 5976	(4) 6537	(4) 5946
	143		(4) 3540	(4) 3410	(4) 3390	(4) 3790	(4) 3500
	208		(4) 1995	(4) 1945	(4) 1894	(4) 2150	(4) 1972
	301		(5) 8161	(5) 8024	(5) 7951	(5) 9567	(5) 8671
1.2	438		(5) 2357	(5) 2316	(5) 2593	(5) 3601	(5) 3150
1.78	650		(6) 6623	(6) 6425	(6) 9611	(5) 1542	(5) 1312
2.60			(6) 3466	(6) 3383	(6) 5728	(6) 8451	(6) 7463
3.80			(6) 2445	(6) 2435	(6) 3959	(6) 4593	(6) 4469
5.58			(6) 1942	(6) 1957	(6) 2894	(6) 2471	(6) 2790
8.18			(6) 1724	(6) 1726	(6) 2331	(6) 1710	(6) 2123
12.0			(6) 1579	(6) 1562	(6) 1960	(6) 1444	(6) 1821
17.6			(6) 1405	(6) 1377	(6) 1620	(6) 1253	(6) 1567
25.7			(6) 1198	(6) 1168	(6) 1289	(6) 1049	(6) 1299

Continued

TABLE 8 (Cont'd)

Decay of Normal Fission Products From U^{235}, U^{238} and Pu^{239}
5. r/hr at 3 ft above an infinite plane for 10^4 fissions per sq ft.

Age			U^{235}		U^{238}	Pu^{239}	
Years	Days	Hours	Thermal	Fission	(8 Mev)	Thermal	Fission
		0.763	(8)9977	(8)9970	(8)9329	(8)8907	(8)8750
		1.12	(8)6648	(8)6632	(8)6172	(8)5866	(8)5761
		1.64	(8)4149	(8)4153	(8)3827	(8)3592	(8)3537
		2.40	(8)2453	(8)2484	(8)2256	(8)2071	(8)2065
		3.52	(8)1410	(8)1450	(8)1303	(8)1166	(8)1196
		5.16	(9)8079	(9)8418	(9)7582	(9)6642	(9)7098
		7.56	(9)4786	(9)5014	(9)4587	(9)3986	(9)4398
		11.1	(9)2964	(9)3094	(9)2897	(9)2555	(9)2821
		16.2	(9)1804	(9)1869	(9)1792	(9)1626	(9)1761
		23.8	(10)9716	(9)1094	(9)1073	(9)1010	(9)1063
	1.45	34.8	(10)6305	(10)6428	(10)6393	(10)6235	(10)6360
	2.13	51.1	(10)3730	(10)3786	(10)3817	(10)3869	(10)3811
	3.12	74.9	(10)2276	(10)2319	(10)2365	(10)2470	(10)2362
	4.57		(10)1483	(10)1524	(10)1556	(10)1645	(10)1546
	6.70		(11)9986	(10)1031	(10)1039	(10)1099	(10)1021
	9.82		(11)6774	(11)6972	(11)6899	(11)7244	(11)6655
	14.4		(11)4490	(11)4587	(11)4462	(11)4650	(11)4226
	21.1		(11)2910	(11)2940	(11)2845	(11)2953	(11)2660
	30.9		(11)1813	(11)1807	(11)1762	(11)1837	(11)1645
	45.3		(11)1061	(11)1039	(11)1034	(11)1092	(12)9777
	66.4		(12)6055	(12)5807	(12)5910	(12)6360	(12)5728
	97.3		(12)3676	(12)3497	(12)3559	(12)3896	(12)3543
	143		(12)2170	(12)2090	(12)2079	(12)2320	(12)2200
	208		(12)1194	(12)1164	(12)1133	(12)1287	(12)1180
	301		(13)4874	(13)4790	(13)4733	(13)5707	(13)5170
1.2	438		(13)1399	(13)1373	(13)1525	(13)2135	(13)1864
1.78	650		(14)3884	(14)3758	(14)5517	(14)9083	(14)7690
2.60			(14)2031	(14)1975	(14)3160	(14)4964	(14)4352
3.80			(14)1444	(14)1432	(14)2213	(14)2692	(14)2594
5.58			(14)1154	(14)1158	(14)1603	(14)1442	(14)1611
8.18			(14)1026	(14)1021	(14)1291	(15)9971	(14)1225
12.0			(15)9432	(15)9293	(14)1094	(15)8452	(14)1057
17.6			(15)8310	(15)8211	(15)9164	(15)7377	(15)9160
25.7			(15)7183	(15)6987	(15)7431	(15)6219	(15)7668

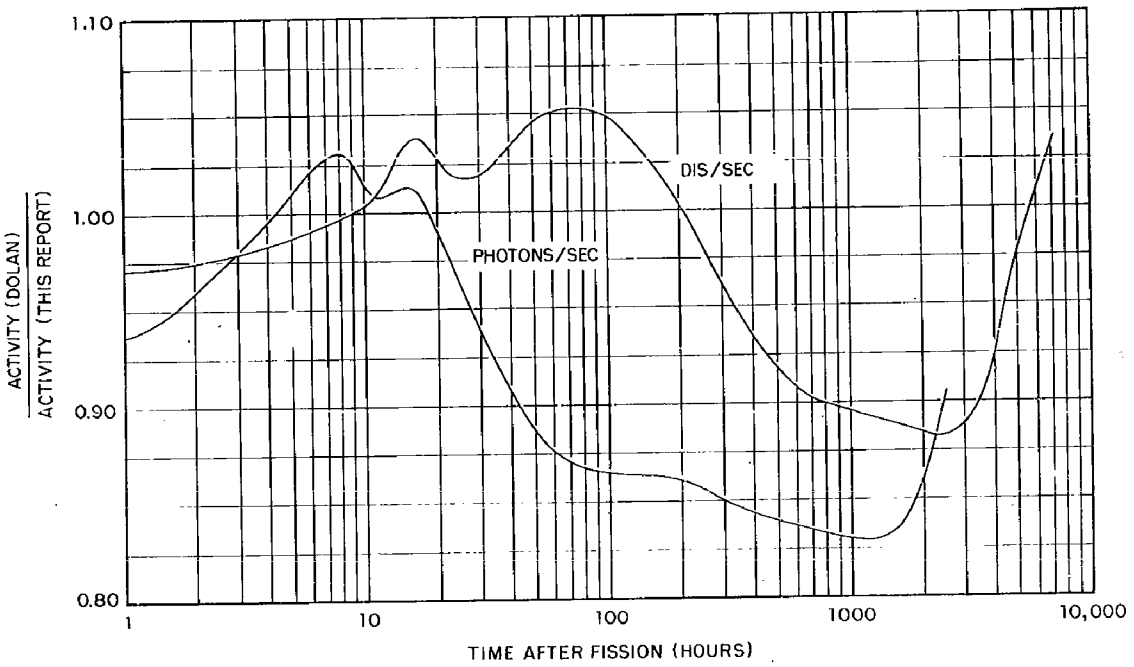

Fig. 3 Comparison of 14.0 Mev Neutron (Dolan[29,30]) to 8 Mev Neutron Fission of U^{238}

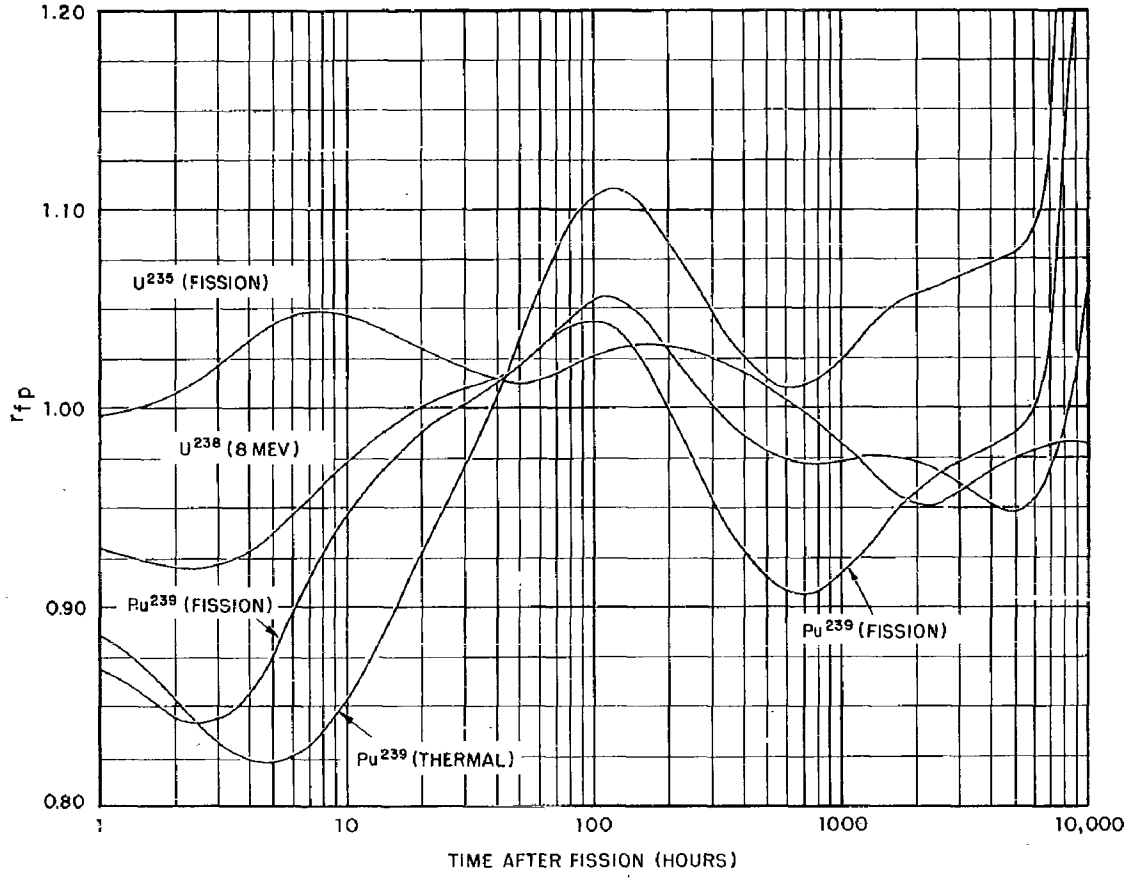

Fig. 4 Gross Air Ionization Rate "R" Factors for Various Types of Fission (hours after fission)

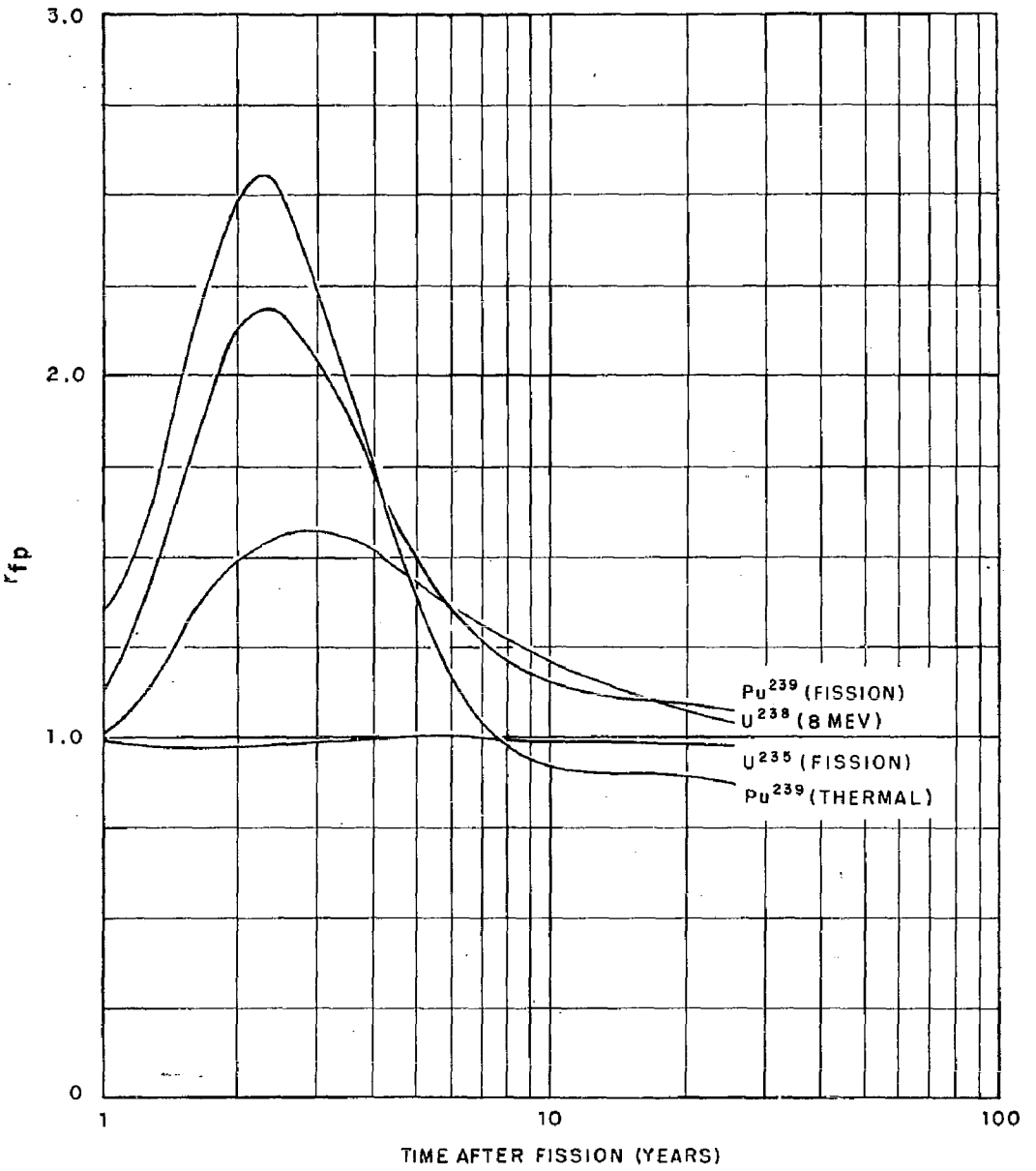

Fig. 5 Gross Air Ionization Rate "R" Factors for Various Types of Fission (years after fission)

nuclide decay schematics) are the mass chain yields and the independent yields of the isotopes in the chain. For times after fission of about 1 hour and greater, the Bolles-Ballou calculations[13] show that the difference in the total disintegration rates based on Present's yield theory from those based on Glendenin's postulate is insignificant. This is due to the fact that at these times after fission most of the chains have decayed to the last one or two active members from short-lived early members. The displacement in the curves of Figs. 3, 4, and 5 from 1.00 are therefore due to differences in the chain yields. The curves show that for times between about 1 hour and 1 year, the maximum error in the ionization rate by use of the data for thermal neutron fission of U^{235} would be about 15 %. The error in the integrated dose for any time period would be less.

The H+1 ionization rates at 3 feet above an infinite smooth contaminated plane for a unit yield distribution of fission products per unit area are summarized in Table 9. The highest value

TABLE 9

Summary of H+1 Ionization-Rates Per Unit Yield Per Unit Area, for 3 Feet Above an Infinite Smooth Contaminated Plane

Type of Fission	H+1 Ionization Rate (Unit Yield/Unit Area)	
	(r/hr at 1 hr)/(fiss/sq ft)	(r/hr at 1 hr)/(KT/sq mi)
U^{235} (thermal)	7.60×10^{-13}	3950
U^{235} (fission)	7.58×10^{-13}	3940
U^{238} (8 Mev)	6.94×10^{-13}	3610
Pu^{239} (thermal)	6.70×10^{-13}	3480
Pu^{239} (fission)	6.54×10^{-13}	3400

is for the thermal neutron fission of U^{235}; the lowest is for fission-neutron fission of Pu^{239}. The same value, 1.45×10^{23} fissions/KT, was used to convert all the rates from fissions to kilotons. The corresponding ionization rate factor derived from ENW is (1240 r/hr at 1 hr)/(KT/sq mi) or about a factor of 3 lower than the values of Table 9. Other authors have made similar calculations and comparisons of these factors and the decay curves for the thermal neutron fission of U^{235}.[31,32,33,34]

SECTION 7

CALCULATION OF THE DISINTEGRATION RATE, AND AIR IONIZATION RATE FROM FRACTIONATED FISSION PRODUCTS OF U^{235}, U^{238}, AND U^{239} CONDENSED WITHIN PARTICLES OF AN IDEALIZED CARRIER MATERIAL

The properties of the idealized carrier material given in Section 2 were that (1) it did not form compounds with the fission product elements or oxides, (2) it dissolved them as stable oxides, (3) and that it had a melting point of 1400°C. The last two properties are somewhat similar to those of some common soil minerals. The selection of the first two properties was made so that a sample calculation of the condensation process could be made by use of the theory utilizing Henry's law of dilute solutions. The process was further idealized, by necessity due to the fact that no values of Henry's law constants were directly available, by the use of Raoult's law of perfect solutions; the latter idealization involved setting Henry's law constant equal to the equilibrium partial pressure of the gaseous species of each element over its own oxide.

The stipulation of the melting temperature is sufficient for computation of the Raoult's law constants from the data of Table 1; these are given in Table 10. The oxygen pressure was taken to be 1 atmosphere as a substitution for the total pressure. The fact that some of the oxides show larger pressure than the rare gases is partly due to the neglect of the difference in heat capacities in the use of the simplified vapor pressure equation at temperatures beyond its range of validity. It was pointed out earlier, however, that errors due to this over-extrapolation would not influence the fractionation computation since the amount condensed of the elements with high vapor pressures would be essentially zero and not sensitive to the exact value of their vapor pressures.

If no carrier material would be present in the fireball along with the fission product elements, or if they were all in the vapor state when the temperature is 1400°C, their partial pressures can be

TABLE 10

Summary of Raoult's Law Constants for the Oxides of Fission Product and Other Elements at 1673°K

Element	k_j (atmos)	Element	k_j (atmos)
Cu	7.4×10^{-6}	Pd	8.7×10^{-7}
Zn	5.5×10^{-5}	Ag	2.9×10^{-3}
Ga	8.5×10^{-4}	Cd	0.12
Ge	0.229	In	9.6×10^{-5}
As	2.6×10^{3}	Sn	7.2×10^{-5}
Se	8.7×10^{4}	Sb	0.339
Br	1.05	Te	4.17
Kr	5.6×10^{3}	I	2.09
Rb	1.20	Xe	4.9×10^{3}
Sr	1.3×10^{-8}	Cs	3.24
Y	6×10^{-19}	Ba	5.0×10^{-7}
Zr	2×10^{-14}	La	2×10^{-15}
Nb	1.6×10^{-7}	Ce	8×10^{-13}
Mo	3.63	Pr	1×10^{-14}
Tc	9.6×10^{3}	Nd	3×10^{-14}
Ru	1.1×10^{-3}	Pm	2×10^{-13}
Rh	9.3×10^{-7}	U	2.2×10^{-5}

estimated from the perfect gas law using V_m as the volume and using the yield factor of 0.5 moles of fission products produced per KT. The partial pressures are summarized in Table 11 for some of the more abundant fission product elements as given by Bolles and Ballou.[13]

TABLE 11

Calculated Partial Pressures and Equilibrium Partial Pressures of Some of the More Abundant Fission Products Dispersed Uniformly in V_m at 1673°K for a Fission Yield of 2.3 MT

Element	Percent No. of Atoms at 1 min	Partial Pressure in Volume (10^{-9} atmos)	Partial Pressure Over Oxide (atmos)
Rb	5	4.2	1.2 (l)[a]
Cs	5	4.2	3.2 (l)
Sr	8	6.7	1.3×10^{-8}(s)
Ba	7	5.8	5.0×10^{-7}(s)
La	4	3.3	2×10^{-15}(s)
Ce	6	5.0	8×10^{-13}(s)
Sb	4	0.84	0.34 (l)
Zr	8	6.7	2×10^{-14}(s)
Nb	6	2.5	1.6×10^{-7}(s)
Mo	8	6.7	3.6 (l)
Te	6	5.0	4.2 (l)

a. s for solid, l for liquid.

Of all the elements listed, only La, Ce, and Zr would have condensed to a solid state at this temperature. The remainder would do so only at lower temperatures. Use of the equations of the variation of the gas volume, temperature, and percent abundance of each element with time could be made to estimate the times that condensation would begin for each. This computation, if other vaporized materials (bomb casing, soil, etc.) were included, could be made to obtain more information about the formation of vapor-condensed particles in the early stages of the whole fallout formation process.

In computing the amount of each mass chain that condensed in the liquid soil, use was made of Eq. 29 to calculate the condensation

"R" factor with reference to the number of fissions. The computation of $r_o(A)$ by use of the Bolles-Ballou[13] values of the independent yields for both Present's and Glendenin's yield theories is illustrated for masses 89, 90, and 140 in Table 12; the value of k_j^9 was determined by dividing the values of k_j in Table 10 by 0.0364. For nuclides other than the end numbers of the chain, the accumulated sum of the $y_i(A)/(1+k_j^9)$ terms up to the indicated chain number, divided by the accumulated percent yield of the chain, gives the $r_o(A)$ value for that nuclide. This converts the partial sums to fractional multipliers for each nuclide in the chain.

The most exact method of computing the amount of each radionuclide present (and its activity) for a given number of fissions would be to use the value of $y_j(A)/(1+k_j^9)$ for each and the appropriate decay formula for the production of the daughter products. But to simplify the computation process, the calculations were made by direct multiplication of the $r_o(A)$ values and the single nuclide d/s values per 10^4 fissions and r/hr values per 10^4 fissions/sq ft. Although this procedure gives higher values for the daughter products in each chain, the error decreases with time. Compared to other possible errors involved in the computation, the error due to this approximation is rather insignificant. For example, the initial fraction for Sr^{89} is 0.010 which increases, after Rb^{89} decays out, to 0.0183; in the exact method of computation, the latter value is reached by 2.40 hr. The $r_o(90)$ value for Sr^{90} is valid from 31.2 minutes and the $r_o(140)$ value for Ba^{140} is essentially valid at 60 seconds.

The $r_o(A)$ values for all the radionuclides used in the computations are summarized in Table 13 for both the Present and Glendenin independent yield theories as calculated by Bolles and Ballou.[13] For more than half of the nuclides, the $r_o(A)$ values from the Glendenin distributions are larger. The computed $r(A)$ values relative to mass 99 for some nuclides of interest are: Sr^{89}, 0.0232 and 0.0200; Sr^{90}, 0.195 and 0.193; I^{131}, 0.914 and 0.108; Cs^{137}, 0.00408 and 0.00455; and Ba^{140}, 0.517 and 0.574. The $r_o(A)$ values indicate that about 85 percent of the total Sr^{90} formed (for the 2.3 MT yield surface burst) would be condensed on (small) solid particles during the second period of condensation along with about 99 percent of the Cs^{137} and its daughter, Ba^{137m}. Some fraction of these amounts would presumably be soluble and biologically available after the particle reached the earth's surface.

The results of the decay computations in d/s per 10^4 fissions and r/hr per 10^4 fissions/sq ft are given in Table 14. The ionization rates for the Glendenin yields are plotted in Fig. 6, with the curve for normal fission products from thermal fission of U^{235}. The

TABLE 12

Computation of $r_o(A)$ for Mass Numbers 89, 90, and 140, for 60 Seconds After Fission

Parameter	Present			Glendenin		
	Kr	Rb	Sr	Kr	Rb	Sr
			Mass Number 89			
$y_j(A)$	0.707	0.283	0.010	0.744	0.248	0.008
k_j^o	1.5×10^5	33.0	3.6×10^{-7}	1.5×10^5	33.0	3.6×10^{-7}
$1+k_j^o$	1.5×10^5	34.0	1.00	1.5×10^5	34.0	1.00
$y_j(A)/(1+k_j^o)$	5×10^{-6}	0.00832	0.010	5×10^{-6}	0.00729	0.008
$r_o(89)$	7×10^{-6}	0.00840	0.0183	7×10^{-6}	0.00735	0.0153
			Mass Number 90			
$y_j(A)$	0.215	0.650	0.135	0.236	0.635	0.129
$y_j(A)/(1+k_j^o)$	1×10^{-6}	0.0191	0.135	1×10^{-6}	0.0187	0.129
$r_o(90)$	7×10^{-6}	0.0221	0.154	7×10^{-6}	0.0215	0.148
	Xe	Cs	Ba	Xe	Cs	Ba
			Mass Number 140			
$y_j(A)$	0.042	0.556	0.402	0.041	0.526	0.433
k_j^o	1.4×10^5	89.0	1.4×10^{-5}	1.4×10^5	89.0	1.4×10^{-5}
$1+k_j^o$	1.4×10^5	90.0	1.00	1.4×10^5	90.0	1.00
$y_j(A)/(1+k_j^o)$	3×10^{-7}	0.0062	0.402	3×10^{-7}	0.0058	0.433
$r_o(140)$	7×10^{-6}	0.0102	0.408	7×10^{-7}	0.0102	0.439

TABLE 13

Summary of $r_o(A)$ Values at 60 Seconds After Fission for Fission Product Nuclides That Contribute to the Gross Activity at 45.8 Minutes After Fission

Nuclide	$r_o(A)$		Nuclide	$r_o(A)$		Nuclide	$r_o(A)$		Nuclide	$r_o(A)$	
	Present	Glendenin		Present	Glendenin		Present	Glendenin		Present	Glendenin
Zn^{72}	0.998	0.998	Nb_1^{95}	1.00	1.00	Sb^{125}	0.998	0.998	Ce^{141}	0.990	0.991
Zn^{74}	0.997	0.998	Nb_2^{95}	1.00	1.00	Sb^{126}	0.967	0.975	Ce^{143}	1.00	1.00
Ga^{72}	0.997	0.998	Nb^{97}	1.00	1.00	Sb^{127}	0.902	0.947	Ce^{144}	1.00	1.00
Ga^{73}	0.985	0.986	Nb^{96}	1.00	1.00	Sb^{128}	0.109	0.111	Ce^{145}	1.00	1.00
Ga^{74}	0.990	0.993	Mo^{99}	0.789	0.765	Sb^{129}	0.0973	0.0974	Ce^{146}	1.00	1.00
Ge^{75}	0.600	0.649	Mo^{101}	0.0396	0.0410	Sb^{131}	0.0970	0.0970	Pr^{143}	1.00	1.00
Ge^{77}	0.183	0.203	Mo^{102}	0.0141	0.0121	Te_1^{125}	0.998	0.998	Pr^{144}	1.00	1.00
Ge^{78}	0.140	0.142	Tc_1^{99}	0.789	0.765	Te_1^{127}	0.902	0.947	Pr^{145}	1.00	1.00
As^{77}	0.137	0.159	Tc^{101}	0.0383	0.0293	Te_2^{127}	0.902	0.947	Pr^{146}	1.00	1.00
As^{78}	0.126	0.138	Tc^{102}	0.0135	0.0112	Te_1^{129}	0.0958	0.0968	Nd^{147}	1.00	1.00
As^{79}	0.0226	0.0288	Ru^{103}	0.266	0.278	Te_2^{129}	0.0941	0.0960	Nd^{149}	1.00	1.00
Se_1^{81}	0.000315	0.000800	Ru^{105}	0.869	0.889	Te_1^{131}	0.0833	0.0902	Nd^{151}	1.00	1.00
Se_2^{81}	0.000143	0.000419	Ru^{106}	0.955	0.960	Te_2^{131}	0.0724	0.0829	Pm^{147}	1.00	1.00
Se_1^{83}	0.0	0.0	Rh_1^{103}	0.266	0.278	Te^{132}	0.0426	0.0563	Pm^{149}	1.00	1.00
Br^{83}	0.00926	0.00808	Rh_1^{105}	0.869	0.890	Te_1^{133}	0.0448	0.0654	Pm^{150}	1.00	1.00
Br^{84}	0.0135	0.0135	Rh_2^{105}	0.870	0.890	Te_2^{133}	0.0350	0.0566	Pm^{151}	1.00	1.00
Kr_1^{83}	0.00926	0.00808	Rh^{106}	0.955	0.960	Te^{134}	0.00904	0.00921	Pm^{152}	1.00	1.00
Kr_1^{85}	0.0279	0.0285	Rh^{107}	0.975	0.975	I^{131}	0.0721	0.0824	Pm^{153}	1.00	1.00
Kr_2^{85}	0.0266	0.0275	Pd^{109}	0.998	0.998	I^{132}	0.0413	0.0554	Sm^{151}	1.00	1.00
Kr^{87}	0.0129	0.0152	Pd^{111}	1.00	1.00	I^{133}	0.0298	0.0517	Sm^{153}	1.00	1.00
Kr^{88}	0.00122	0.00171	Pd^{112}	1.00	1.00	I^{134}	0.0115	0.0108	Sm^{155}	1.00	1.00
Rb^{88}	0.00213	0.00213	Ag_1^{109}	0.998	0.998	I^{135}	0.0170	0.0170	Sm^{156}	1.00	1.00
Rb^{89}	0.00840	0.00735	Ag^{111}	0.999	0.999	Xe_1^{131}	0.0721	0.0824	Sm^{158}	1.00	1.00
Rb_2^{91}	0.0291	0.0290	Ag^{112}	1.00	1.00	Xe_1^{133}	0.0298	0.0517	Eu^{155}	1.00	1.00
Sr^{89}	0.0183	0.0153	Ag^{113}	0.964	0.963	Xe_2^{133}	0.0298	0.0517	Eu^{156}	1.00	1.00
Sr^{90}	0.154	0.148	Ag^{115}	0.929	0.928	Xe_1^{135}	0.0164	0.0166	Eu^{157}	1.00	1.00
Sr^{91}	0.236	0.243	Cd_1^{115}	0.928	0.927	Xe_2^{135}	0.0157	0.0162	Eu^{158}	1.00	1.00
Sr^{92}	0.921	0.922	Cd_2^{115}	0.910	0.910	X^{138}	0.0	0.0	Gd^{159}	1.00	1.00
Sr^{93}	0.999	0.998	Cd^{117}	0.563	0.550	Cs^{137}	0.00322	0.00348	Tb^{161}	1.00	1.00
Y^{90}	0.154	0.148	Cd^{118}	0.379	0.372	Cs^{138}	0.00146	0.00135			
Y_1^{91}	0.236	0.243	Cd^{120}	0.237	0.237	Cs^{139}	0.0111	0.0112			
Y_2^{92}	0.236	0.243	In_1^{115}	0.910	0.910	Ba_1^{137}	0.00322	0.00348			
Y^{92}	0.921	0.923	In^{117}	0.564	0.551	Ba^{139}	0.0744	0.0863			
Y^{93}	0.999	0.998	In^{118}	0.379	0.372	Ba^{140}	0.408	0.439			
Y^{94}	1.00	1.00	In^{119}	0.395	0.398	Ba^{141}	0.990	0.991			
Zr^{95}	1.00	1.00	Sn^{121}	0.846	0.846	Ba^{142}	1.00	1.00			
Zr^{97}	1.00	1.00	Sn^{123}	0.991	0.991	La^{140}	0.408	0.439			
			Sn^{125}	0.998	0.998	La^{141}	0.990	0.991			
			Sn^{126}	0.998	0.998	La^{142}	1.00	1.00			
						La^{143}	1.00	1.00			

100

TABLE 14

Decay of Fractionated Fission Products for Close-In Fallout From a 2.3 MT Yield Surface Detonation on an Ideal Soil That Melts at 1400°C

1. dis/sec for 10^4 fissions

Age			Present				Glendenin			
Years	Days	Hours	U^{235}		U^{238}	Pu^{239}	U^{235}		U^{238}	Pu^{239}
			Thermal	Fission	(8 Mev)	(Fission)	Thermal	Fission	(8 Mev)	(Fission)
		0.763	0.6579	0.6476	0.6417	0.6827	0.6609	0.6503	0.6441	0.6852
		1.12	0.4273	0.4195	0.4194	0.4560	0.4301	0.4220	0.4218	0.4485
		1.64	0.2739	0.2695	0.2706	0.2851	0.2762	0.2717	0.2727	0.2873
		2.40	0.1840	0.1820	0.1821	0.1896	0.1855	0.1835	0.1837	0.1912
		3.52	0.1334	0.1326	0.1314	0.1360	0.1344	0.1334	0.1324	0.1371
		5.16	(1)9914	(1)9856	(1)9702	0.1008	(1)9967	(1)9906	(1)9760	0.1014
		7.56	(1)7139	(1)7094	(1)6966	(1)7266	(1)7171	(1)7124	(1)7002	(1)7307
		11.1	(1)4854	(1)4818	(1)4756	(1)4980	(1)4876	(1)4838	(1)4781	(1)5007
		16.2	(1)3092	(1)3063	(1)3064	(1)3214	(1)3108	(1)3078	(1)3082	(1)3233
		23.8	(1)1895	(1)1872	(1)1911	(1)2000	(1)1906	(1)1883	(1)1923	(1)2013
	1.45	34.8	(1)1159	(1)1143	(1)1193	(1)1241	(1)1168	(1)1151	(1)1202	(1)1251
	2.13	51.1	(2)6946	(2)6839	(2)7312	(2)7545	(2)7007	(2)6900	(2)7380	(2)7617
	3.12	74.9	(2)3995	(2)3949	(2)4309	(2)4412	(2)4042	(2)3996	(2)4361	(2)4466
	4.57		(2)2350	(2)2344	(2)2557	(2)2595	(2)2388	(2)2382	(2)2598	(2)2637
	6.70		(2)1494	(2)1501	(2)1594	(2)1597	(2)1525	(2)1532	(2)1627	(2)1629
	9.82		(2)1041	(2)1046	(2)1069	(2)1057	(2)1065	(2)1071	(2)1094	(2)1081
	14.4		(3)7587	(3)7599	(3)7522	(3)7389	(3)7770	(3)7782	(3)7704	(3)7560
	21.1		(3)5599	(3)5578	(3)5433	(3)5240	(3)5718	(3)5695	(3)5551	(3)5347
	30.9		(3)4030	(3)3997	(3)3780	(3)3814	(3)4098	(3)4062	(3)3943	(3)3877
	45.3		(3)2773	(3)2740	(3)2664	(3)2647	(3)2807	(3)2771	(3)2699	(3)2680
	66.4		(3)1864	(3)1836	(3)1791	(3)1816	(3)1878	(3)1848	(3)1808	(3)1832

Continued

TABLE 14 (Cont'd)

Decay of Fractionated Fission Products for Close-In Fallout From a 2.3 MT Yield Surface Detonation on an Ideal Soil That Melts at 1400°C

1. dis/sec for 10^4 fissions

Age			Present				Glendenin			
			U^{235}		U^{238}	Pu^{239}	U^{235}		U^{238}	Pu^{239}
Years	Days	Hours	Thermal	Fission	(8 Mev)	(Fission)	Thermal	Fission	(8 Mev)	(Fission)
	97.3		(3)1257	(3)1238	(3)1208	(3)1262	(3)1262	(3)1242	(3)1216	(3)1270
	143		(4)8305	(4)8219	(4)7960	(4)8619	(4)8302	(4)8207	(4)7975	(4)8640
	208		(4)4848	(4)4799	(4)4724	(4)5422	(4)4856	(4)4806	(4)4737	(4)5438
	301		(4)2695	(4)2666	(4)2697	(4)3311	(4)2698	(4)2668	(4)2702	(4)3318
1.20	438		(4)1456	(4)1422	(4)1515	(4)1990	(4)1456	(4)1431	(4)1516	(4)1994
1.78			(5)8179	(5)7961	(5)8766	(4)1192	(5)8179	(5)7960	(5)8774	(4)1194
2.60			(5)4422	(5)4264	(5)4844	(5)6586	(5)4421	(5)4262	(5)4848	(5)6597
3.80			(5)2191	(5)2086	(5)2430	(5)3173	(5)2189	(5)2083	(5)2430	(5)3177
5.58			(5)1041	(6)9836	(5)1134	(5)1341	(5)1039	(6)9808	(5)1133	(5)1341
8.18			(6)5823	(6)5531	(6)6005	(6)6332	(6)5800	(6)5504	(6)5988	(6)6320
12.0			(6)3179	(6)3123	(6)3142	(6)3095	(6)3158	(6)3099	(6)3126	(6)3083
17.6			(6)1745	(6)1797	(6)1674	(6)1587	(6)1728	(6)1778	(6)1661	(6)1577
25.7			(7)9877	(6)1069	(7)9457	(7)8715	(7)9750	(6)1054	(7)9361	(7)8643

Continued

TABLE 14 (Cont'd)

Decay of Fractionated Fission Products for Close-In Fallout From a 2.3 MT Yield Surface Detonation on an Ideal Soil That Melts at 1400°C

2. r/hr at 3 ft above an infinite plane for 10^4 fissions per sq ft

Age			Present				Glendenin			
Years	Days	Hours	U^{235}		U^{238}	Pu^{239}	U^{235}		U^{238}	Pu^{239}
			Thermal	Fission	(8 Mev)	(Fission)	Thermal	Fission	(8 Mev)	(Fission)
		0.763	(8)4123	(8)4040	(8)3861	(8)3995	(8)4136	(8)4052	(8)3872	(8)4006
		1.12	(8)2644	(8)2582	(8)2474	(8)2547	(8)2655	(8)2593	(8)2483	(8)2557
		1.64	(8)1576	(8)1544	(8)1479	(8)1501	(8)1585	(8)1552	(8)1487	(8)1509
		2.40	(9)9181	(9)9082	(9)8668	(9)8617	(9)9241	(9)9140	(9)8724	(9)8672
		3.52	(9)5495	(9)5592	(9)5308	(9)5190	(9)5629	(9)5628	(9)5343	(9)5225
		5.16	(9)3547	(9)3478	(9)3384	(9)3287	(9)3569	(9)3495	(9)3406	(9)3309
		7.56	(9)2252	(9)2273	(9)2164	(9)2092	(9)2266	(9)2286	(9)2179	(9)2107
		11.1	(9)1408	(9)1421	(9)1371	(9)1318	(9)1418	(9)1431	(9)1381	(9)1329
		16.2	(10)8455	(10)8498	(10)8382	(10)8015	(10)8530	(10)8574	(10)8461	(10)8094
		23.8	(10)4913	(10)4901	(10)4965	(10)4740	(10)4969	(10)4959	(10)5023	(10)4797
	1.45	34.8	(10)2933	(10)2905	(10)2996	(10)2866	(10)2976	(10)2949	(10)3040	(10)2909
	2.13	51.1	(10)1728	(10)1707	(10)1784	(10)1716	(10)1761	(10)1741	(10)1818	(10)1750
	3.12	74.9	(11)9607	(11)9540	(10)1014	(11)9808	(11)9872	(11)9817	(10)1042	(10)1007
	4.57		(11)5453	(11)5486	(11)5864	(11)5653	(11)5671	(11)5715	(11)6085	(11)5868
	6.70		(11)3422	(11)3489	(11)3631	(11)3450	(11)3599	(11)3676	(11)3809	(11)3620
	9.82		(11)2440	(11)2502	(11)2502	(11)2340	(11)2579	(11)2647	(11)2638	(11)2467
	14.4		(11)1820	(11)1863	(11)1805	(11)1676	(11)1920	(11)1968	(11)1901	(11)1765
	21.1		(11)1351	(11)1375	(11)1312	(11)1223	(11)1417	(11)1444	(11)1375	(11)1280
	30.9		(12)9628	(12)9710	(12)9211	(12)8708	(11)1001	(11)1010	(12)9572	(12)9033
	45.3		(12)6585	(12)6571	(12)6225	(12)6014	(12)6763	(12)6751	(12)6395	(12)6167

Continued

TABLE 14 (Cont'd)

Decay of Fractionated Fission Products for Close-In Fallout From a 2.3 MT Yield Surface Detonation on an Ideal Soil That Melts at 1400°C

2. r/hr at 3 ft above an infinite plane for 10^4 fissions per sq ft

Age			Present				Glendenin			
Years	Days	Hours	U^{235}		U^{238}	Pu^{239}	U^{235}		U^{238}	Pu^{239}
			Thermal	Fission	(8 Mev)	(Fission)	Thermal	Fission	(8 Mev)	(Fission)
	66.4		(12)4518	(12)4467	(12)4217	(12)4179	(12)4579	(12)4526	(12)4278	(12)4234
	97.3		(12)3186	(12)3141	(12)2945	(12)2976	(12)3200	(12)3153	(12)2961	(12)2991
	143		(12)2106	(12)2081	(12)1939	(12)1989	(12)2109	(12)2083	(12)1943	(12)1993
	208		(12)1141	(12)1131	(12)1057	(12)1107	(12)1141	(12)1131	(12)1058	(12)1108
	301		(13)4668	(13)4630	(13)4462	(13)4891	(13)4670	(13)4631	(13)4466	(13)4897
1.20	438		(13)1273	(13)1255	(13)1372	(13)1700	(13)1274	(13)1255	(13)1373	(13)1703
1.78	650		(14)2724	(14)2633	(14)4156	(14)6249	(14)2727	(14)2634	(14)4162	(14)6269
2.60			(15)9056	(15)8800	(14)1945	(14)3021	(15)9074	(15)8810	(14)1947	(14)3032
3.80			(15)3501	(15)3656	(15)9833	(14)1354	(15)3509	(15)3660	(15)9835	(14)1358
5.58			(15)1035	(15)1325	(15)4457	(15)4520	(15)1038	(15)1327	(15)4445	(15)4528
8.18			(16)2883	(16)4991	(15)2113	(15)1393	(16)2900	(16)4998	(15)2100	(15)1390
12.0			(16)1265	(16)2320	(15)1117	(16)5624	(16)1279	(16)2328	(15)1107	(16)5592
17.6			(17)7741	(16)1147	(16)5945	(16)2965	(17)7889	(16)1158	(16)5878	(16)2948
25.7			(17)5072	(17)6337	(16)3057	(16)1622	(17)5219	(17)6458	(16)3027	(16)1619

Fig. 6 Air Ionization Rate at 3 ft Above a Smooth Infinite Plane Uniformly Contaminated With Fractional Fission Products From 10^4 Fissions/sq ft, in Melted Fallout Particles From a 2.3 MT Yield Surface Detonation. Rates for normal fission products from thermal neutron fission of U^{235} are given for comparison.

A,B. Hours after fission
C,D. Days after fission
E,F. Years after fission

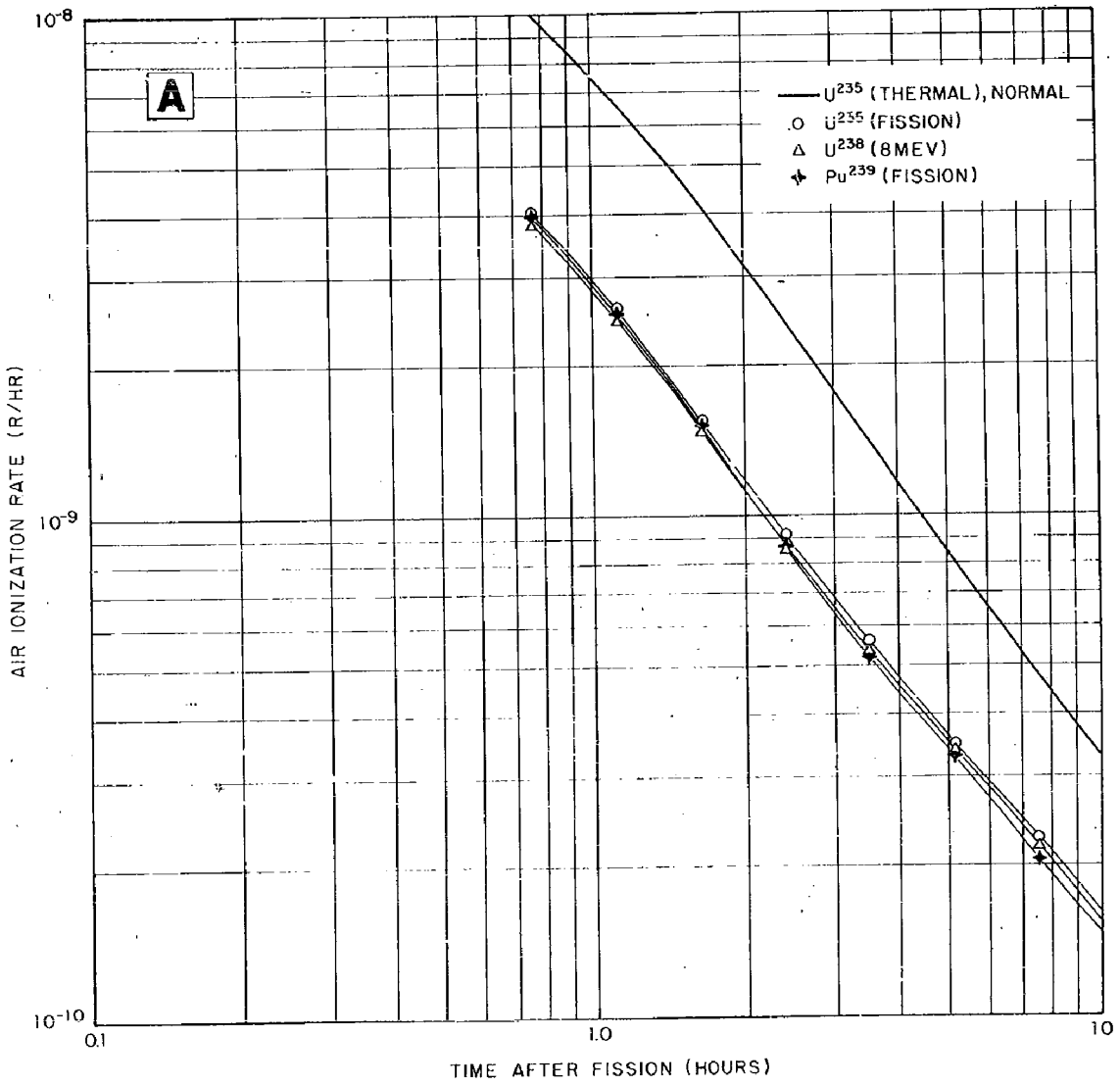
A
U^{235} (THERMAL), NORMAL
U^{235} (FISSION)
U^{238} (8MEV)
Pu^{239} (FISSION)
10^{-8}
10^{-9}
10^{-10}
AIR IONIZATION RATE (R/HR)
0.1
1.0
10
TIME AFTER FISSION (HOURS)

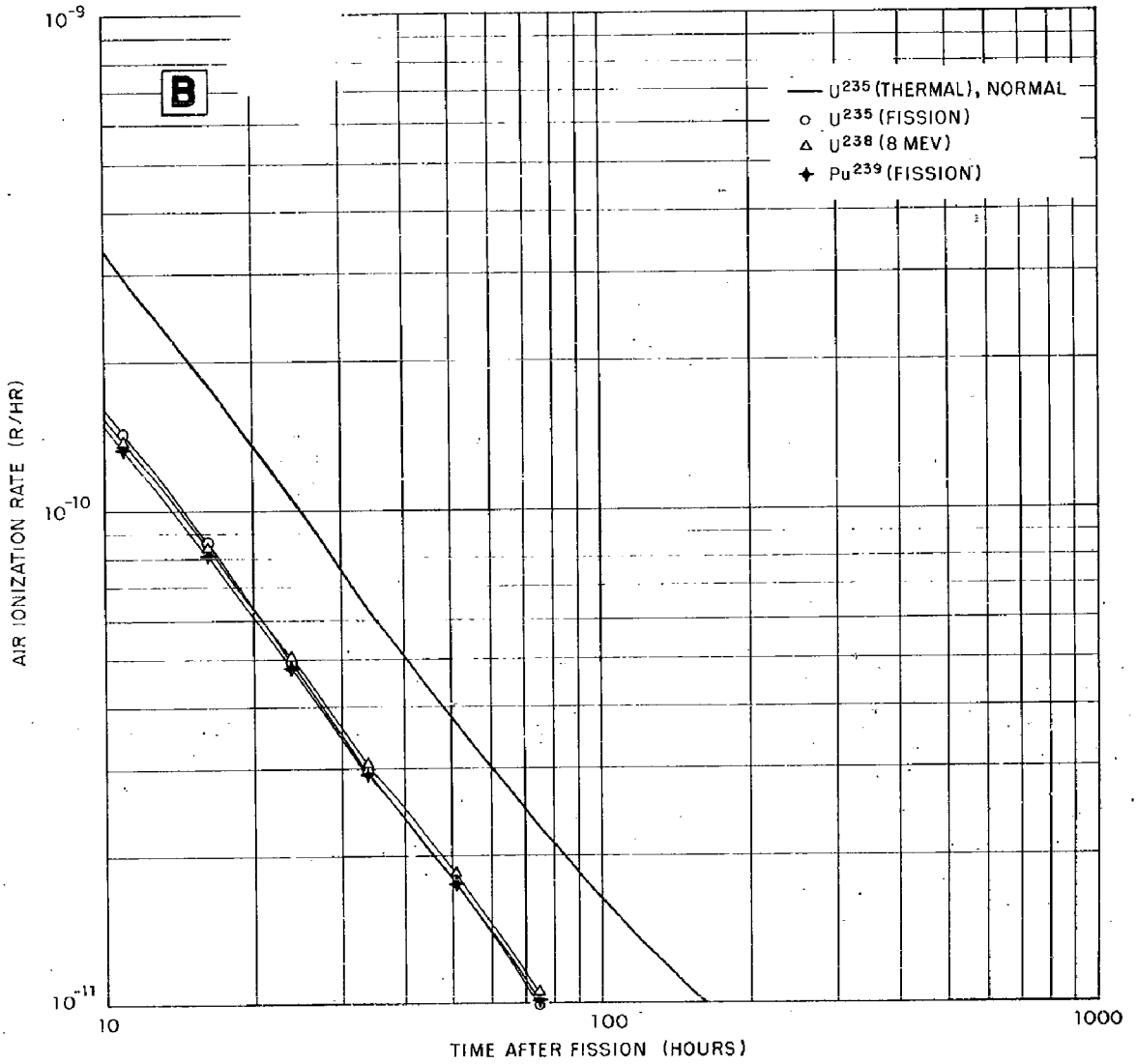
B
10^{-9}
10^{-10}
10^{-11}
AIR IONIZATION RATE (R/HR)
10
100
1000
TIME AFTER FISSION (HOURS)
U^{235} (THERMAL), NORMAL
U^{235} (FISSION)
U^{238} (8 MEV)
Pu^{239} (FISSION)

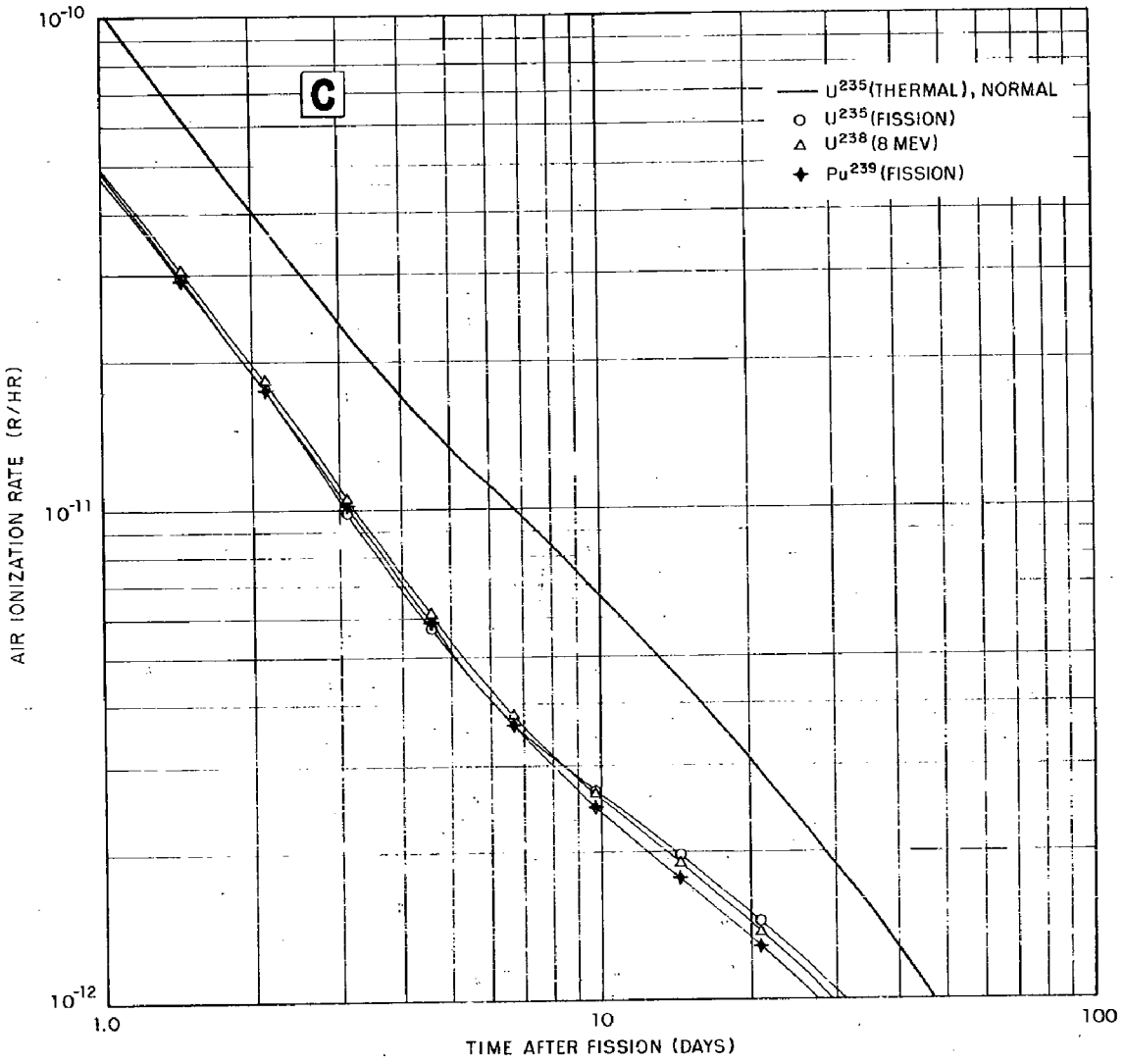
C
U^{235}(THERMAL), NORMAL
U^{235}(FISSION)
U^{238}(8 MEV)
Pu^{239}(FISSION)
10^{-10}
10^{-11}
10^{-12}
AIR IONIZATION RATE (R/HR)
1.0
10
100
TIME AFTER FISSION (DAYS)

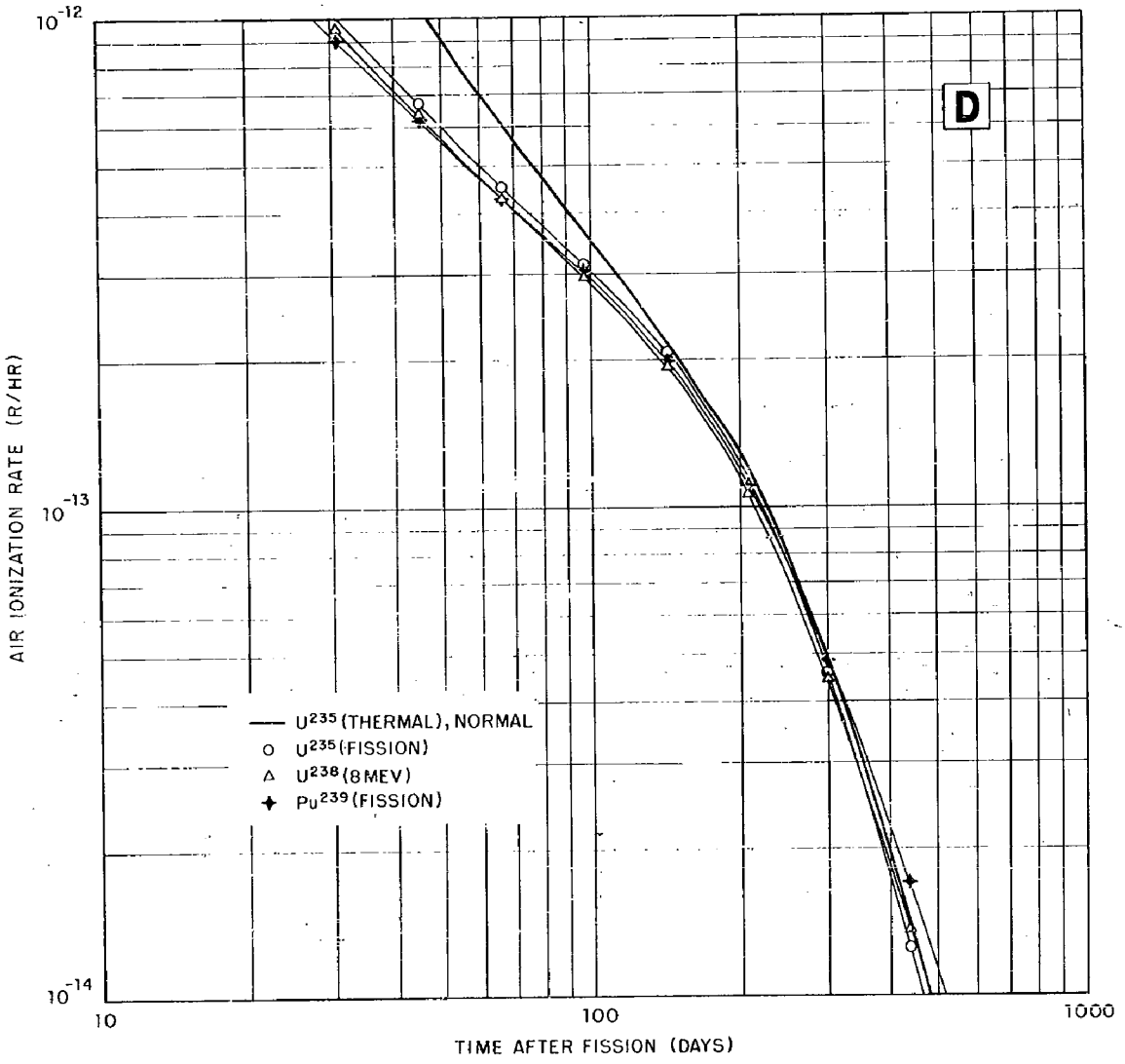
D
AIR IONIZATION RATE (R/HR)
10^{-12}
10^{-13}
10^{-14}
10
100
1000
TIME AFTER FISSION (DAYS)
U^{235} (THERMAL), NORMAL
U^{235} (FISSION)
U^{238} (8 MEV)
Pu^{239} (FISSION)

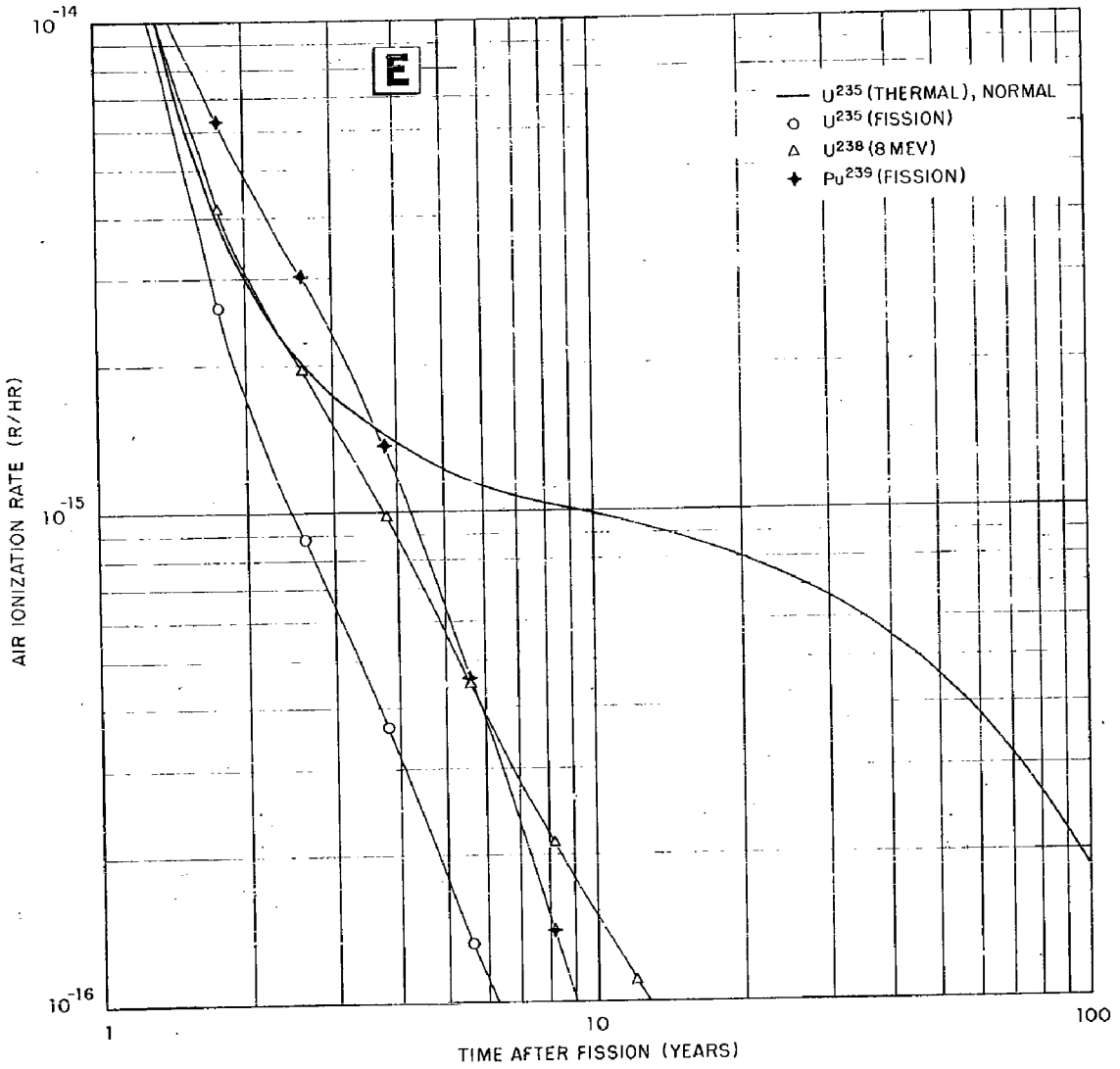
E
10^{-14}
10^{-15}
10^{-16}
AIR IONIZATION RATE (R/HR)
1
10
100
TIME AFTER FISSION (YEARS)
U^{235} (THERMAL), NORMAL
U^{235} (FISSION)
U^{238} (8 MEV)
Pu^{239} (FISSION)

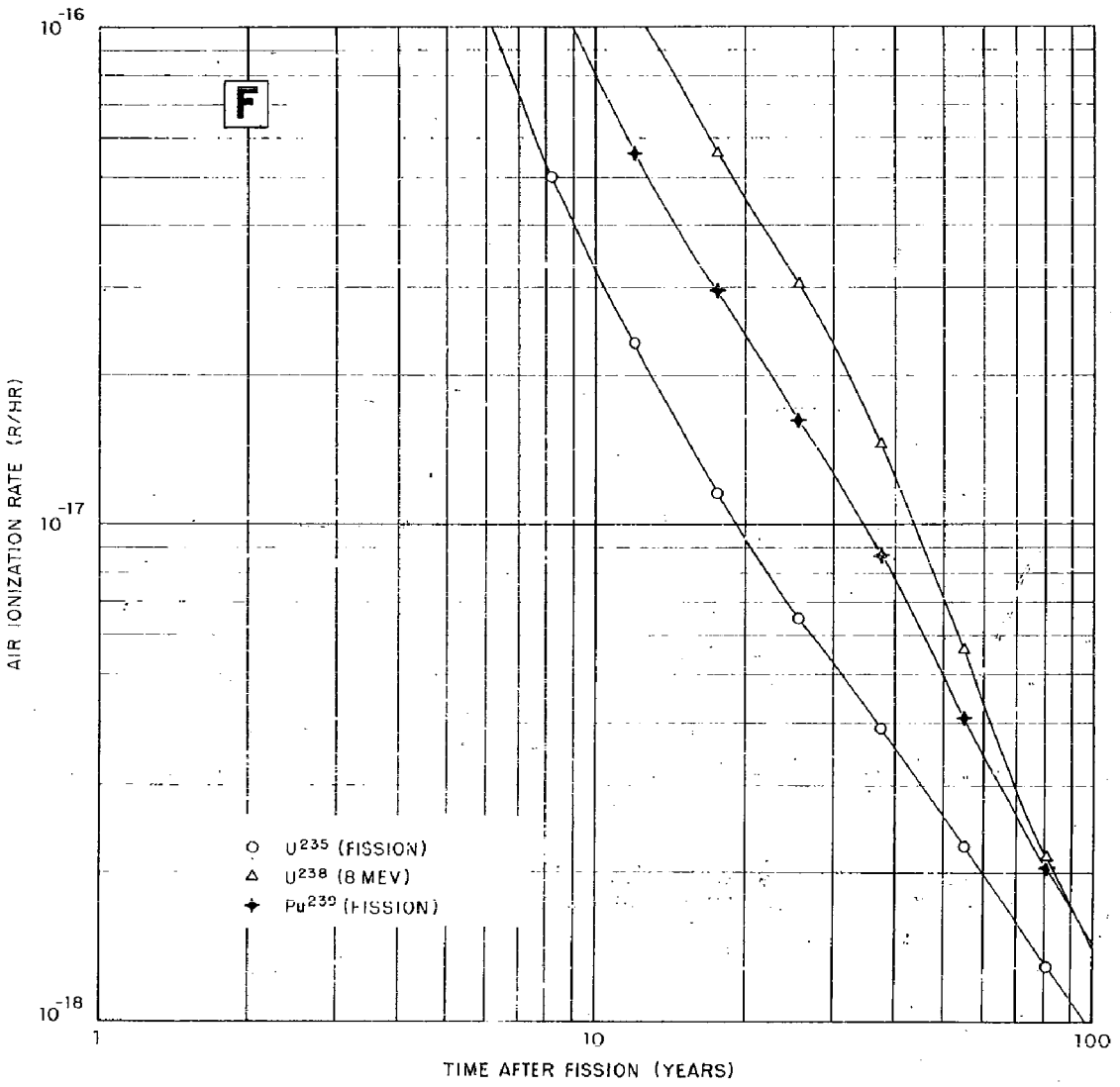
F
AIR IONIZATION RATE (R/HR)
10^{-16}
10^{-17}
10^{-18}
1
10
100
TIME AFTER FISSION (YEARS)
U^{235} (FISSION)
U^{238} (8 MEV)
Pu^{239} (FISSION)

gross fission product "R" factor, r_{fp}, which is defined as the ratio of the ionization rate for the fractionated products to that for the unfractionated products from thermal fission of U^{235} is given in Fig. 7. Up to about 5000 hrs (200 days), the differences in the r_{fp} values for the different types of fission are not large. At 1 hr after fission, the r_{fp} values for U^{238} (8 Mev), U^{235} (fission) range from 0.37 to 0.40. The minimum at about 150 hrs is where I^{131} and Ba^{140}-La^{140} are in high abundance and the maximum at about 3500 hrs is where Zr^{95}-Nb^{95} are in high abundance. The large r_{fp} values after 10,000 hrs for Pu^{239} (fission) is due to the larger yields of some of the rare earth nuclides.

The decay curves were calculated only for radionuclides dissolved in liquid soil particles and therefore apply only to a group of particles in the fallout of a given size range (say, those that separated from the fireball between about 50 and 70 seconds after burst). The r_{fp} values for smaller particles would generally be larger and even approach values that are the inverse of those shown in Fig. 7. The r_{fp} values for the world-wide fallout might approach 1 minus the r_{fp} values of Fig. 7.

The differences in the d/s and r/hr rates between those based on Present's theory of yield and Glendenin's are insignificant. The calculations for both sets were made because, when the condensation process is considered, the later decay rates are very much dependent on the independent nuclide yields present at the time of cessation of the first phase of the condensation process. Thus it appears that, for yields in the MT yield range and for soil melting at temperatures below 2000°K, the gross decay of the fractionated fissions is not sensitive to the differences in the independent nuclide yields from the two theories. It would be expected, however, that the differences in the gross decay curves would increase somewhat as the yield decreased and the soil melting point increased.

The H+1 air ionization rate in units of KT's per square mile for the various types of fission for the 2.3 MT surface burst are listed in Table 15. These values cannot be directly applied to the fraction of a weapon per unit area that produces a given radiation intensity as would be measured with a survey meter three feet above an extended flat contaminated area. First, some induced activities will be produced; if only the production of U^{239}-Np^{239} is considered,[35] a yield of 1 atom U^{239} per fission would increase the above values by 0.34×10^{-13} (r/hr)/fission/sq ft) or 180 (r/hr)/(KT/sq mi). Second, a Co^{60} calibrated survey instrument, with operator, will give a meter reading at 3 ft above the surface about 25 % lower than the true air ionization rate.[28] Third, a real surface is not

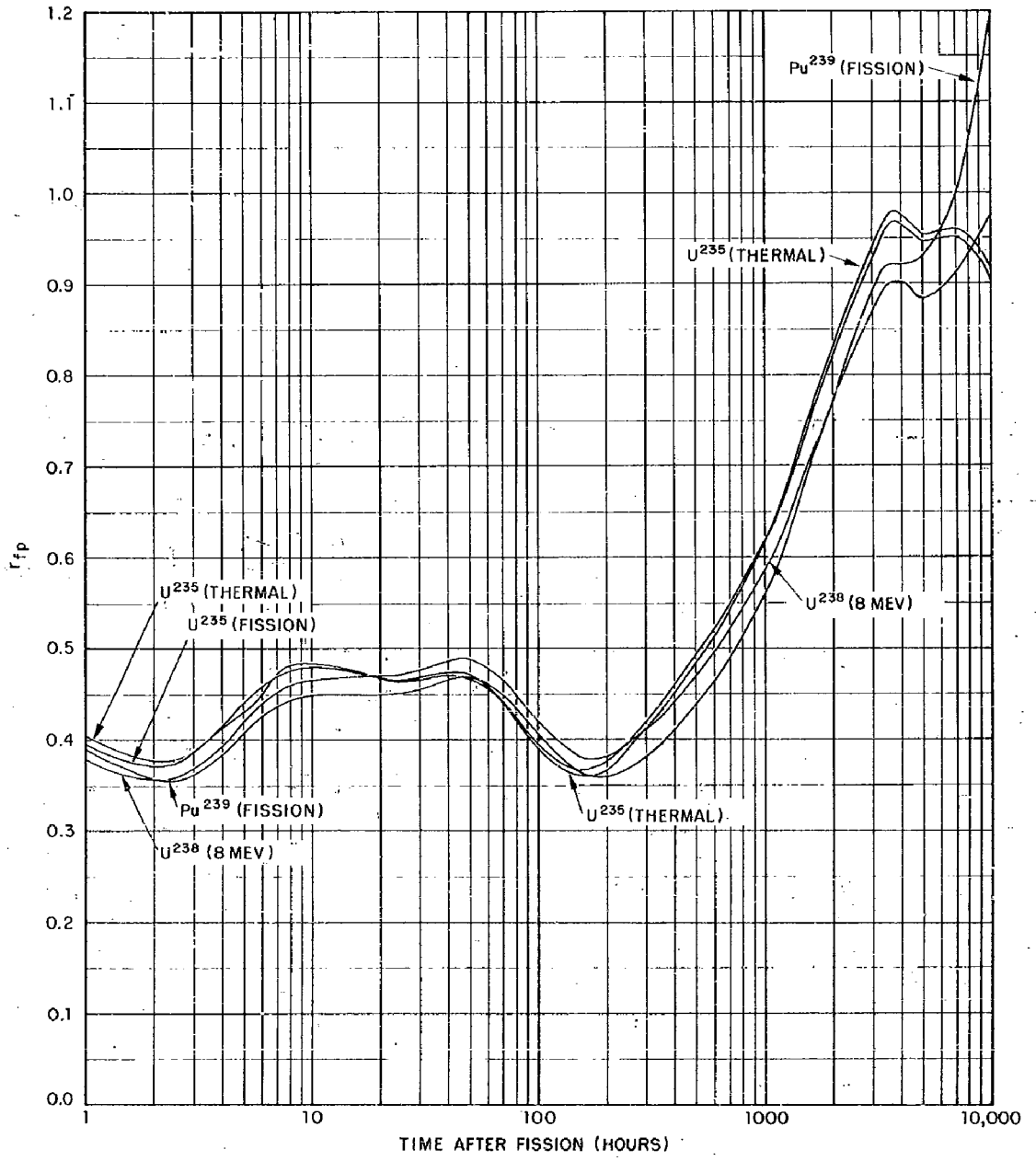

Fig. 7 Variation of the Gross Ionization Rate "R" Factor for the Fractionated Fission Products With Time After Fission

TABLE 15

Air Ionization 3 ft Above the Surface at H+1 for Unit Yield Fallout Distributions on an Ideal Plane, for Fractionated Fission Products From a 2.3 MT Surface Detonation

Type of Fission	Air Ionization (Unit Yield/Unit Area)	
	(r/hr at 1 hr)/(fiss/sq ft)[a]	(r/hr at 1 hr)/(KT/sq mi)[a]
U^{235}, thermal neutron	3.00×10^{-13}	1,560
U^{235}, fission neutrons	2.96×10^{-13}	1,540
U^{238}, 8 Mev neutrons	2.85×10^{-13}	1,480
Pu^{239}, fission neutrons	2.92×10^{-13}	1,520

a. Glendenin's Postulate.

smooth so that actual air ionization at 3 ft above the surface will again be less than that given in Table 15. If the terrain roughness were such as to reduce the ionization rate by 20 %, the combination of the three factors would give about 1000 (r/hr)/(KT/sq mi) as the "observed" value of the ratio for 8 Mev neutron fission of U^{238}. Unfortunately, this conversion factor between r/hr and KT/sq mi will not be constant over the whole region of heavy fallout. At further downwind distances where the fractionation would be less, the observed conversion factor may approach or even exceed the value, (3610 + 180) X 0.6, or 2270 (r/hr)/(KT/sq mi) for the U^{238} (8 Mev) fission. Even with fractionation, the values in Table 15 are higher than the factor derived from ENW[14] (1240 r/hr/(KT/sq mi)). However no specifications as to yield and type of detonation are given for the information in ENW; hence the value from that reference is more appropriately associated with the data of Section 6 even though its numerical value is much nearer to those given here.

The factors given in Table 15 do not have the precise relation to fissions or KT's the way the factors given in Section 6 for normal fission products do. The original mixture of fission products which is directly related to the yield has been altered in many ways. It is possible to compute the values in Table 15 because

the fraction of each nuclide produced and condensed has been calculated on the basis of the original fission yield. In an experimental evaluation of the factor, the yield representation of a square foot of fallout contamination is unknown. A representation can be made to some degree of accuracy by a radiochemical analysis of the fallout material and a measurement of the air ionization rate (corrected to H+1 or other reference time). The selection of the radionuclides for analysis should depend on some knowledge of the type of particles present. For the types of particles represented by the calculations given here, an analysis that gave the abundance of the radionuclides with $r_o(A)$ values of 1.00 (see Table 13) should give the same value of the factor as discussed for those in Table 15. It may be noted that Mo^{99}, for the conditions of these calculations, would give factors that are 27 to 31 % high. In the real fallout where a mixture of particle sizes and types are present, it would appear that the selection of the appropriate radionuclides and their yield representation should depend on other factors than the originalmass chain yield and its chain decay characteristics.

Approved by:

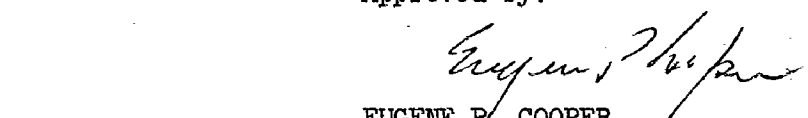

EUGENE P. COOPER
Associate Scientific Director

REFERENCES

1. C.E. Adams, I.G. Popoff, N.R. Wallace. The Nature of Individual Radioactive Particles. I. Surface and Underground ABD Particles From Operation JANGLE. U.S. Naval Radiological Defense Laboratory Report, USNRDL-374, 28 November 1952 (Unclassified).

2. C.E. Adams. The Nature of Individual Radioactive Particles. II. Fallout Particles From M-Shot, Operation IVY. U.S. Naval Radiological Defense Laboratory Report, USNRDL-408, 1 July 1953 (Unclassified).

3. C.E. Adams, J.P. Wittman. The Nature of Individual Radioactive Particles From an ABD of Operation UPSHOT-KNOTHOLE, U.S. Naval Radiological Defense Laboratory Report, USNRDL-940, 24 February 1954 (Unclassified).

4. C.E. Adams. The Nature of Individual Radioactive Particles. IV. Fallout Particles From the First Shot Operation CASTLE. U.S. Naval Radiological Defense Laboratory Technical Report, USNRDL TR-26, 17 January 1955 (Unclassified).

5. C.E. Adams. The Nature of Individual Radioactive Particles. V. Fallout Particles From Operation REDWING. U.S. Naval Radiological Defense Laboratory Technical Report, USNRDL TR-133, 1 February 1957 (Classified).

6. C.E. Adams, J.D. O'Connor. The Nature of Individual Radioactive Particles. VI. Fallout Particles From a Tower Shot, Operation REDWING. U.S. Naval Radiological Defense Laboratory Technical Report, USNRDL TR-208, 25 March 1958 (Unclassified).

7. C.E. Adams, N.H. Farlow, W.R. Schell. The Compositions, Structures, and Origins of Radioactive Fallout Particles. U.S. Naval Radiological Defense Laboratory Technical Report, USNRDL TR-209, 3 February 1958 (Unclassified).

8. R.K. Fuller. The Specific Activity-Size Relations and Solubility of Fallout From Shot Shasta, Operation PLUMBBOB. U.S. Naval Radiological Defense Laboratory Technical Report (in preparation).

9. K.H. Larson, J.W. Neel. Summary Statement of Findings Related to the Testing Program at Nevada Test Site, Fallout From Nuclear Tests, Hearings, JCAE, Vol. 3. p. 2006-2019, May 5-8, 1959.

10. W.D. Kingery, J. Am. Ceram. Soc. 42, 6-10 (1959).

11. C.E. Adams. The Condensation of Rubidium Vapor Onto Hot Oxide Surfaces. U.S. Naval Radiological Defense Laboratory Technical Report, USNRDL TR-355, 7 August 1959.

12. Kenjiro Kimura, International Conference on the Peaceful Uses of Atomic Energy, Geneva, Switzerland, Vol. 7, pages 196-209, 1956.

13. R.C. Bolles, N.E. Ballou. Calculated Abundances of U^{235} Fission Products. U.S. Naval Radiological Defense Laboratory Report, USNRDL-456, 30 August 1956.

14. The Effects of Nuclear Weapons. U.S. Govt. Printing Office, Washington, D.C., 1957.

15. D.R. Stull, G.C. Sinke. The Thermodynamic Properties of the Elements in Their Standard State. The Dow Chemical Company, March 1955.

16. C.E. Lapple. Fallout Control. Stanford Research Institute, SRIA-3, August 1958.

17. L.E. Glendenin. Technical Report No. 35, Massachusetts Institute of Technology, Cambridge, Mass., 1949.

18. R.D. Present, Phys. Rev. 72, 7, 1947.

19. Seymour Katcoff, Nucleonics, Vol. 16, No. 4, p. 78, 1958.

20. L.R. Bunney, et al, Fission Yields in Neutron Fission of Pu^{239}. U.S. Naval Radiological Defense Laboratory Technical Report, USNRDL TR-268, 10 October 1958.

21. E.P. Steinberg, L.E. Glendenin. Survey of Radiochemical Studies of the Fission Process, International Conference on the Peaceful Uses of Atomic Energy, Vol. 7, p. 3-14, 1956.

22. A.C. Pappas. The Delayed Neutron Precursors in Fission. International Conference on the Peaceful Uses of Atomic Energy, Vol. 15, p. 583, 1958.

23. A.C. Wahl. Nuclear Charge Distribution in Fission: Cumulative Yields of Short-Lived Krypton and Neon Isotopes From Thermal-Neutron Fission of U^{235}. J. Inorg. Nucl. Chem. 6, 263-77, 1958.

24. L.E. Glendenin, C.D. Coryell, R.R. Edwards. Radiochemical Studies: The Fission Products, NNES, Plutonium Project Record, Div. IV, 9, 489, McGraw Hill, New York (1951).

25. A.C. Herrington, Massachusetts Institute of Technology, Laboratory for Nuclear Science, Annual Progress Report, p. 37, 1 June 1957 - 31 May 1958.

26. C.F. Miller. Proposed Decay Schemes of the Fission Products and Other Radionuclides. U.S. Naval Radiological Defense Laboratory Technical Report, USNRDL TR-160, 27 May 1957.

27. P.D. LaRiviere. Proposed Decay Schemes of the Fission Products and Other Radionuclides; Revision I. U.S. Naval Radiological Defense Laboratory Technical Report (in publication).

28. C.F. Miller, P. Loeb. Ionization Rate and Photon Pulse Decay of Fission Products From the Slow Neutron Fission of U^{235}. U.S. Naval Radiological Defense Laboratory Technical Report, USNRDL TR-247 (1958).

29. P.T. Dolan. Calculated Abundances and Activities of the Products of High Energy Neutron Fission of Uranium-238, DASA (Formerly AFSWP) 525, May 1959.

30. P.J. Dolan. Gamma Spectra of Uranium-238 Fission Products at Various Times After Fission. DASA (Formerly AFSWP) 526, May 1959.

31. Ralph E. Lapp. Local Fallout Radioactivity. Bull. Atomic Scientists, Vol. XV, No. 5, p. 181 (1959).

32. Harold A. Knapp. A Review of Information on the Gamma Energy Radiation Rate From Fission Products, and its Significance for Studies of Radioactive Fallout, Biological and Environmental Effects of Nuclear War. Hearings, JCAE, p. 113, June 1959.

33. J.F. Perkins, R.W. King. Energy Release From the Decay of Fission Products. Nuclear Sci. and Eng. 3, 726, June 1958.

34. W.E. Knabe, G.E. Putnam. The Activity of the Fission Products of U^{235}. General Electric Co., APEX-448, Oct. 1958.

35. N.G. Stewart, R.N. Crooks, E.M.R. Fisher. The Radiological Dose to Person in the U.K. Due to Debris From Nuclear Test Explosions Prior to January 1956, The Nature of Radioactive Fallout and Its Effects on Man. Hearings, JCAE, p. 1690, June 1957.

U. S. NAVAL RADIOLOGICAL DEFENSE LABORATORY
SAN FRANCISCO 24, CALIFORNIA

220
BD:mm

SEP 3 0 1960

From: Commanding Officer and Director
To: Distribution for Technical Report USNRDL-TR-425

Subj: U. S. Naval Radiological Defense Laboratory Report USNRDL-TR-425 entitled "A Theory of Formation of Fallout from Land-Surface Nuclear Detonations and Decay of the Fission Products" by C. F. Miller; errata for

1. It is requested that the following corrections be made in subject report:

p. iv - last paragraph, first sentence, add "are presented" after "fission of Pu^{239}."

p. 11 - Equation 11 is to read as follows: $RT/np/p_o = \frac{47M}{\rho d}$

p. 15 - Equation 21 is to read as follows: $n_j^o = \frac{n_j k_j}{(n(\ell)/V)RT}$

p. 27 - Equation 70 is to read as follows: $n'_{jA} = \frac{k_j^o y_{jA}}{1 + k_j^o} \cdot \frac{-Vp_{jA}^s}{RT}$

p. 32 - line 3 reads "Combining Eqs. 57 and 58 gives"

Change to read "Combining Eqs. 74 and 75 gives"

p. 45 - line 1 - correct typographical error in spelling of word "expansion"

p. 46 - line 8 reads "Substituting Eqs. 103, 104, and"

Change to read "Substituting Eqs. 103, 105, and"

p. 49 - line 23 reads "then T_2 from Eq. 112 is"

Change to read "then T_2 from Eq. 123 is"

p. 50 - Equation 131 closes as follows: $\int_{t_m}^{t_f} t^{-1.490}\, dt$

220
BD:mm

Subj: U. S. Naval Radiological Defense Laboratory Report USNRDL-TR-425 entitled "A Theory of Formation of Fallout from Land-Surface Nuclear Detonations and Decay of the Fission Products" by C. F. Miller; errata for

Change this portion of the equation to read as follows: $\int_{t_m}^{t_f} t^{-1.590}\,dt$

p. 58 - footnote ** reads " . . . ; determined from Eq. 121b"

Change to read " . . . ; determined from Eq. 149b"

p. 63 - line 14 reads "of Pdt for Eq. 176, is"

Change to read "of Pdt for Eq. 177, is"

p. 64 - last line, add "so that" after "per molecule"

p. 66 - line 14 reads " . . . ; for other yields Eq. 178"

Change to read " . . . ; for other yields Eq. 179"

p. 98 - third paragraph, seventh line reads " . . . ; I^{131}, 0.914 and 0.108"

Change to read " . . . ; I^{131}, 0.0914 and 0.108".

T. J. Mathews

T. J. MATHEWS
By direction

UNCLASSIFIED

UNCLASSIFIED